# MAST III – SASME Project
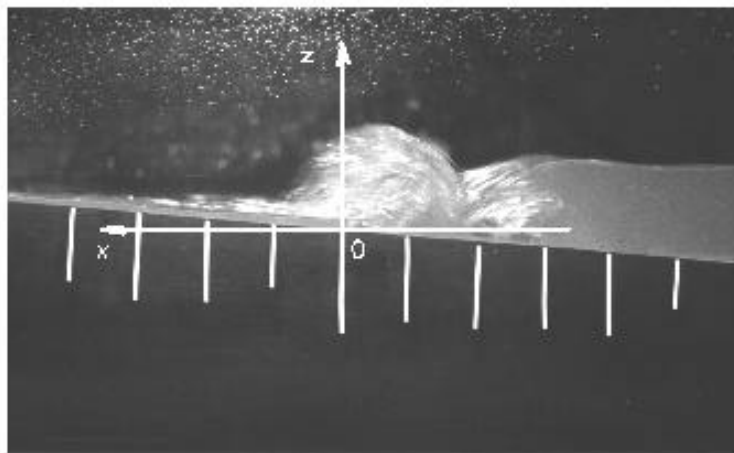
## Surf and Swash Zone Mechanics

---

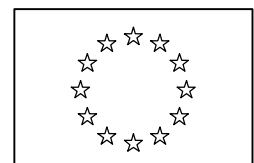# Swash zone hydrodynamics on a 1:10 bottom slope: laboratory data

Marco Petti, Sandro Longo, Stefano Sadun, Matteo Tirindelli



**Department of Civil Engineering**
*Hydraulic Laboratory*
University of Firenze

**December 1998**

*SASME Report FIUD-01-98*

# Swash zone hydrodynamics on a 1:10 bottom slope: laboratory data

Marco Petti (*),  Sandro Longo (°)

Stefano Sadun (^),  Matteo Tirindelli (^)

(*)    Dipartimento di Georisorse e Territorio, University of Udine
(°)    Dipartimento di Ingegneria Civile, University of Parma
(^)    Dipartimento di Ingegneria Civile, University of Firenze

# Contents

## List of Figures and Tables

*Fig. 2.1- Wave flume.*
*Fig. 2.2 - Generation and acquisition box system.*
*Fig. 2.3 - Fixed and movable gauges.*
*Fig. 2.4 - Typical calibration of a vertical wave gauge*
*Fig. 2.5 - Systematic error in run up meter measures.*
*Fig. 2.6 - Typical calibration of the run up meter.*
*Fig. 2.8 - Laser Doppler Velocimeter system.*
*Fig. 2.9 - LDV system sketch.*
*Fig. 2.10 - LDV signal selection.*
*Fig. 2.11 - Videocamera of the Image analysis system.*
*Fig. 3.1 - Experimental set-up and location of wave gauges.*
*Fig. 3.2 - Location of the wave gauges in the surf e swash-zone.*
*Fig. 3.3 - Laser Doppler velocimeter position.*
*Fig. 3.4 - Videocamera position.*
*Fig. 3.5 - Breaking range covered with performed tests.*
*Fig. 4.1a - Test RH040T30: phase analysis for gauges 1-8.*
*Fig. 4.1b - Test RH040T30: phase analysis for gauges 9-11 and 13.*
*Fig. 4.2 - Test RH040T20: Set up profiles, crest and trough envelopes.*
*Fig. 4.3 - Sketch for flux evaluation.*
*Fig. 4.4 - Test RH040T20: flux analysis in the zero section (gauge S8).*
*Fig. 4.5 - Measure sections for velocity measurements.*
*Fig. 4.6 - RH040T20: velocity profiles in the lower section.*
*Fig. 4.7 - RH040T20: velocity profiles in the mid-section.*
*Fig. 4.8 - RH040T20: velocity profiles in the upper section.*
*Fig.4.9 - Test RH040T30: instantaneous velocity and turbulence fluctuations in the lower section, z = 2.5 mm.*
*Tab. I - Videocamera characteristics.*
*Tab. II - Regular waves.*
*Tab. III - Irregular waves.*
*Tab. IV - Breaking parameters.*
*Tab. V - Test RH040T20: water levels evaluated referring to S.W.L.*
*Tab. VI - Regular waves: water levels evaluated at the run up meter referring to S.W.L.*
*Tab. VII - Irregular waves: water levels evaluated at the run up meter referring to S.W.L.*

**Annex 1**

*Fig.A1-1.* Experimental set-up and location of the wave gauges.
*Fig.A1-2.* Reference system and location of the wave gauges in the surf and swash zone.
*Fig.A1-3.* Calibration of gauges 1-4.
*Fig.A1-4.* Calibration of gauges 5-12.
*Fig.A1-5.* Concrete bottom surface profiles. Specimen A.
*Fig.A1-6.* Concrete bottom surface profiles. Specimen B.
*Fig.A1-7.* Concrete bottom surface profiles. Specimen C.

**Annex 2**

*Tab.A2-I Test RH040T20:* water levels evaluated referring to S.W.L.
*Tab.A2-II Test RH040T25:* water levels evaluated referring to S.W.L.
*Tab.A2-III Test RH040T30:* water levels evaluated referring to S.W.L.
*Tab.A2-IV Regular waves:* water levels evaluated at the run up meter referring to S.W.L.
*Fig.A2-1. Test RH040T20:* phase analysis of gauges 1-8.
*Fig.A2-2. Test RH040T20:* phase analysis of gauges 9-10 and 13.
*Fig.A2-3. Test RH040T20:* Set up profiles, crest and trough envelopes.
*Fig.A2-4. Test RH040T25:* phase analysis of gauges 1-8.
*Fig.A2-5. Test RH040T25:* phase analysis of gauges 9-10 and 13.
*Fig.A2-6. Test RH040T25:* Set up profiles, crest and trough envelopes.
*Fig.A2-7. Test RH040T30:* phase analysis of gauges 1-8.
*Fig.A2-8. Test RH040T30:* phase analysis of gauges 9-10 and 13.
*Fig.A2-9. Test RH040T30:* Set up profiles, crest and trough envelopes.

**Annex 3**

*Tab. A3-1.* Irregular waves: water levels evaluated at the run up meter referring to S.W.L.
*Fig.A3-1. Test IH040T20*: time recording of gauges 1-4.
*Fig.A3-2. Test IH040T20*: time recording of gauges 5-8.
*Fig.A3-3. Test IH040T20*: time recording of gauges 9,10 and 13.
*Fig.A3-4. Test IH040T25*: time recording of gauges 1-4.
*Fig.A3-5. Test IH040T25*: time recording of gauges 5-8.
*Fig.A3-6. Test IH040T25*: time recording of gauges 9,10 and 13.
*Fig.A3-7. Test IH040T30*: time recording of gauges 1-4.
*Fig.A3-8. Test IH040T30*: time recording of gauges 5-8.

# 1. Introduction

Wave set-up has been measured on impermeable fixed plane beaches by a number of researchers, i.e. Bowen et al. (1968), Gourlay (1978), Van Dorn (1976, 1978), Hansen and Svendsen (1979), Stive and Wind (1982), and Stive (1985). In all these measurements the beach slopes range between 0.022 and 0.1. As a consequence of the many difficulties in measuring the water level in a partially wet and dry area, none of the methods used (inverted tube, piezometers) have given satisfactory observations in the swash zone (Gourlay, 1992).

Starting from the results of the research up to now, a new series of experiments have been carried out, on different beach slopes and with different surf similarity parameter values. The main aim is to take detailed measurements of fluid velocity and free surface levels in the swash zone.

The first series of the experiments took place in the flume of the Department of Civil Engineering, University of Florence, on a 1:10 impermeable sloping beach. We mainly measured free surface elevation in different sections, run-up and run-down levels and fluid velocities. The specific equipment consisted of twin wire wave gauges (also as run-up meter), image analysis and Laser Doppler Velocimetry.

The waves tested in the tank are mainly monochromatic, but we refer also to some bichromatic irregular waves.

The Wave Flume was operated by Mauro Gioli, Muzio Mascherini, Stefano Sadun and Matteo Tirindelli. The experiment execution, data analysis and report drawing up were conducted by the following research team:

Marco Petti, University of Udine, Italy, principal investigator;
Sandro Longo, University of Parma, Italy;
Stefano Sadun, University of Florence, Italy, M.Sc. student;
Matteo Tirindelli, University of Florence, Italy, M.Sc. student.

## 2.  Experimental facilities

In this chapter a general description of the facilities used to perform experimental tests in SASME project is given.


## 2.1  Wave flume

The wave flume located in the Hydraulic Laboratory of the Department of Civil Engineering in Florence is 48 m long, 0.8 m wide, and 0.8 m high, and is built completely of steel and glass. The maximum water depth that can be used in the flume is 0.6 m. At one end of the flume a wave maker is installed, which consists of a paddle moved by an electronic-controlled hydraulic system. The mechanical structure which supports the paddle allows it to work as a piston, flap, or cradle type.

Fig.2.1- *Wave flume.*

The displacement of the paddle is controlled with a hydraulic servo-valve moved by a computer system through an electric low voltage signal ; a feedback checks the paddle displacement.

The acquisition system consists of a personal computer equipped with an Intel Pentium processor, two boards A/D and D/A 12 bits converters, and one analogue low pass filter. A high level software (Petti, 1988, 1992) programmes the runs of the waves in the flume, shows in real time, collects and stores the signals coming from 32 acquisition channels connected with as many gauges.



Fig. 2.2 - *Generation and acquisition box system.*

Additional software developed in Delft NL performs a second order generation.

## 2.2 Wave gauges

Water level oscillations are measured by resistive wave gauges. They consist of twin parallel wire (Ø=0.3 mm) meters; the measurement of the resistance between the wires may be accomplished in several ways, but high frequency AC methods offer

significant advantage and have been used. The wires are connected to a 4 KHz oscillator, able to supply current, and are fixed to an insulating support (*movable* gauges) or with two ends directly to the bottom of the flume (*fixed* gauges) with brass screws. The resistance between the wires is proportional to the water level and is converted in output voltage in the range 0÷10 Volt; it is possible to adjust the electrical gain of the circuit to improve the resolution. The gain is relatively high for swash zone gauges, where the expected water level fluctuations are in the order of a few centimetres. The characteristic Voltage vs. water level, if the field around the wires is homogeneous and symmetrical, is linear.
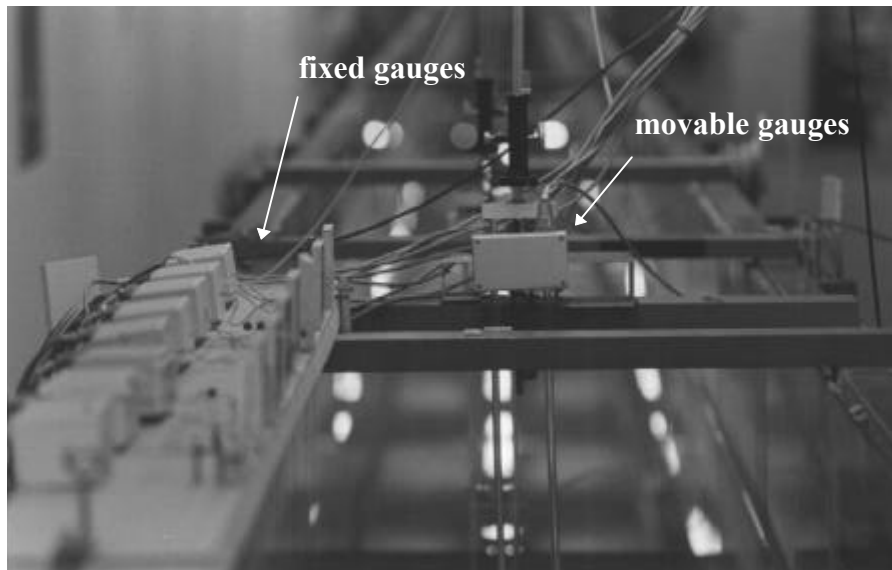


Fig. 2.3 - *Fixed and movable gauges*.

### 2.2.1 Calibration of wave gauges

The voltage output of each resistive gauge has to be related to metric water level signal. The input-output (cm-V) relation is expressed by a linear function:

$$\boldsymbol{h} = aV + b \tag{2.1}$$

for vertical gauges (both movable and fixed); this is a consequence of the symmetry of the electrical field around the wires and the absence of interfering inputs. The calibration is carried out in static conditions; the operating sequence consists of:

       1) setting the water level in the flume (step ~1 cm);

       2) accurate measurement of the level reached through a point gauge with an overall accuracy of 0.1 mm;

       3) acquisition of the wave gauges signal for several seconds.

For movable gauges, point 1) can be performed by moving the gauge rather than the water level in the flume. In Fig. 2.4 a typical calibration output for a vertical gauge is shown.
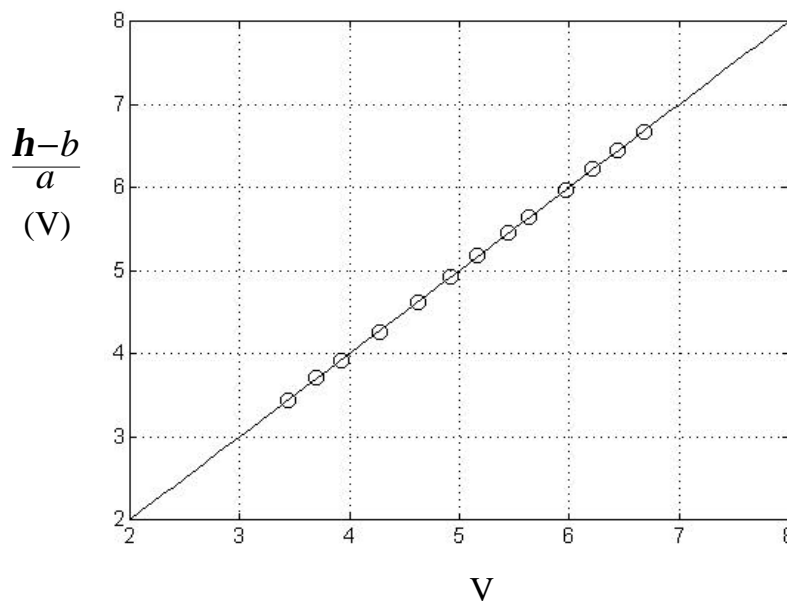


Fig. 2.4 - *Typical calibration of a vertical wave gauge*.

During tests the linearity and the stability of wave gauges is periodically checked by repeating the calibration steps; the electronics for signal manipulation is stable while the main causes of bias and lack of precision are the surface contamination of the wires and the water resistance variation. The level of electric noise, evaluated as the standard deviation of the output signal in still water conditions, is correspondent to an error in

water level measurement equal to a maximum of:

$$\Delta\eta = \pm1 \text{ mm}$$

with a transient error in dynamic conditions, partially due to tension surface effects, included in this value.

## 2.3  Run up meter

The run up meter consists of twin wires laid down in parallel to the beach bottom face, covering the whole swash range. With such a configuration the system shows the effect of the lack of symmetry of the electromagnetic field due to the presence of the bottom layers. Leaning the wires close to the bottom of the flume causes the signal to lose its validity because of the meniscus effects (meniscus between the bottom and the wires) and of the already mentioned boundary effects. On lifting them, the signal gains validity but the output is non linear, especially at the extremes of the oscillation range; a systematic geometrical error is also introduced, as sketched in Fig. 2.5.
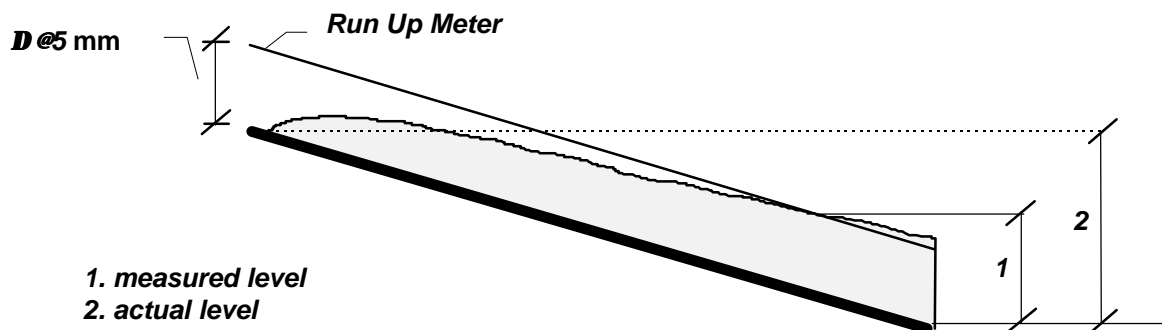


Fig. 2.5 - *Systematic error in run up meter measures.*

A good compromise has been found by placing the wires at a fixed distance of 5 mm from the bottom. To correct the systematic geometrical error, a video image analysis (§2.5) has been used, comparing the position of the bore front as detected by video images with the position as recorded by the run up meter. The behaviour seems different in back swash and up swash and the interpretation of capillary effects can be

debated. The problem is of particular interest especially concerning run down height estimates, that involve a very small thickness of water, and needs further discussion. In Fig. 2.6 a typical calibration curve of the run up meter is sketched.
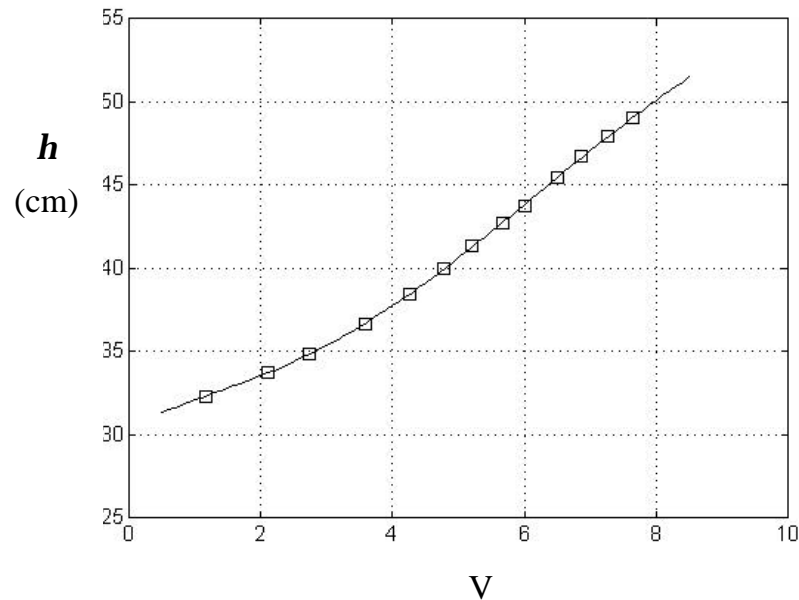


Fig. 2.6 - *Typical calibration of the run up meter*.

The estimated error varies linearly from maximum run-down to maximum run-up; a fifth order polynomial function is necessary to fit the calibration data to make a non-linearity error equal to the other errors.

## 2.4  Laser Doppler Velocimeter

A Laser Doppler He-Ne 30 mW system for local velocity measurements has been used with a measurement volume as an ellipsoid whose axes are of the order of 1 mm (Fig. 2.8). The optical modular system is composed of cover and retarder lenses (to stabilise the direction of polarisation), a beamsplitter, a beam waist adjuster (to avoid errors in beams interference), a Bragg cell (to introduce the frequency shift necessary for detecting velocity orientation), a pinhole section and a frontal achromatic lens (f=310 mm) that provides for the beams convergence onto the measurement volume

inside the wave tank (Fig. 2.9). The Doppler frequency information is collected by a photomultiplier (*PM*). A frequency shifter device introduces an adjustable frequency ($f_s$) that distinguishes the orientation of velocity.



Fig. 2.8 - *Laser Doppler Velocimeter system.*
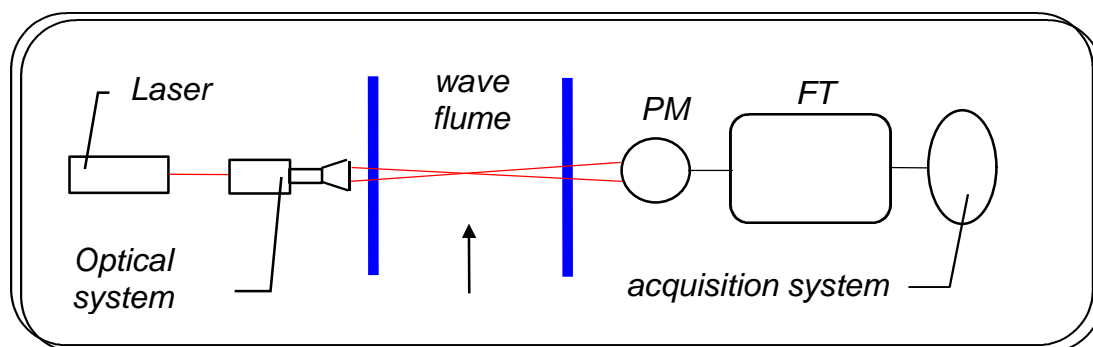


Fig. 2.9 - *LDV system sketch.*

### 2.4.1  Signal collecting and elaboration

Signal elaboration is carried out through a *frequency tracker (FT)* device, suitable for multiparticle origin signals. The linear output function between velocity and voltage is:

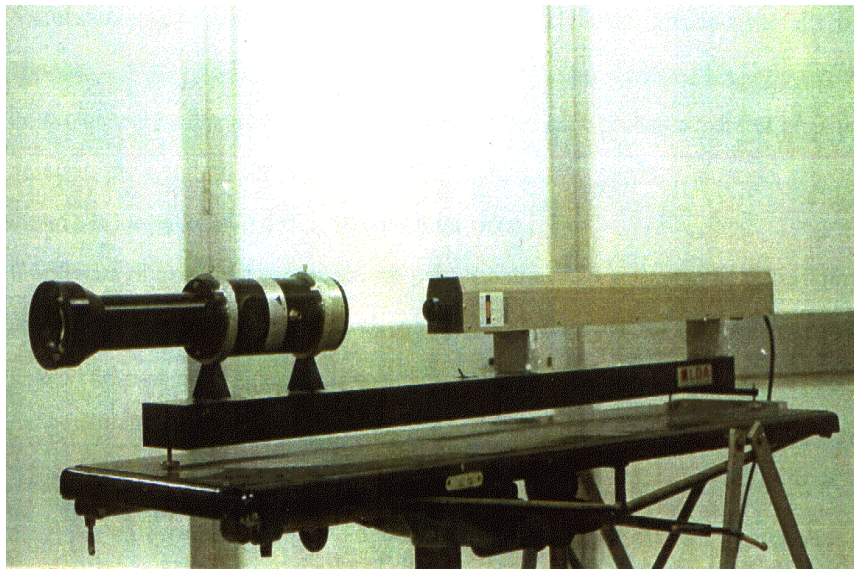$$V_{out} = \frac{10f_D}{R} \pm \frac{10f_s}{R} = \frac{10}{R}\left(\frac{u}{3.18} \pm f_s\right) \qquad (2.2)$$

where $V_{out}$ [V] is the output tension, $f_D$ [Hz] is the Doppler frequency, $R$ [MHz] is the upper limit of the chosen frequency range, $f_s$ [MHz] is the shift frequency, $u$ [m/s] is the velocity and 3.18 is a coefficient depending upon the optical set-up and laser radiation wave length. To increase light scattering and consequently the Signal/Noise ratio, aluminium powder ($\varnothing$=10 µm) is used as a tracer. The error in velocity measurements declared by DISA-DANTEC is 1% of the selected frequency range ; with the used set-up (frequency range =0.1-1 MHz) that means:

$$u_{actual} = u_{measured} \pm 2.8 \text{ cm/s}$$

The main problem with LDV measurements in the swash zone is related to the periodic backwash: the absence of water, or simply air bubbles crossing through the measurement volume, unlock the signal. The locking-unlocking sequence is not strictly predictable, even in presence of regular wave trains; for this reason we selected the valid signal directly through visual observation of the raw time series plot defining a Boolean function $f(t)$ (Fig. 2.10).
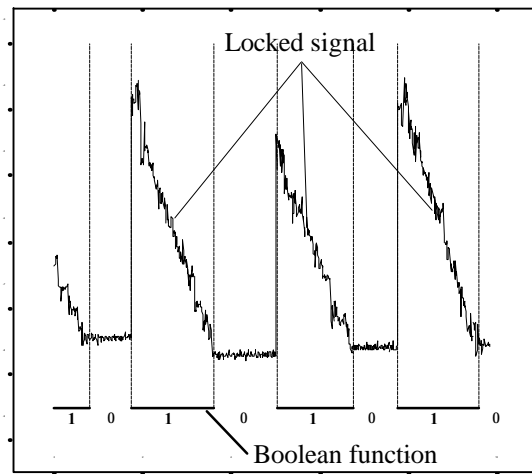
Fig. 2.10 - *LDV signal selection.*

## 2.5  Image analysis

A digital videocamera *Panasonic model AG-EZ1E* has been used for image analysis, coupled with *Matrox* video-board, frame-grabber and appropriate software.

Tab. I - *Videocamera characteristics.*

| recording system: | DIGITAL VIDEO SD  format |
|---|---|
| lens: | zoom 1:10    variable speed; F 1.6; focal length 6 ¸ 60 mm |
| shutter frequency: | 50 ¸ 8000 Hz |
| standard illumination: | 1400 lux |

In the present experiments, Video Image Analysis has been used for qualitative preliminary analyses of the breaking process and field of motion, run up and run down height estimates (correction and calibration of the run up meter), the location of the breaking point and assessments of breaking wave height. Placing appropriate markers (points or lines) on the field and on the frames, precise metric estimates are possible

after carrying out calibration. Lighting has been assured using a white-hot lamp of limited power.



Fig. 2.11 - *Videocamera of the Image analysis system.*

## 3. Experiments

In this chapter, a description of the experiments performed on 1:10 sloping beach is given.

## 3.1 Set-up

A concrete bottom 1:10 sloping beach was built up starting 37.5 m from the paddle; its surface was finished in order to reduce its roughness. Three specimens have been collected out of the maximum water level, assuming that the wave action is not strong enough to smooth the surface. The geometric scale of the roughness has been evaluated through a detailed analysis of the specimens using a Laser interferometric pick-up transverse unit (RTH Form Talysurf-120L), according to ISO 4287. The average height value of the crests is around 30 μm without evident differences among the specimens ; the bottom surface is quite regular, without apparent 3-D effects induced on the wave field.

For water level measurements a series of 12 resistive gauges were used: 4 movable, at different positions along the flume, and 8 fixed located in the surf and swash zone (Fig. 3.1).
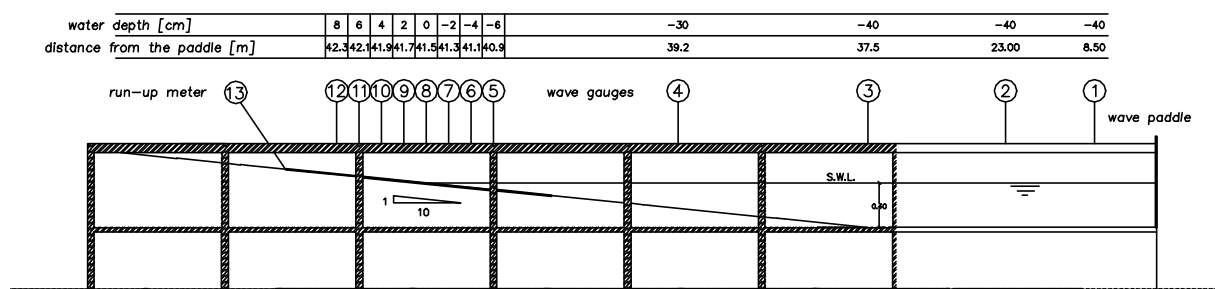


Fig. 3.1 – *Experimental set-up and location of wave gauges.*

Three of the four movable gauges (1÷3) were placed on the plane bottom part of the flume, at distances from the paddle of 8.5, 23 and 37.5 m; their output was used to check the generated wave forms. The fourth wave gauge (4) was positioned at 39.2

meters from the wave paddle. Eight fixed gauges (5-12) were placed at intervals of 20 cm (this was the best compromise to avoid reciprocal interference and to cover the measures zone with an adequate resolution) across the swash zone (Fig. 3.2). Finally, a run up meter (gauge 13) was placed parallel to the bottom in the swash zone, to measure the bore front position. It was insulated from the concrete surface to prevent short-circuiting of the resistance and 5 mm away to avoid meniscus and consequent output distortion.
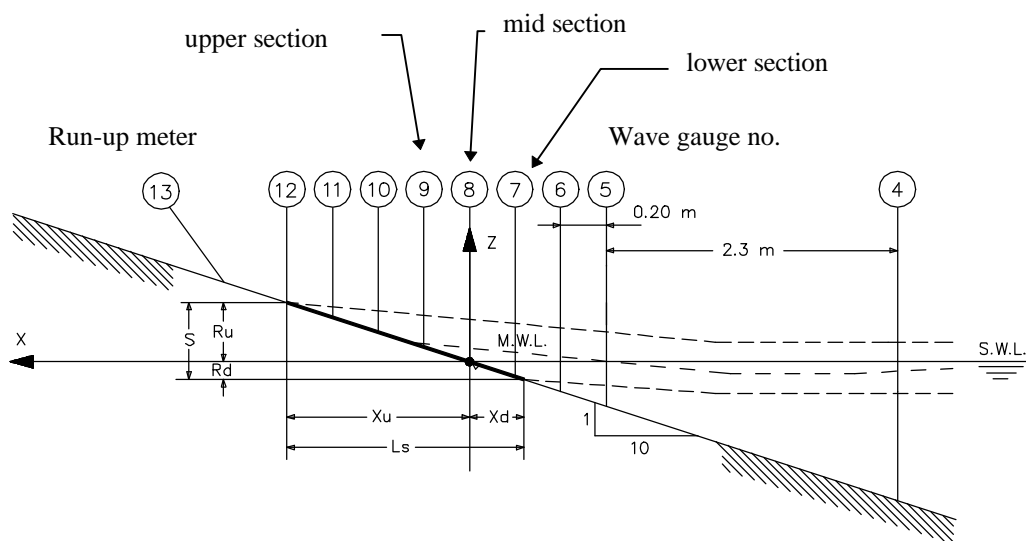


Fig. 3.2 – *Location of the wave gauges in the surf and swash-zone.*

Particular attention was given to the calibration of the gauges in the swash zone, which is characterised by an uprush/backwash cycle with the gauges wet only for a fraction of the wave period. During backwash the gauges did not have a linear characteristic around the zero water level; moreover the output had a transient error and reached the correspondent zero level voltage output only after a time interval. This was due to the local conditions at the toe of the gauge (residual water around the screws, distortion induced by the concrete bottom). These signals were corrected by detecting the output discontinuity that marks the water front crossing during backwash.

Instantaneous velocities have been measured in the swash zone by a LDV system (Fig. 3.3) in forward scatter, at several points equally spaced with 1 mm step along the vertical starting at 0.5 mm from the bottom and in three different sections. The three sections were in the still water level intersection with the slope (**mid** section), 20 cm shoreward (**upper** section), and the last at 20 cm seaward (lower section). The position of the upper section was reduced to +5 cm for the shorter waves, in order to catch the velocity signal for a sufficiently long enough time.
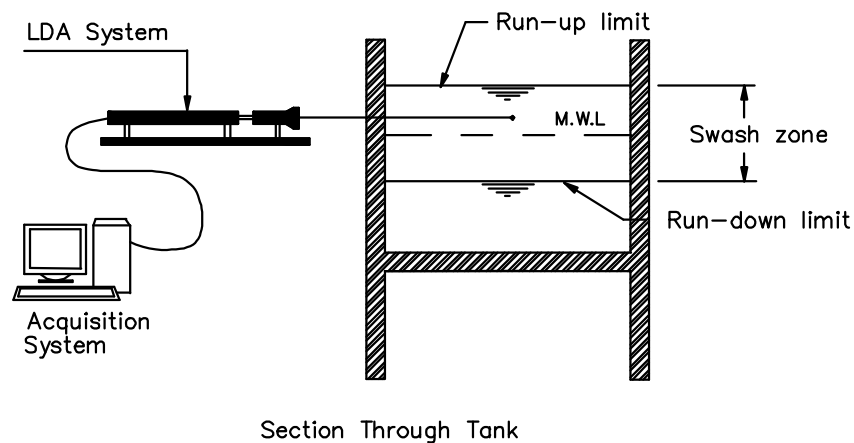


Fig. 3.3 – *Laser Doppler velocimeter position.*

An image analysis system was used to improve run up and run down measurements (Fig. 3.4). Camera positions were fixed at different angles: the camera was placed above the wave flume for swash zone measures; a lateral point of view was used for the breaking process analysis. The video image analysis was very useful to evaluate the transfer function of the run-up meter, carefully calibrated in order to correct the distortion due to meniscus.
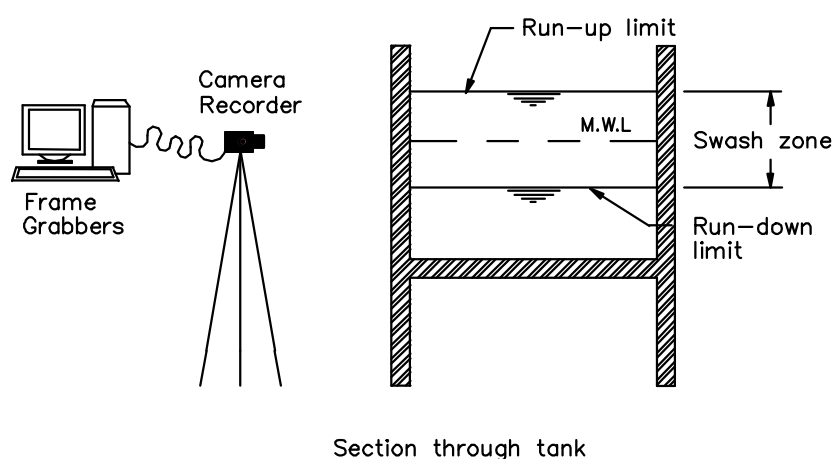
Fig. 3.4 – *Videocamera position.*

## 3.2 Tests

Three regular wave trains and three bichromatic irregular wave trains were generated in the flume. Each test was performed strictly according to the following "rules":

1) maintaining the still water level in the flume equal to 40 cm;

2) waiting 15 minutes between two successive tests in order to get actual still water conditions;

3) checking gauge measurements through the acquisition system for the entire length of each test.

The whole set of **regular wave** tests performed is summarised in Tab. II, subscripts "$_1$" refer to data collected at gauge *S1*. The whole set of **irregular wave** tests performed is summarised in Tab. III. In this case subscript "$_s$" means significant value while "$_1$" refers again to data collected at gauge *S1*. Over-scripts $^{(1)}$ and $^{(2)}$ refer to first and second component of the bichromatic train generated.

Tab. II - *Regular waves.*

| Test | $H_1$ [cm] | $T$ [s] | $H_1/L_1$ [-] | Sampling rate [Hz] | Acquisition time [s] |
|------|-----------|---------|---------------|---------------------|----------------------|
| *RH040T20* | 3.5 | 2.0 | 0.0088 | 100 | 600 |
| *RH040T25* | 3.4 | 2.5 | 0.0069 | 100 | 600 |
| *RH040T30* | 3.8 | 3.0 | 0.0064 | 100 | 600 |

Tab. III - *Irregular waves.*

| Test | $H_{S1}$ [cm] | $T_{S1}$ [s] | $T^{(1)}$ [s] | $T^{(2)}$ [s] | Sampling rate [Hz] | Acquisition time [s] |
|------|--------------|-------------|---------------|---------------|---------------------|----------------------|
| *IH040T20* | 3.5 | 2.0 | 1.9 | 2.1 | 100 | 600 |
| *IH040T25* | 3.4 | 2.5 | 2.3 | 2.7 | 100 | 600 |
| *IH040T30* | 3.8 | 3.0 | 2.8 | 3.2 | 100 | 600 |

Velocity measurements  in several points (§ 4.3) required many runs for each regular wave, thus a repetitiveness analysis was carried out. This was done successfully by checking the wave height and wave period collected by gauge *S1* for the whole set of tests. Using data collected with gauge *S1* (control gauge), accounting for the shoaling effect, surf similarity parameters $\xi_b$ and $I_b$ were estimated for each wave train (Gourlay, 1992):

$$x_b = \frac{1.45 \cdot \tan(J)}{\left(H_0 / L_0\right)^{0.36}} \qquad\qquad I_b = \frac{1}{2.5 \cdot x_b}$$

The results are reported in Tab. IV ; the last column contains the reflection coefficients. The breaking ranges in the tests are reported in Fig. 3.5.
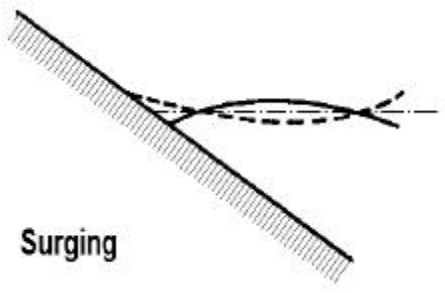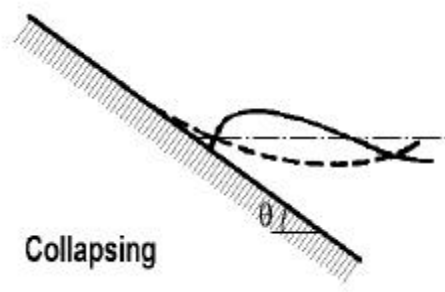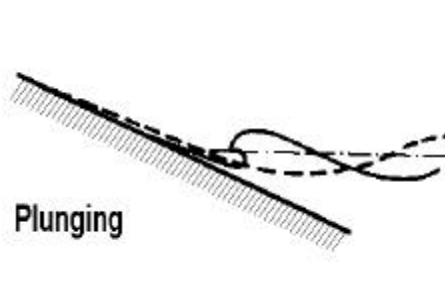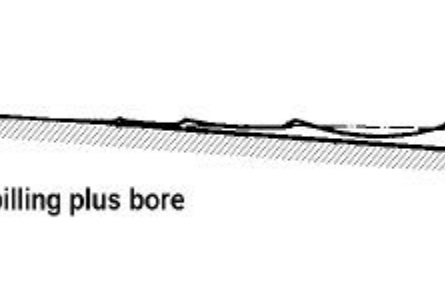
| | | |
|---|---|---|
| Surging | | $\xi_b > 2$ |
| Collapsing | *Tests:*<br>*RH040T30*<br>*RH040T25* | $1.14 < \xi_b < 2$ |
| Plunging | *Test:*<br>*RH040T20* | $0.80 < \xi_b < 1.14$ |
| Plunging plus bore | | $0.40 < \xi_b < 0.80$ |
| Spilling plus bore | | $\xi_b < 0.2$ |

Fig. 3.5 – *Breaking range covered with performed tests.*

Tab. IV. - *Breaking parameters.*

| Test | $\xi_b$ | $I_b$ | breaking type | $K_r$ |
|------|---------|-------|---------------|-------|
| *RH040T20* | 0.987 | 0.404 | *plunging* | 0.16 |
| *RH040T25* | 1.298 | 0.307 | *collapsing* | 0.27 |
| *RH040T30* | 1.437 | 0.278 | *collapsing* | 0.34 |

## 4. Measurements

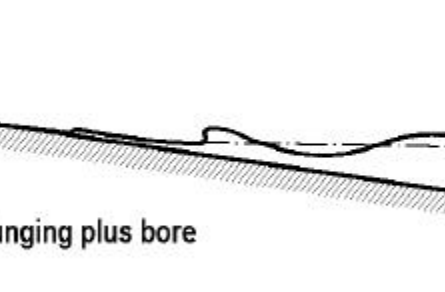Measurements of water levels, velocity, mass flux and turbulence levels have been performed on data collected for each test.

Experimental tests in a wave flume are always influenced by the particular experimental set-up used. Our tests simulated open-sea conditions in front of a beach and the problem of the waves reflected by the beach and re-reflected by the paddle had to be faced, as its influence could seriously undermine the representative nature of the measurements.

To tackle this problem a post-analysis was carried out: using the shallow water celerity formula ($c = \sqrt{gh} = 1.981$ [m/s] ), different time intervals were chosen for data analysis of each gauge in order to avoid low frequency components released from re-reflection of the paddle and to avoid data being influenced by resonance seiches, estimated to have a period $\approx 40$ s in the tested conditions.

## 4.1 Water levels

The **phase** averaged water levels $h(t)$ were calculated for each gauge:

$$h(t) = \frac{1}{N} \sum_{k=0}^{N-1} \hbar(t + kT) \qquad 0 \pounds t < T \qquad (4.1)$$

where $\hbar(t)$ represents instantaneous oscillation from SWL, $N$ is the number of waves in the chosen time interval and $T$ is wave period.

In Fig. 4.1a-b an example of phase averaged analysis is shown for each gauge, referring to test RH040T30. The analyses for all the tests are reported in Annex 1.
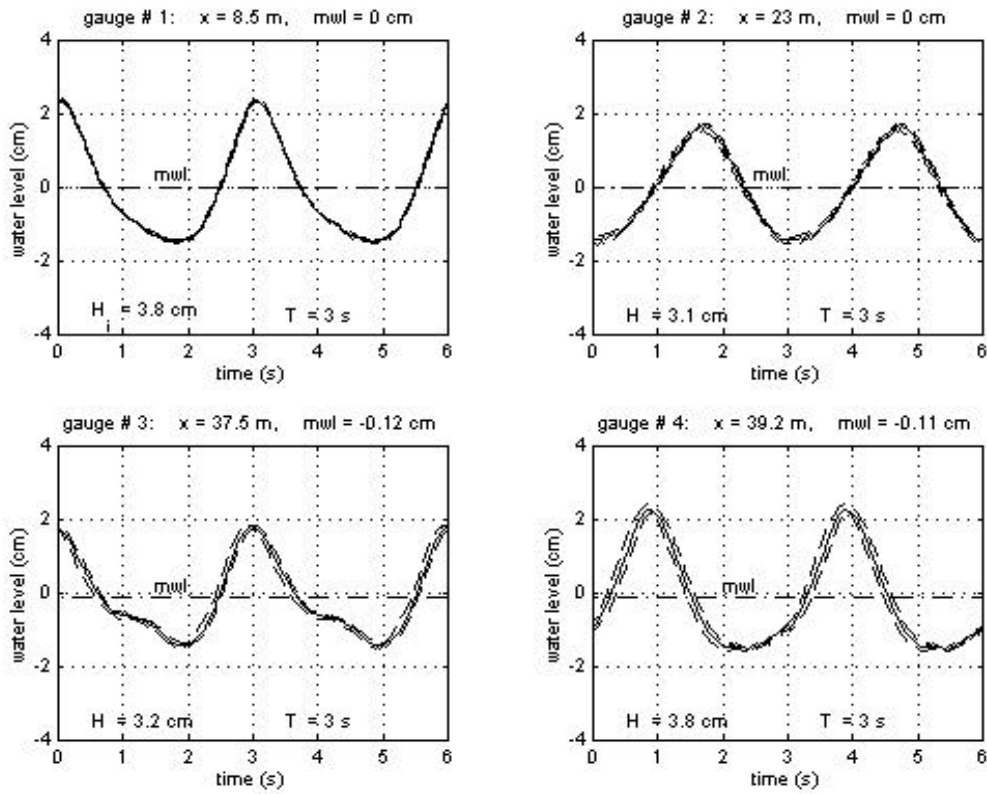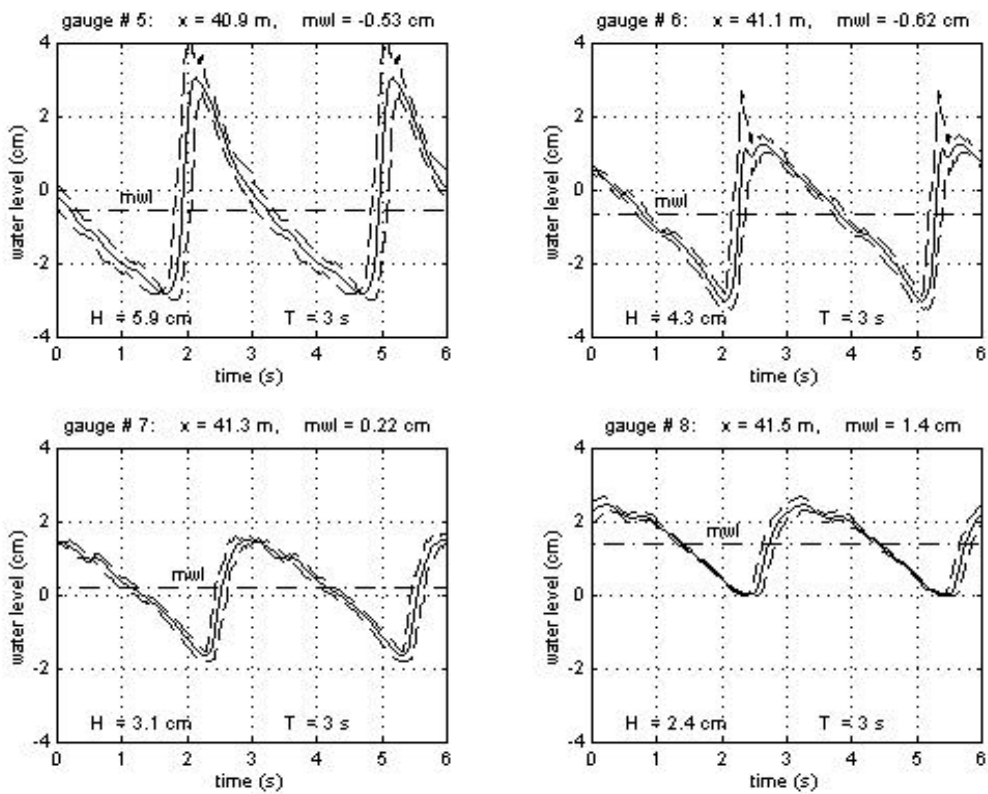
Fig. 4.1a - *Test RH040T30: phase analysis for gauges 1-8. Dashed lines are the envelopes of maximum and minimum levels recorded in all sets of measurements.*
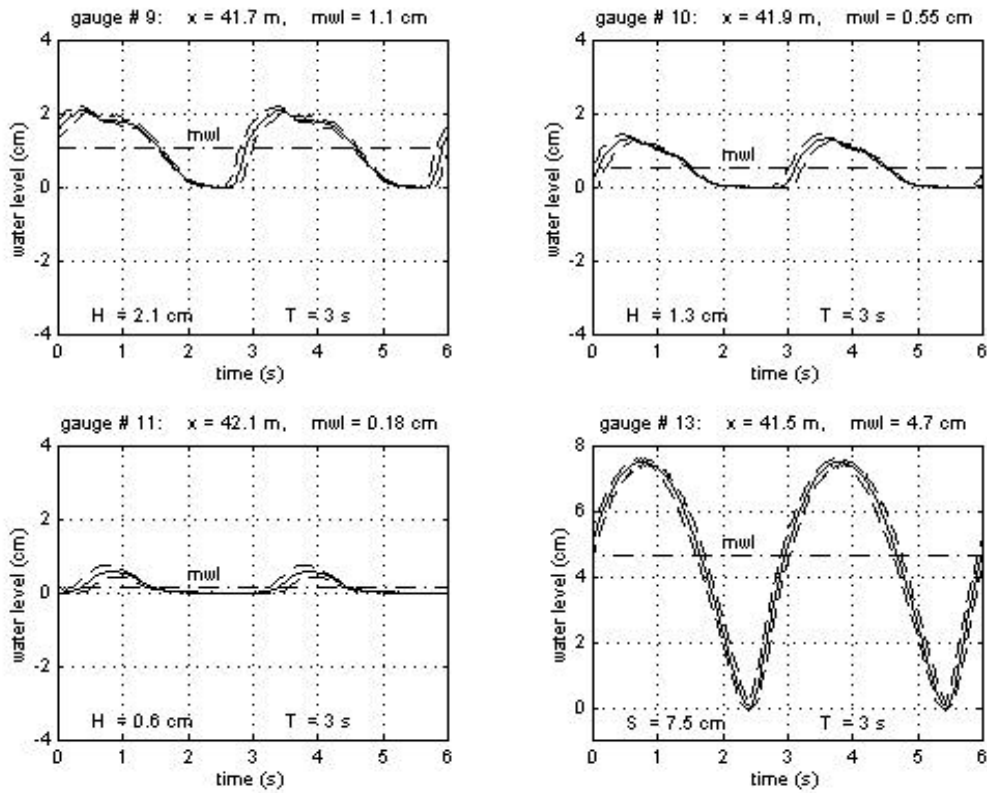
Fig. 4.1b - *Test RH040T30: phase analysis for gauges 9-11 and 13. Dashed lines are the envelopes of maximum and minimum levels recorded in all sets of measurements.*

The **time averages** have been performed through the relation:

$$\bar{\hbar} = \frac{1}{T} \int_0^T \hbar(t) \; dt,$$ 
(4.2)

and **phasic averages** through:

$$\langle \boldsymbol{h} \rangle = \frac{\sum_i \int_{\Delta T_i} \hbar(t)\,dt}{\sum_i \Delta T_i}$$
(4.3)

where $\Delta T_i$ are the time steps during water presence. The operators are linear and can be applied in sequence without rank. Numerical values of time and phasic averages,

maximum and minimum values, and wave heights estimated for each gauge are reported in Tabs. V. Fig. 4.2 shows time and phasic averages, crest and trough spatial envelopes for Test RH040T20 (see Annex 2 for all tests).

Tab. V - *Test RH040T20: water levels evaluated referring to S.W.L. ($h_{max}$ = max values, <$h$>= phasic average values, $\overline{\eta}$ = time average values, $h_{min}$ = min values, H = wave height)*

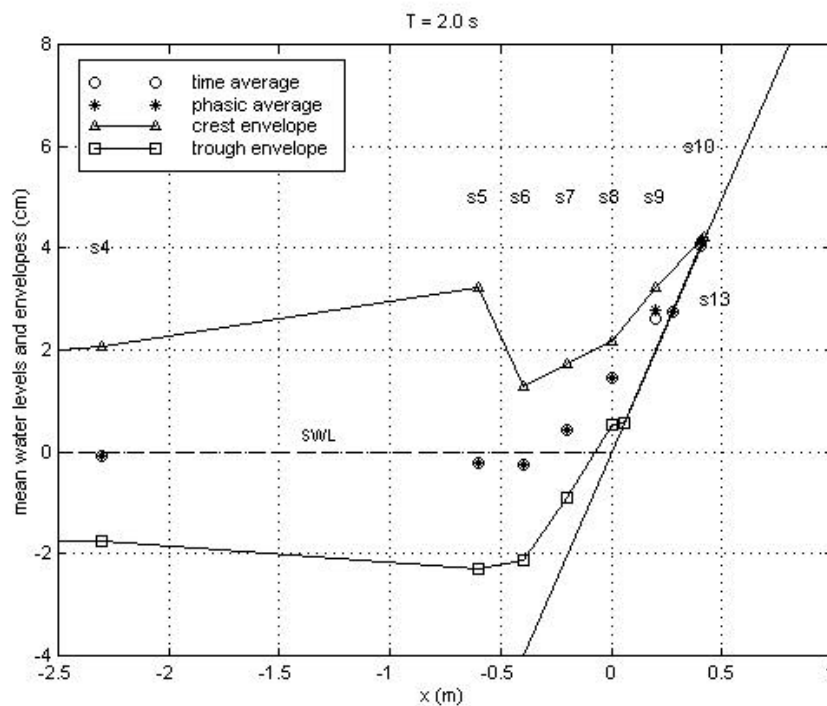| Gauge # | $\eta_{max}$ (cm) | <$\eta$> (cm) | $\overline{\eta}$ (cm) | $\eta_{min}$ (cm) | $H$ (cm) |
|---|---|---|---|---|---|
| **1** | 1.9 | 0.0 | 0.0 | -1.6 | 3.5 |
| **2** | 1.8 | 0.0 | 0.0 | -1.7 | 3.5 |
| **3** | 1.6 | 0.0 | 0.0 | -1.7 | 3.4 |
| **4** | 2.1 | 0.1 | 0.1 | -1.7 | 3.8 |
| **5** | 3.2 | -0.2 | -0.2 | -2.3 | 5.5 |
| **6** | 1.3 | -0.3 | -0.3 | -2.1 | 3.4 |
| **7** | 1.7 | 0.4 | 0.4 | -0.9 | 2.6 |
| **8** | 2.2 | 1.4 | 1.4 | 0.5 | 1.6 |
| **9** | 3.2 | 2.8 | 2.6 | 2.0 | 1.2 |
| **10** | 4.1 | 4.1 | 4.0 | 4.0 | 0.1 |
| **11** | / | / | / | / | / |
| **12** | / | / | / | / | / |



Fig. 4.2 - Test RH040T20: *Set up profiles, crest and trough envelopes.*

Data collected by run up meter S13 permit us to evaluate the run-up ($R_u$), run-down ($R_d$), the amplitude of the swash-zone (*S*), and the time averaged level $\overline{\eta}$ reported in Tab. VI.

Tab. VI - *Regular waves: water levels evaluated at the run up meter referring to S.W.L. ($R_u$ = run up, <**h**>= phasic averaged values, $\overline{\eta}$ = time averaged values, $R_d$ = run down, S = swash amplitude)*

| Test # | $R_u$ (cm) | <η>=$\overline{\eta}$ (cm) | $R_d$ (cm) | S (cm) |
|--------|------------|---------------------------|------------|--------|
| RH040T20 | 4.2 | 2.8 | 0.6 | 3.6 |
| RH040T25 | 5.5 | 3.5 | 0.2 | 5.3 |
| RH040T30 | 7.5 | 4.7 | 0.1 | 7.5 |

In Tab. VII the same results estimated for bichromatic waves are reported (see Annex 3 for more details).

Tab. VII - *Irregular waves: water levels evaluated at the run up meter referring to S.W.L. ($Ru_{max}$ = max run up, $\overline{\eta}$ = time averaged values, $Rd_{min}$ = min run down, S = swash amplitude)*

| Test # | $Ru_{max}$ (cm) | $\overline{\eta}$ (cm) | $Rd_{min}$ (cm) | S (cm) |
|--------|-----------------|------------------------|-----------------|--------|
| IH040T20 | 4.2 | 2.2 | -0.2 | 4.4 |
| IH040T25 | 5.1 | 1.9 | -1.4 | 6.5 |
| IH040T30 | 6.9 | 2.7 | -2.5 | 9.4 |

## 4.2  Mass fluxes

On the base of phase averaged surface oscillations $h(t)$ collected at gauges located in the surf zone mass, flux has been estimated in the zero section by the continuity equation:

$$uh|_{x=0} = \frac{\partial V}{\partial t} \qquad (4.4)$$

where *uh* is the mass flux trough the section *x=0*, $h = \mathbf{h} + d$ the sum of water level (referred to SWL) and still water depth, and *V* the volume included between the section under evaluation and the instantaneous coastal line.

The volume *V* has been estimated using the phase-phasic averaged levels recorded by gauges *S8-S12* assuming a plane surface between two successive gauges :

$$V(t) = \frac{\Delta x}{2} \left[ \sum_{i=8}^{12} 2h_i(t) - h_8 - h_{12} \right] \qquad 0 \pounds t < T \qquad (4.5)$$

where $\Delta x$ is the constant horizontal distance between two successive gauges, equal to 20 cm (Fig. 4.3).
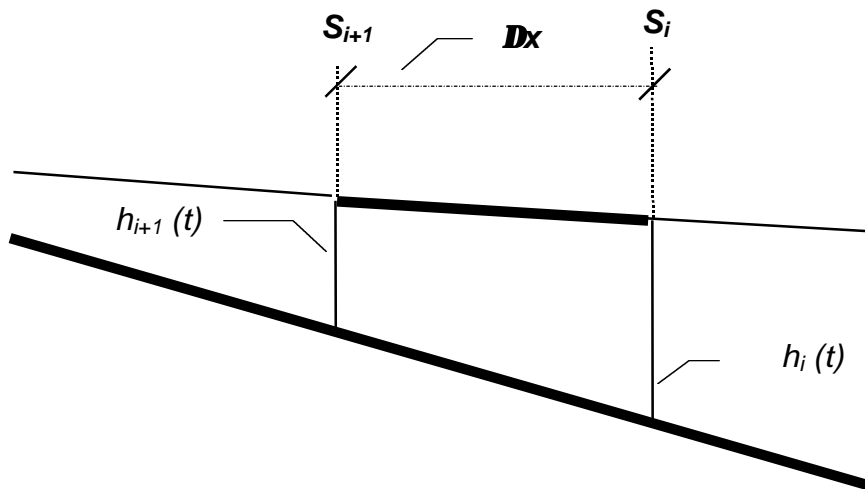


Fig. 4.3 - *Sketch for flux evaluation.*

The time series *V(t)* were filtered eliminating frequency oscillations $f > 2$ Hz. Fig. 4.4 shows flux analyses for regular test RH040T20 ; the analyses for all tests are reported in Annex 4.
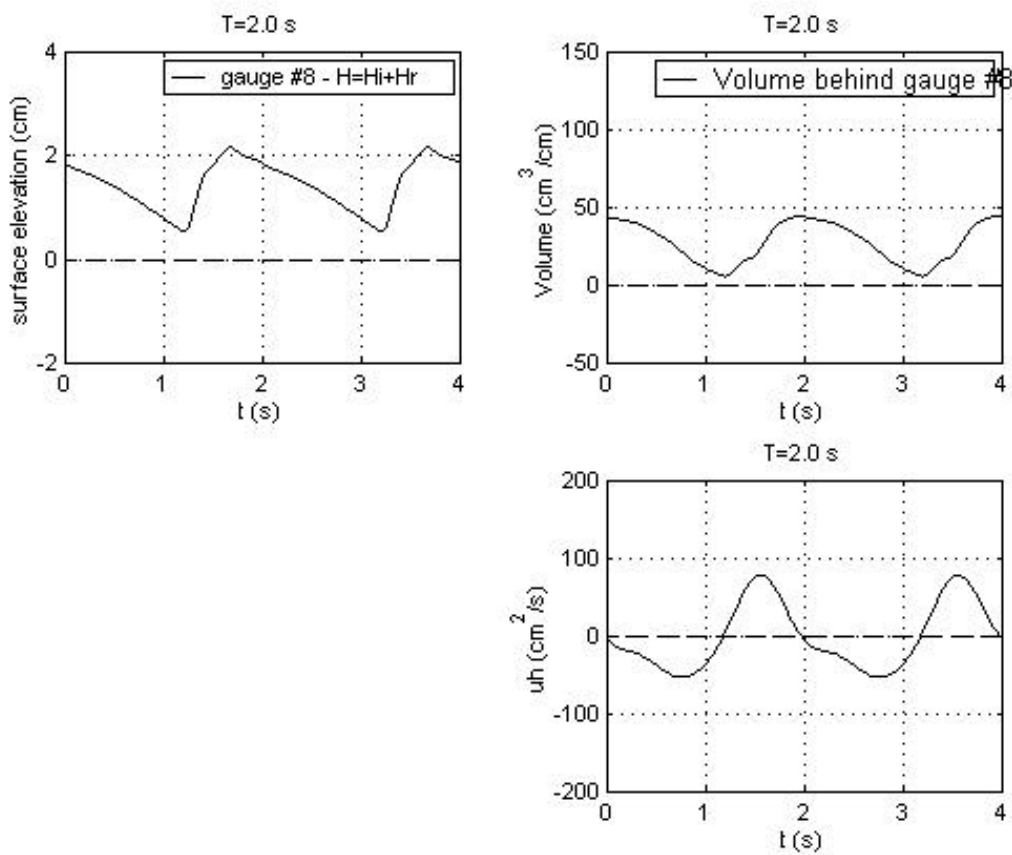
Fig. 4.4 - *Test RH040T20: flux analysis in the zero section (gauge S8).*

## 4.3 Fluid velocities

Velocity measurements along three vertical sections (the *lower*, *mid* and *upper* sections) in the inner region and swash zone were collected (Fig. 4.5). LDV was directed along the three sections in successive steps of 1 mm, starting at 0.5 mm from the bottom. Many runs for each regular wave were necessary in order to cover the whole vertical measure for each section. The upper section in the test RH040T20 was fixed at  $x$=+5 cm rather than $x$ =+20 cm, because stream thickness was not significant in section *S9*.
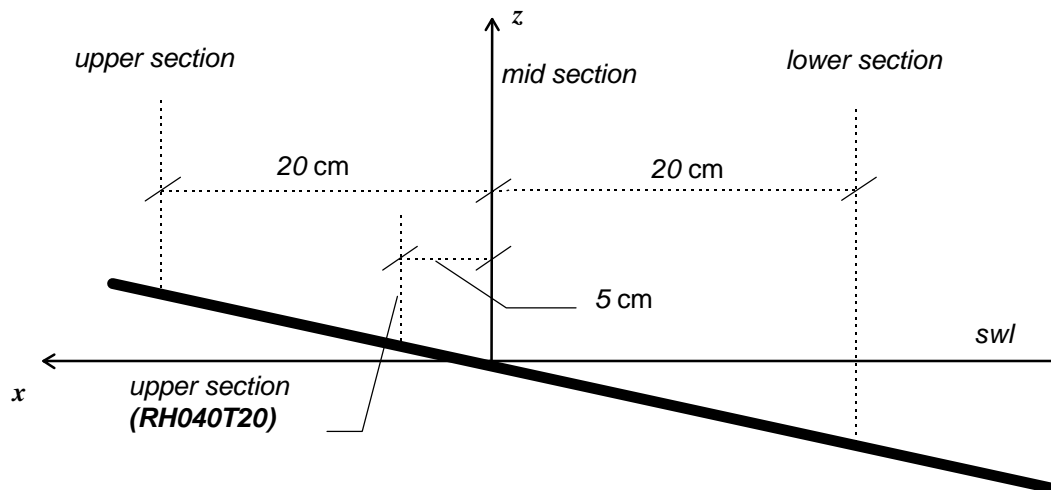
Fig. 4.5 - *Measure sections for velocity measurements.*

The velocity profiles have been calculated as phase-phasic averages over a cycle in time intervals at 31.5-61.5 s, 30.4-62.8 s and 31.5-70.5 s for all regular waves :

$$u(t) = \frac{\sum_{k=0}^{N-1} \hat{u}(t+kT)f(t+kT)}{\sum_{k=0}^{N-1} f(t+kT)} \qquad 0 \pounds t < T \tag{4.6}$$

where $\hat{u}(t)$ is the instantaneous fluid velocity and $f$ is the Boolean phasic function equal to 1 if the signal is locked otherwise equal to zero ; note that $f$ is not a simple indicator of water presence, even though it is null in the absence of water. An estimation using a weighted (phase-phasic) average with weights proportional to the square root of the difference between the run-up during the cycle and the mean run-up has also been carried out, in order to filter possible disturbances and to detect possible modulations in turbulence. The results are nearly the same as the results obtained without weighting the single cycle contribution, confirming negligible spurious effects in the chosen time interval analysis. Fig. 4.6, 4.7, and 4.8 show profiles for the three sections for test RH040T20, with time step = T/8; the whole set of analyses is reported in Annex 6.
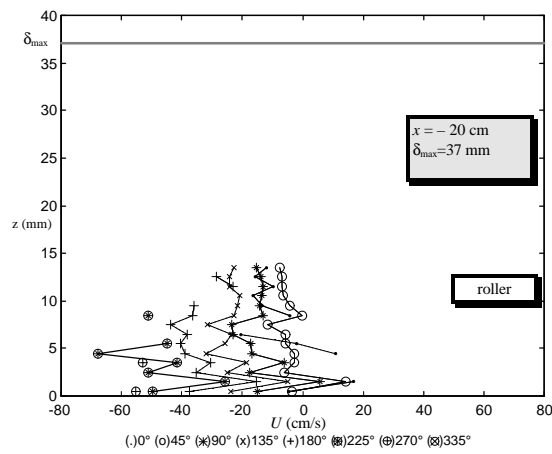
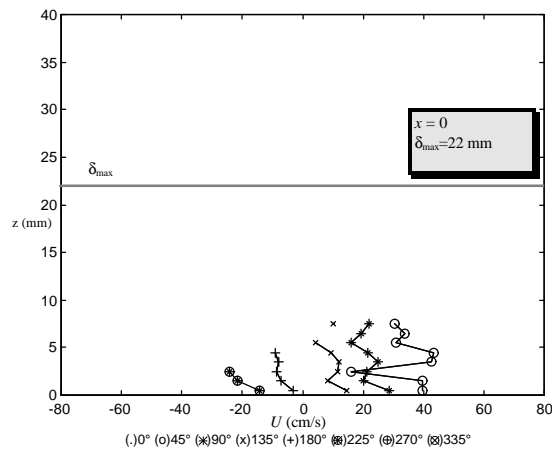Fig. 4.6 - *RH040T20: velocity profiles in the lower section.*



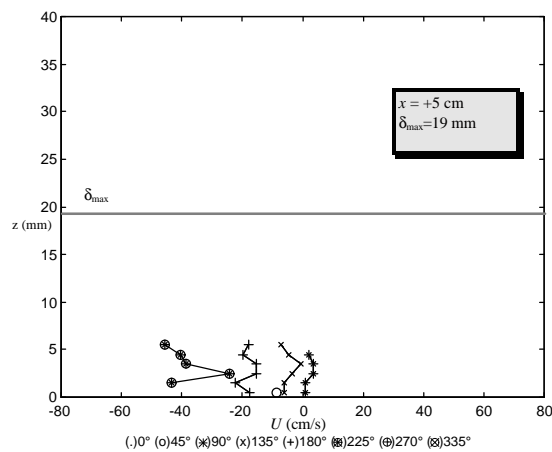Fig. 4.7 - *RH040T20: velocity profiles in the mid section.*



Fig. 4.8 - *RH040T20: velocity profiles in the upper section.*

Velocity profiles are irregular in the roller sections, as a consequence of the short time analysis in respect to the roller fluctuations; they are quite regular and flat in the other sections, with some evident boundary effects in the mid-section for the 3.0 s period wave.

## 4.4 Turbulence

The turbulence component along the main flow direction has been evaluated filtering the raw signal by subtracting its mobile average (Fig. 4.11).

$$u'(t) = (\hat{u}(t) - \tilde{u}(t)) \tag{4.7}$$

where $\tilde{u}(t)$ is the mobile average of the instantaneous fluid velocity. The mobile average time interval is equal to 0.1 s and has been chosen observing the spectra of the signal and separating the low frequency and the relatively high frequency (>10Hz) contributions. Note that the acquisition rate is equal to 100 Hz, allowing for the detection of a maximum frequency component equal to 50 Hz.

One of the component of the Reynolds stress, i.e. the variance of the velocity parallel to the bottom, is expressed as the square of the instantaneous velocity fluctuation:

$$u'^2(t) = (\hat{u}(t) - \tilde{u}(t))^2 \tag{4.8}$$

The result has been phase-phasic averaged obtaining the turbulent fluctuations cycle at different height levels over the bed :

$$\left\langle u'^2(t) \right\rangle = \frac{\sum_{k=0}^{N-1} (\hat{u}(t+kT) - \tilde{u}(t+kT))^2 f(t+kT)}{\sum_{k=0}^{N-1} f(t+kT)} \qquad 0 \pounds t < T \tag{4.9}$$
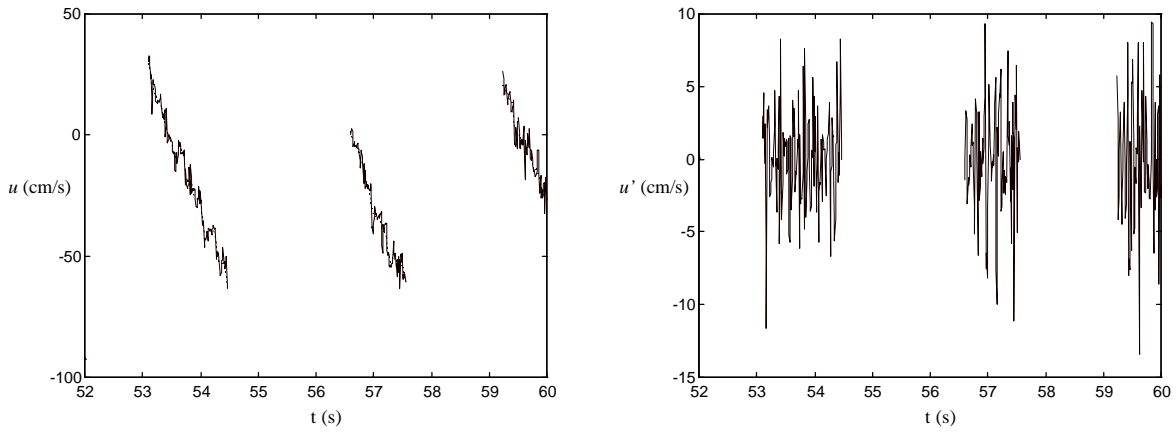
Fig. 4.9 - *Test RH040T30: instantaneous velocity and turbulence fluctuations in the lower section, z = 2.5* mm

Two simple estimators of the turbulence cycle, the mean value over a cycle and its standard deviation (non dimensional respect to the mean value over a cycle), are reported in Annex 6, calculated as:

$$E \propto \overline{u'^2} = \frac{\int\limits_0^{NT} \left(\hat{u}(t) - \tilde{u}(t)\right)^2 f(t)dt}{\int\limits_0^{NT} f(t)dt} \tag{4.10}$$

$$u'^2_{STD} \Big/ \sqrt{\overline{u'^2}} = \sqrt{\frac{\int\limits_0^{NT} \left[\left(\hat{u}(t) - \tilde{u}(t)\right)^2 - \overline{u'^2}\right]^2 f(t)dt}{\overline{u'^2}}} \tag{4.11}$$

By observing the results for the three different sections it seems that the maxima of the turbulent energy are not located near the bottom but in the upper part of the flowing layer (lower section) and in the mid part for the two other sections. Note that the results are limited at best to 60% of the maximum local layer thickness, moreover with a limited persistence time of the signal for the higher measurement points. Turbulence variation over a cycle is generally higher at the mean level of the measuring window.

Turbulence level near the bottom can be used as reference for bottom stress computation. The plots of turbulence level at the first point (z=0.5 mm) over the bed show a time lag of the maxima in the three measuring sections during upwash, with the secondary maxima corresponding to the backwash. The mean near bottom turbulence level is higher in the mid-section.

## 4.5 Summary and further tests

An experimental investigation on surf and swash zone of a 1:10 sloping beach has been presented. It has been possible to evaluate the free surface elevation in several sections in surf and swash zones, fluid velocity in three sections and mass fluxes; the data have been elaborated obtaining turbulence estimation in several points in three sections.

The $2^{nd}$ year SASME Project schedule refers to experiments on a 1:5 fixed impermeable beach, with the same set of regular and bichromatic waves.

## 5. Acknowledgements

## 6. References

Baldock, T.E., Holmes, P. e Horn, D.P., (1997). "Low frequency swash motion induced by wave grouping", *Coastal Eng.*, 32, 197-222.

Battjes, J.A., (1974). "Surf similarity", *Proc. of 14$^{th}$ Int. Conf. on Coastal Eng.*, 1419-1438.

Battjes, J.A. and Roos, A., (1976). "Characteristics of flow in run-up of periodic waves", *Proc. of 15$^{th}$ Int. Conf. on Coastal Eng.*,781-795.

Bowen, A.J., Inman, D.L. and Simmons, V.P. (1968). "Wave set-down and set-up", *J. Geophys. Res.,* 73, 2569-2577.

Fredsøe, J. and Deigaard, R., (1992). *Mechanics of Coastal Sediment Transport*, World Scientific Publishing, Singapore.

Gourlay, M.R., (1992). "Wave set-up, wave run-up and beach water table: Interaction between surf-zone hydraulics and groundwater hydraulics", *Coastal Eng.*, 17, 93-144.

Hansen, J.B. and Svendsen, I.A., (1979). "Regular waves in shoaling water-experimental data. Tech. Univ. Denmark, Inst. Hydrodyn. and Hydr. Eng., Lyngby. Series Paper No. 21.

Kriebel, D.L., (1994). "Swash-zone wave characteristics from supertank", *Proc. of 24th Int. Conf. on Coastal Eng.*, 2207-2221.

Stive, M.J.F., (1985). "A scale comparison of waves breaking on a beach", *Coastal Eng.*, 9, 151-158.

Van Dorn, W.G., (1976). "Set-up and run-up in shoaling breakers", *Proc. of 15th Int. Conf. on Coastal Eng.*, 738-751.

Van Dorn, W.G., (1978). "Breaking invariants in shoaling waves", *J. Geophys. Res.,* 83, 2981-2988.

## Annex 1

Reference system, calibration of wave gauges, surface roughness profiles of the bottom

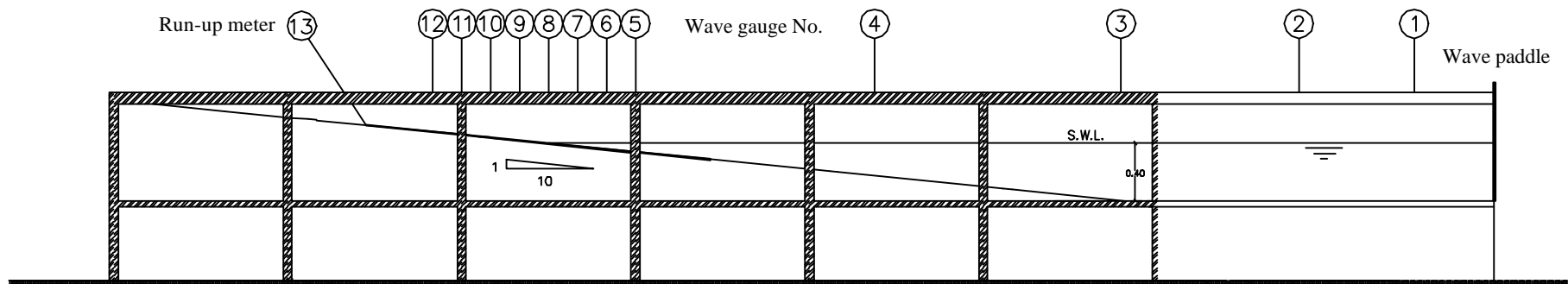| Still water level (cm) | 8 | 6 | 4 | 2 | 0 | −2 | −4 | −6 | −30 | −40 | −40 | −40 |
|---|---|---|---|---|---|---|---|---|---|---|---|---|
| Distance from the paddle (m) | 42.3 | 42.1 | 41.9 | 41.7 | 41.5 | 41.3 | 41.1 | 40.9 | 39.2 | 37.5 | 23.00 | 8.50 |



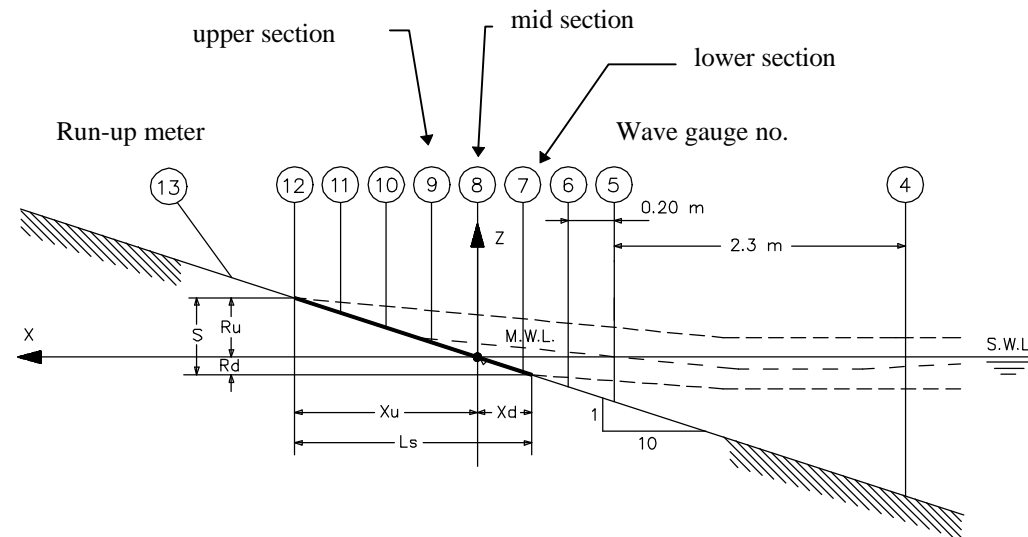**Fig.A1-1** *Experimental set-up and location of the wave gauges.*

**Fig.A1-2** *Reference system and location of the wave gauges in the surf and swash zone.*
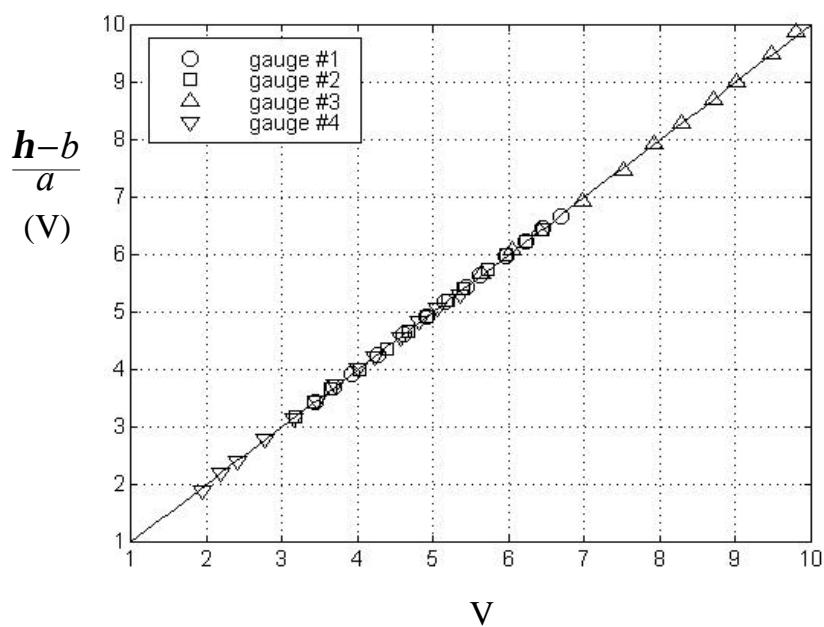
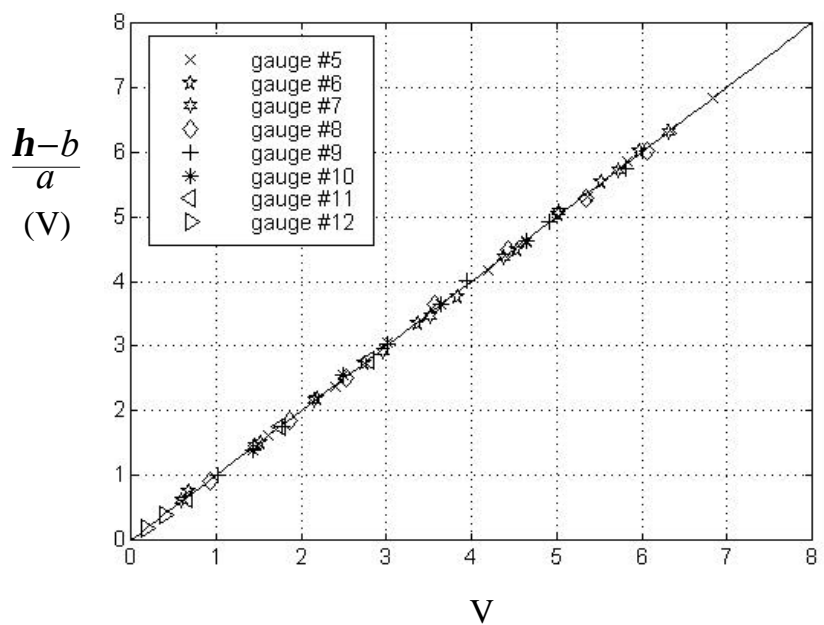**Fig.A1-3** *Calibration of gauges 1-4.*



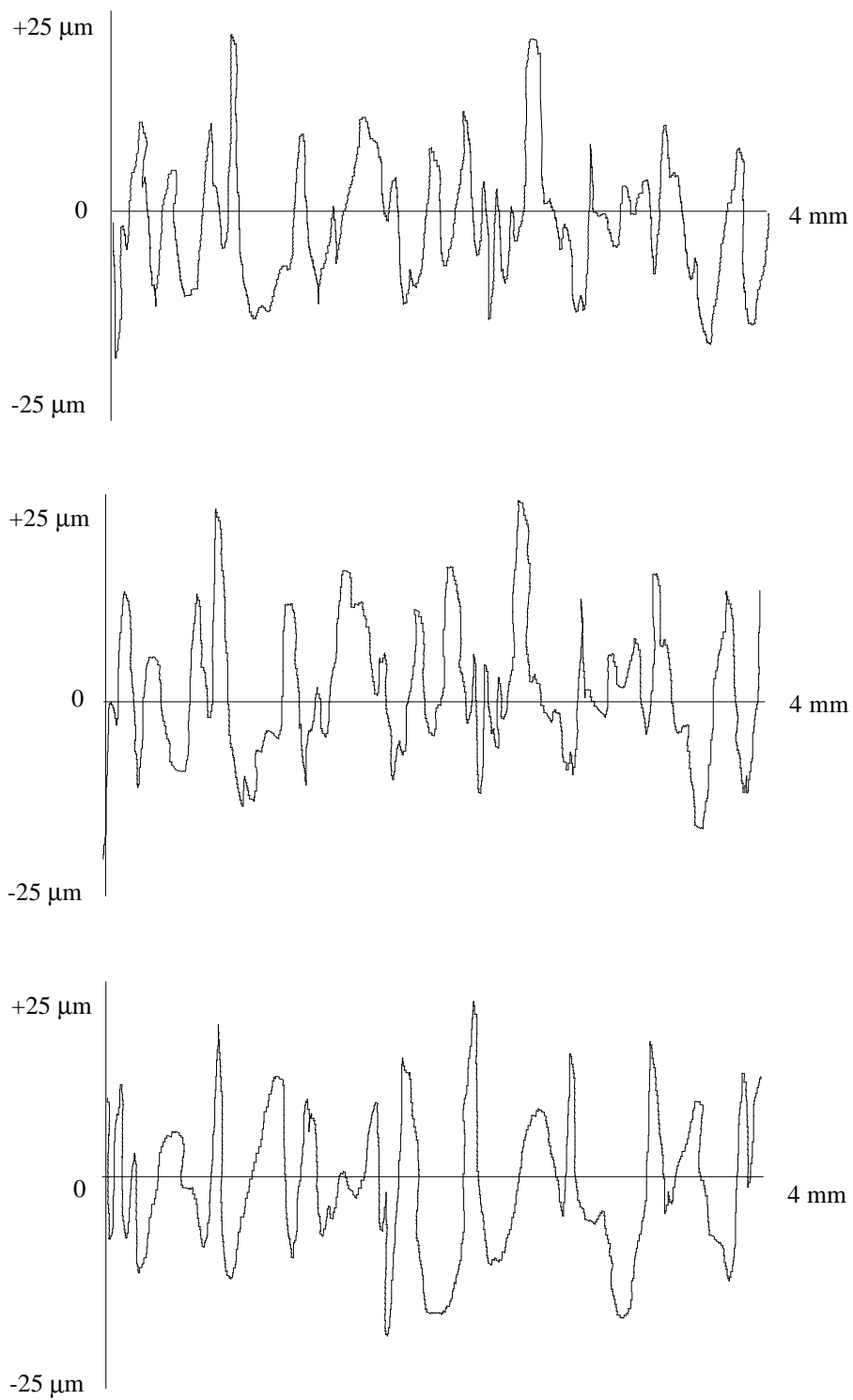**Fig.A1-4** *Calibration of gauges 5-12.*

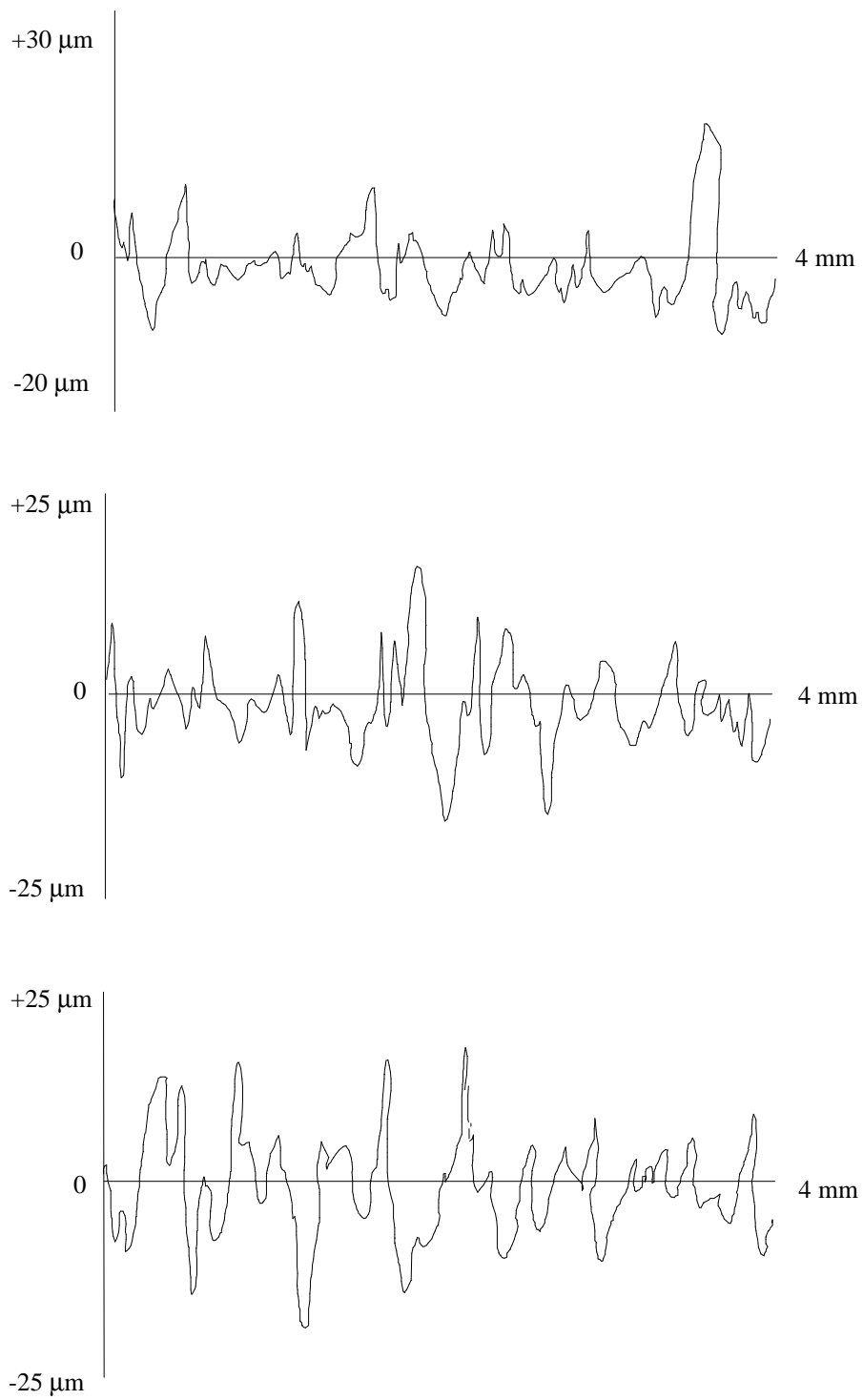**Fig.A1-5** *Concrete bottom surface profiles. Specimen A.*

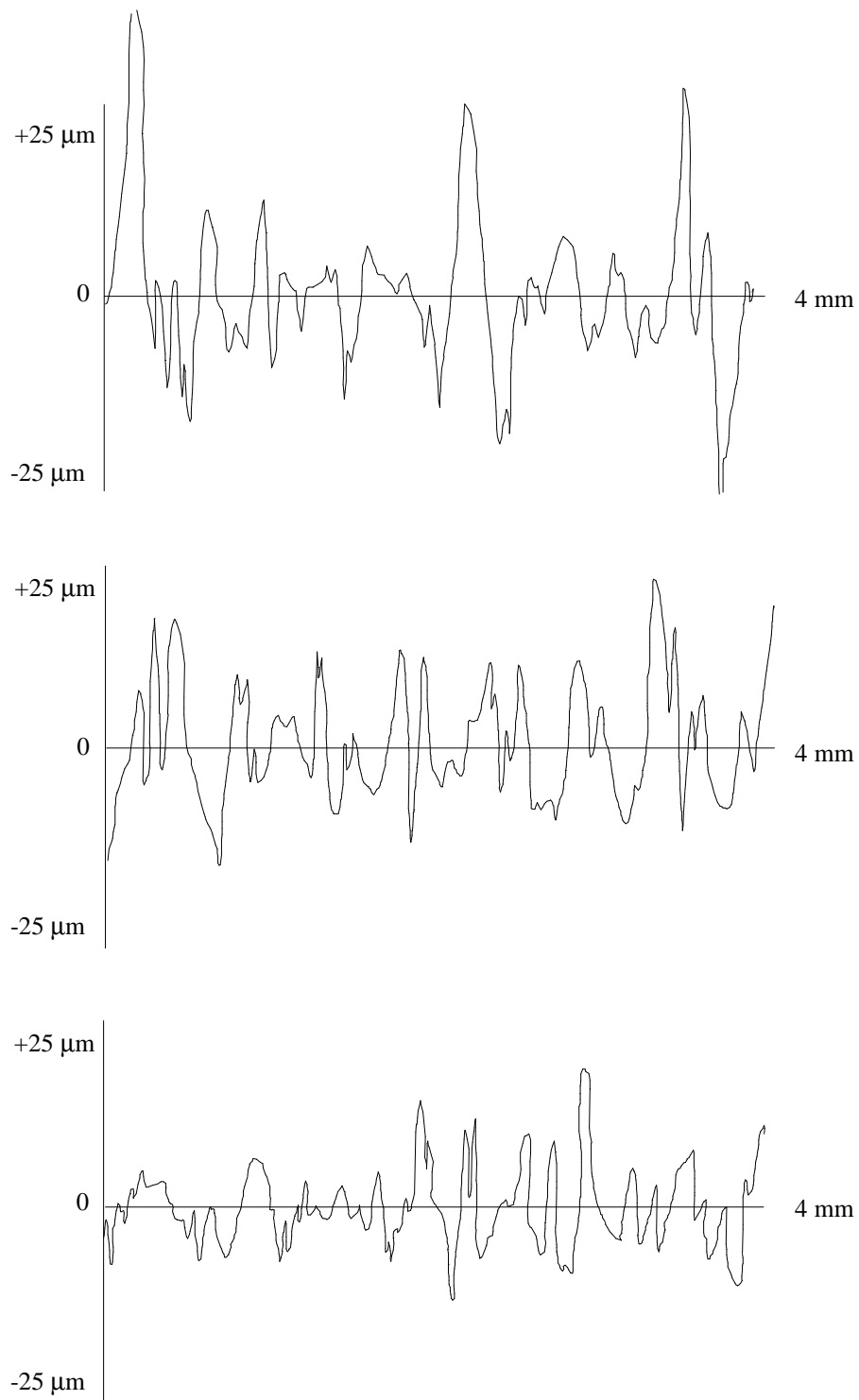**Fig.A1-6** *Concrete bottom surface profiles. Specimen B.*

**Fig.A1-7** *Concrete bottom surface profiles. Specimen C.*

# Annex 2

Phase analysis of regular wave tests:

- RH040T20
- RH040T25
- RH040T30

**Tab.A2-I** *Test RH040T20: water levels evaluated referring to S.W.L. ($\mathbf{h}_{max}$ = max values, $<\mathbf{h}>$ = phasic average values, $\overline{\eta}$ = time average values, $\mathbf{h}_{min}$ = min values, H = wave height)*

| Gauge # | $\eta_{max}$ (cm) | $<\eta>$ (cm) | $\overline{\eta}$ (cm) | $\eta_{min}$ (cm) | $H$ (cm) |
|---|---|---|---|---|---|
| **1** | 1.9 | 0.0 | 0.0 | -1.6 | 3.5 |
| **2** | 1.8 | 0.0 | 0.0 | -1.7 | 3.5 |
| **3** | 1.6 | 0.0 | 0.0 | -1.7 | 3.4 |
| **4** | 2.1 | 0.1 | 0.1 | -1.7 | 3.8 |
| **5** | 3.2 | -0.2 | -0.2 | -2.3 | 5.5 |
| **6** | 1.3 | -0.3 | -0.3 | -2.1 | 3.4 |
| **7** | 1.7 | 0.4 | 0.4 | -0.9 | 2.6 |
| **8** | 2.2 | 1.4 | 1.4 | 0.5 | 1.6 |
| **9** | 3.2 | 2.8 | 2.6 | 2.0 | 1.2 |
| **10** | 4.1 | 4.1 | 4.0 | 4.0 | 0.1 |
| **11** | / | / | / | / | / |
| **12** | / | / | / | / | / |

**Tab.A2-II** *Test RH040T25: for caption see Tab. A2-I.*

| Gauge # | $\eta_{max}$ (cm) | $<\eta>$ (cm) | $\overline{\eta}$ (cm) | $\eta_{min}$ (cm) | H (cm) |
|---|---|---|---|---|---|
| **1** | 2 | 0.0 | 0.0 | -1.4 | 3.4 |
| **2** | 1.9 | 0.0 | 0.0 | -1.5 | 3.4 |
| **3** | 1.9 | 0.0 | 0.0 | -1.4 | 3.3 |
| **4** | 2.2 | -0.1 | -0.1 | -1.7 | 3.9 |
| **5** | 2.6 | -0.3 | -0.3 | -2.8 | 5.4 |
| **6** | 2.6 | -0.3 | -0.3 | -2.3 | 4.9 |
| **7** | 1.6 | 0.3 | 0.3 | -1.2 | 2.8 |
| **8** | 2.1 | 1.3 | 1.3 | 0.2 | 1.9 |
| **9** | 3.6 | 3.1 | 2.8 | 2.0 | 1.6 |
| **10** | 4.7 | 4.5 | 4.3 | 4.0 | 0.7 |
| **11** | / | / | / | / | / |
| **12** | / | / | / | / | / |

**Tab.A2-III** *Test RH040T30: for caption see Tab. A2-I.*

| Gauge # | $\eta_{max}$ (cm) | $<\eta>$ (cm) | $\overline{\eta}$ (cm) | $\eta_{min}$ (cm) | $H$ (cm) |
|---|---|---|---|---|---|
| **1** | 2.4 | 0.0 | 0.0 | -1.5 | 3.8 |
| **2** | 1.7 | 0.0 | 0.0 | -1.4 | 3.1 |
| **3** | 1.8 | 0.0 | 0.0 | -1.4 | 3.2 |
| **4** | 2.3 | -0.1 | -0.1 | -1.5 | 3.8 |
| **5** | 3.1 | -0.5 | -0.5 | -2.8 | 5.9 |
| **6** | 1.2 | -0.6 | -0.6 | -3 | 4.3 |
| **7** | 1.5 | 0.2 | 0.2 | -1.6 | 3.1 |
| **8** | 2.5 | 1.4 | 1.4 | 0.0 | 2.4 |
| **9** | 4.1 | 3.4 | 3.1 | 2.0 | 2.1 |
| **10** | 5.3 | 4.8 | 4.6 | 4.0 | 1.3 |
| **11** | 6.6 | 6.4 | 6.2 | 6.0 | 0.6 |
| **12** | / | / | / | / | / |

**Tab.A2-IV**- *Regular waves: water levels evaluated at the run up meter referring to S.W.L. ($R_u$ = run up, $<h>$= phasic averaged values, $\overline{\eta}$ = time averaged values, $R_d$ = run down, S = swash amplitude)*

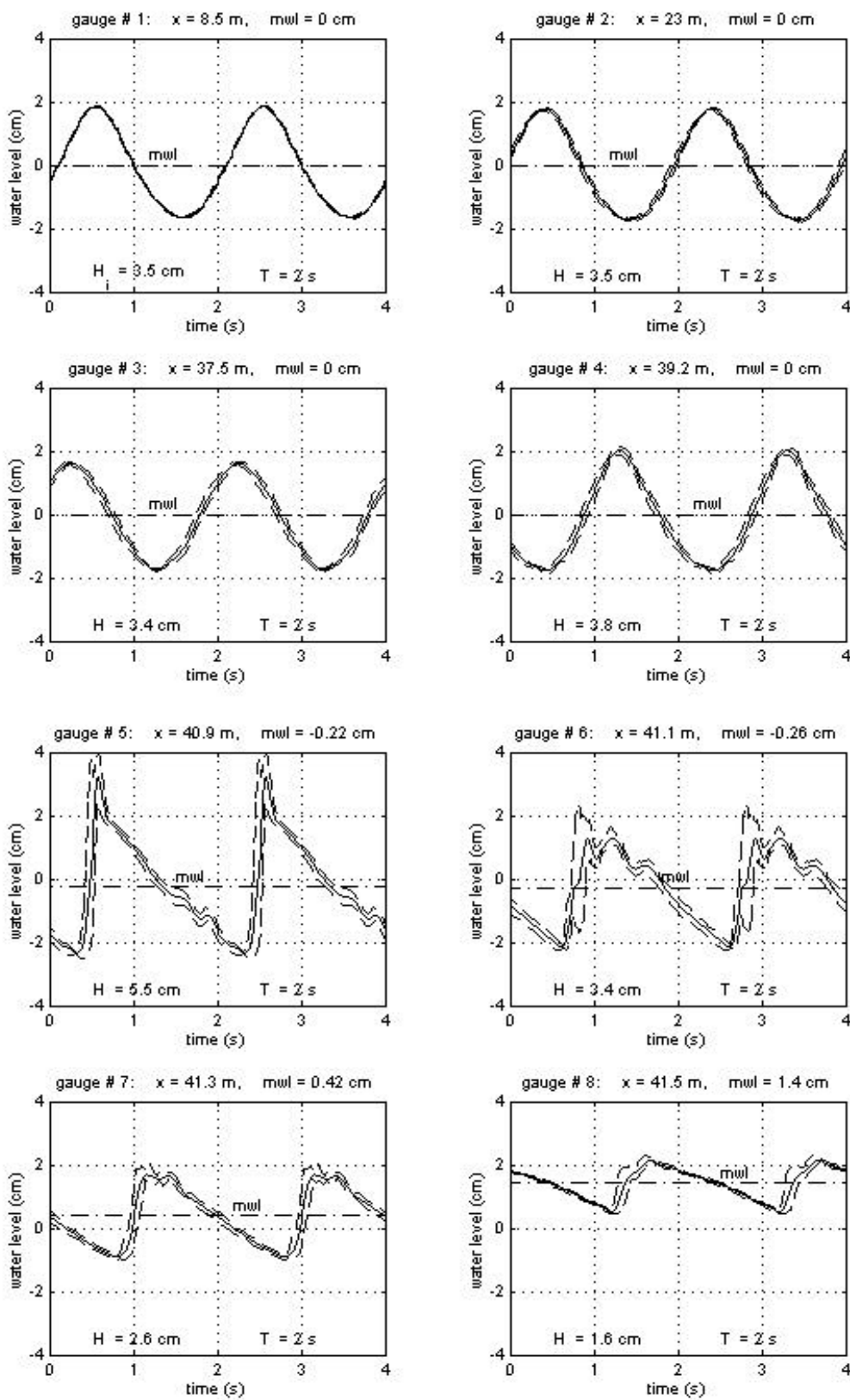| Test # | $R_u$ (cm) | $<\eta>=\overline{\eta}$ (cm) | $R_d$ (cm) | $S$ (cm) |
|---|---|---|---|---|
| *RH040T20* | 4.2 | 2.8 | 0.6 | 3.6 |
| *RH040T25* | 5.5 | 3.5 | 0.2 | 5.3 |
| *RH040T30* | 7.5 | 4.7 | 0.1 | 7.5 |

**Fig.A2-1. Test RH040T20:** *phase analysis of gauges 1-8. Dashed lines are the envelopes of maximum and minimum levels recorded in all sets of measurements.*
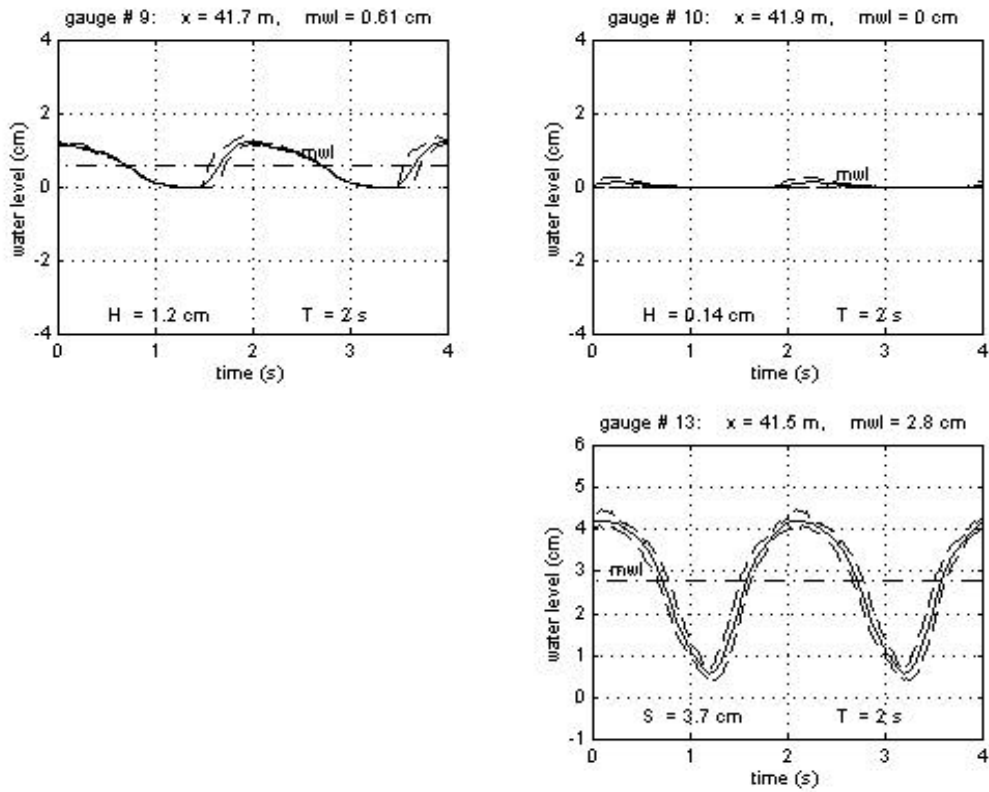
**Fig.A2-2. Test RH040T20***: phase analysis of gauges 9-10 and 13. Dashed lines are envelopes of maximum and minimum levels recorded in all sets of measurements.*



**Fig.A2-3. Test RH040T20:** *Set up profiles, crest and trough envelopes.*

**Fig.A2-4. Test RH040T25**: *phase analysis of gauges 1-8. Dashed lines are the envelopes of maximum and minimum levels recorded in all sets of measurements.*

**Fig.A2-5. Test RH040T25**: *phase analysis of gauges 9-10 and 13. Dashed lines are the envelopes of maximum and minimum levels recorded in all sets of measurements.*
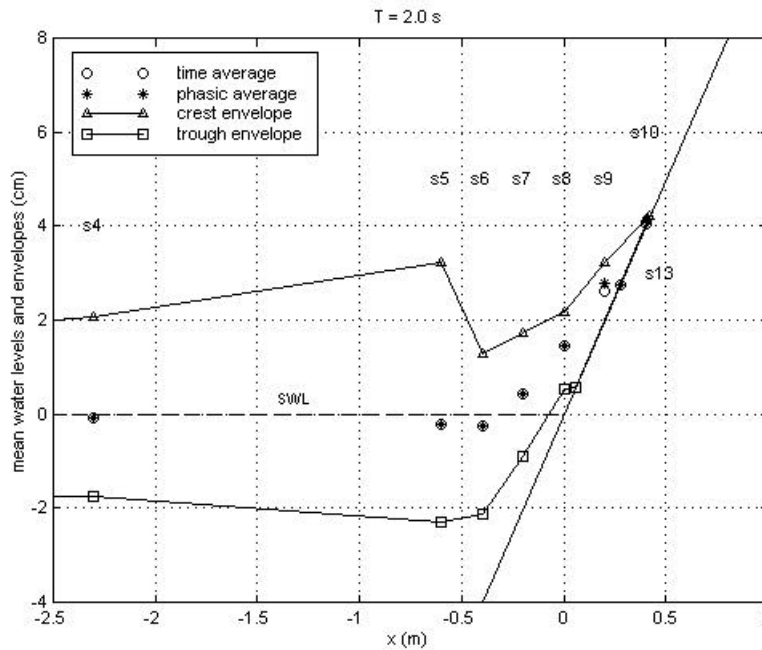


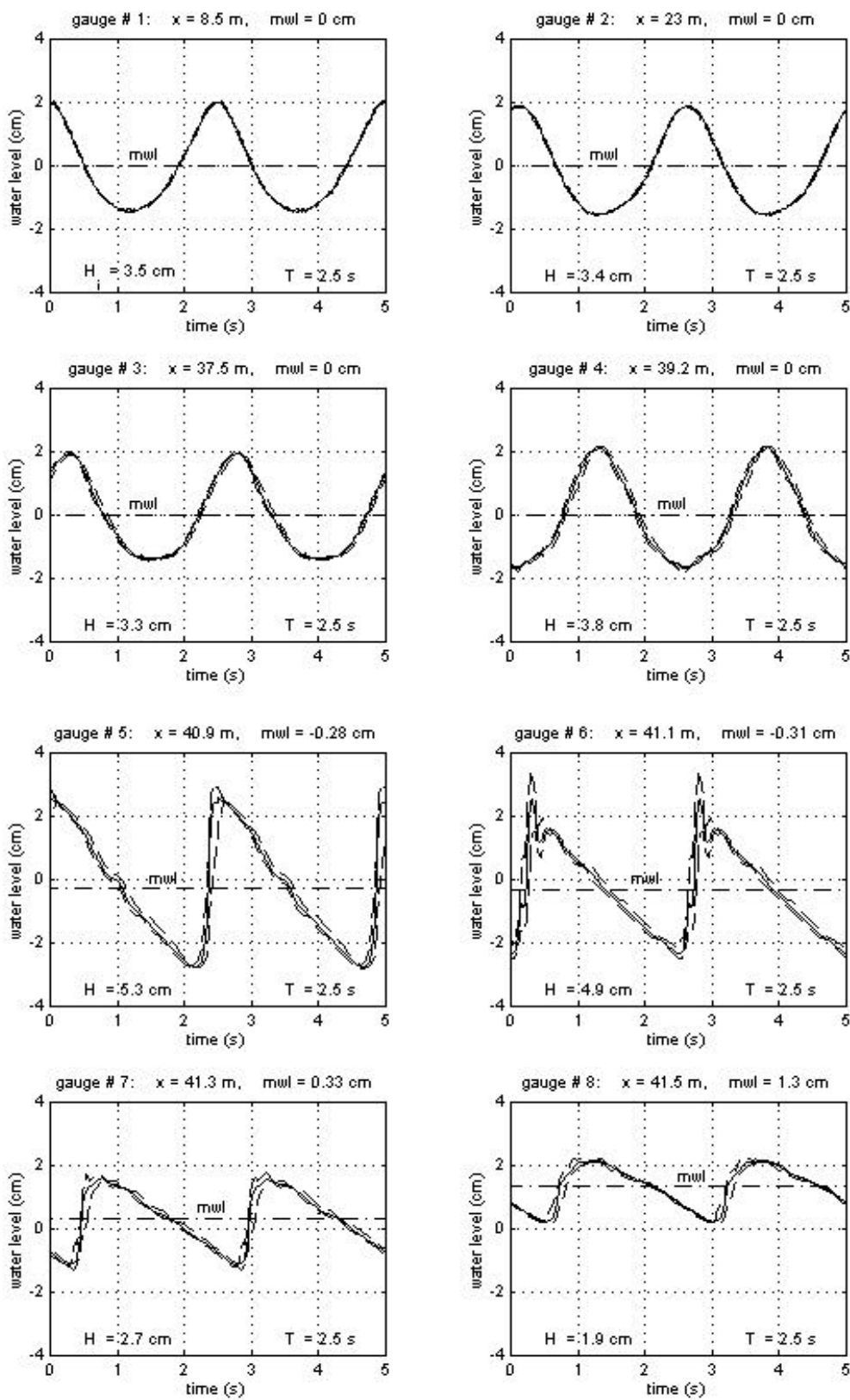**Fig. A2-6. Test RH040T25:** *Set up profiles, crest and trough envelopes.*

**Fig.A2-7. Test RH040T30**: *phase analysis for gauges 1-8. Dashed lines are the envelopes of maximum and minimum levels recorded in all sets of measurements.*
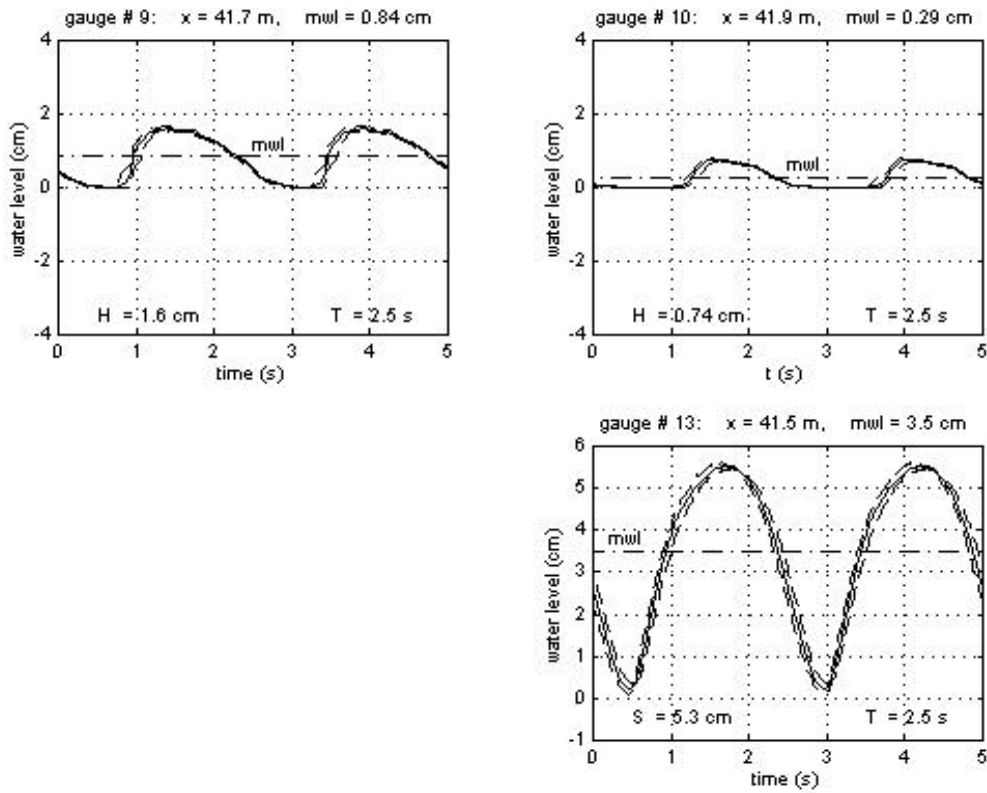
**Fig.A2-8. Test RH040T30**: *phase analysis for gauges 9-11 and 13. Dashed lines are the envelopes of maximum and minimum levels recorded in all sets of measurements.*
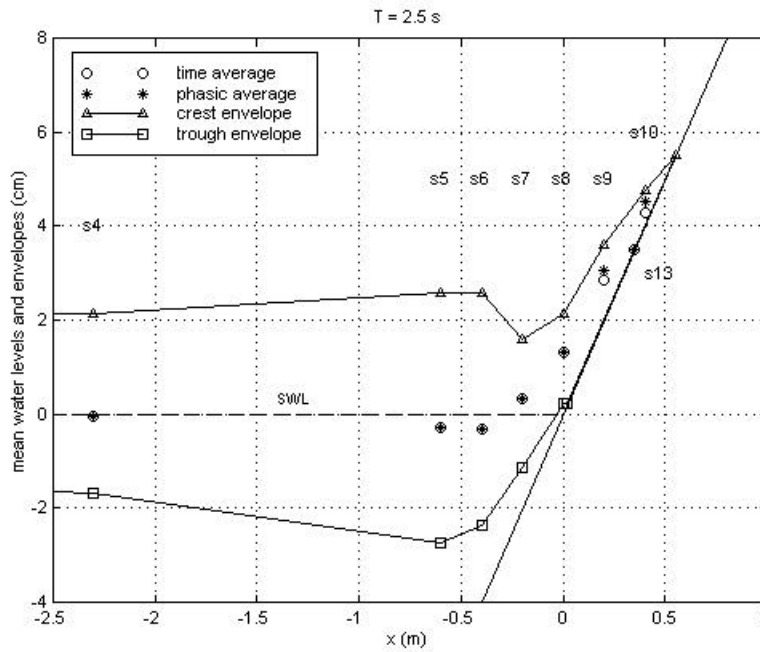


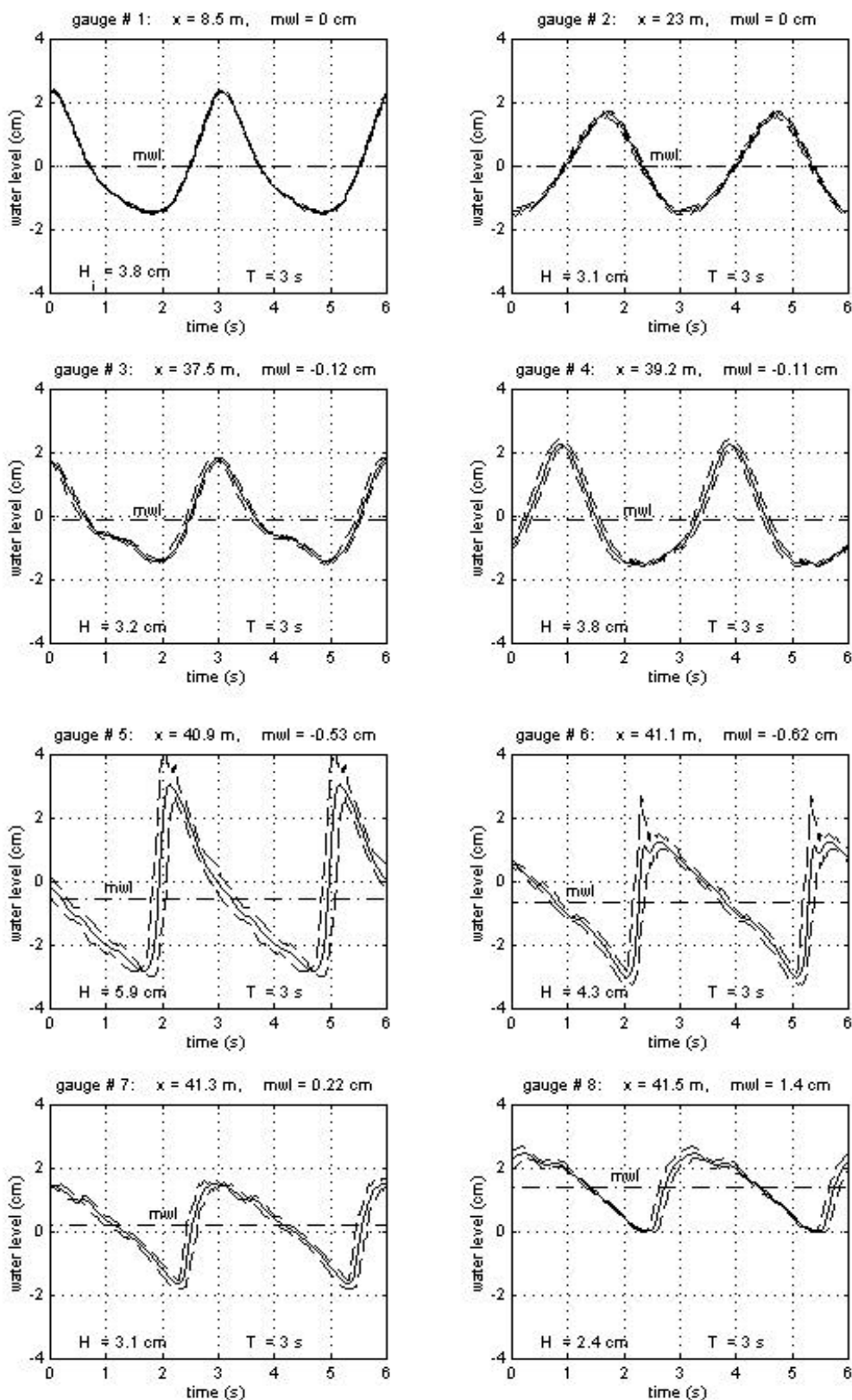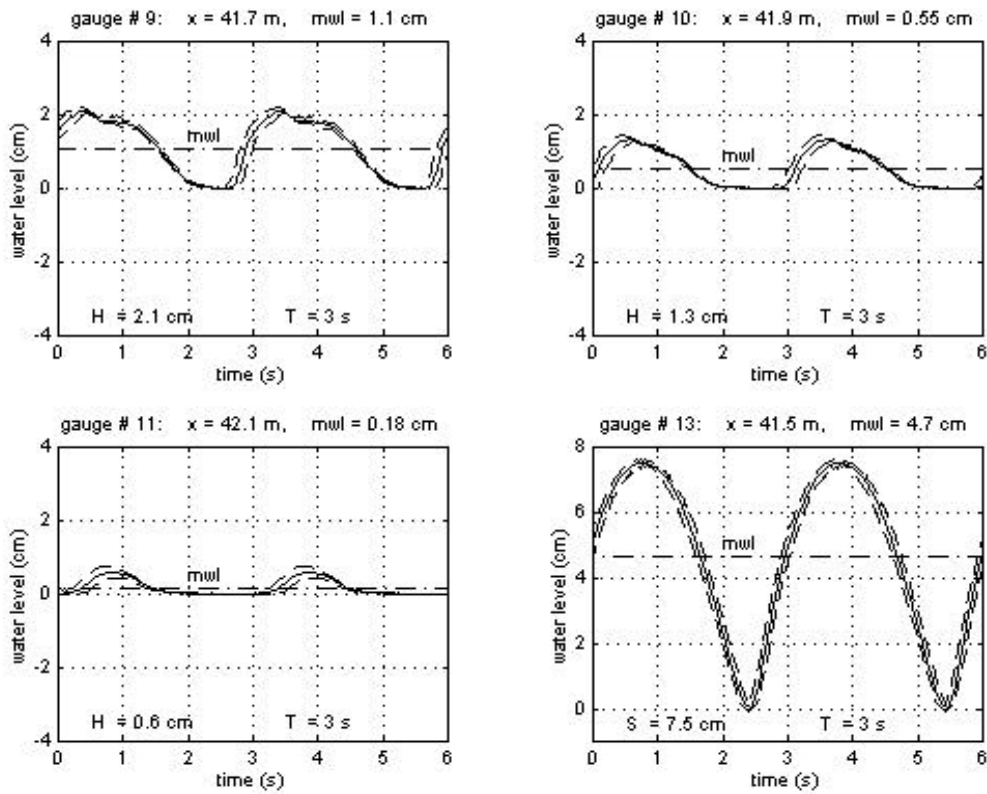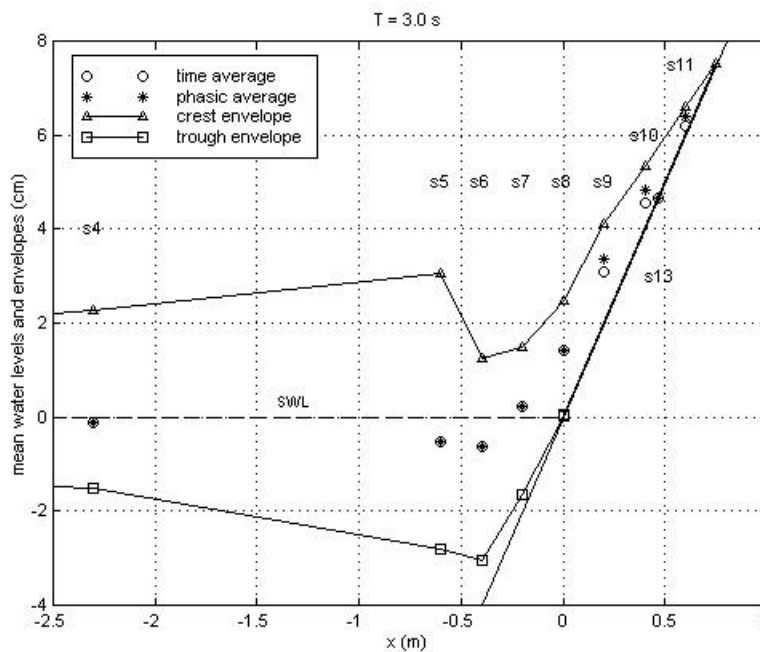**Fig. A2-9. Test RH040T30**: *Set up profiles, crest and trough envelopes.*

# Annex 3

Analysis of irregular wave tests:

- IH040T20
- IH040T25
- IH040T30

**Tab. A3-1.** - *Irregular waves: water levels evaluated at the run up meter referring to S.W.L. ($Ru_{max}$ = max run up, $\overline{\eta}$ = time averaged values, $Rd_{min}$ = min run down, S = swash amplitude)*

| Test # | $Ru_{max}$ (cm) | $\overline{\eta}$ (cm) | $Rd_{min}$ (cm) | S (cm) |
|--------|------|------|------|------|
| *IH040T20* | 4.2 | 2.2 | -0.2 | 4.4 |
| *IH040T25* | 5.1 | 1.9 | -1.4 | 6.5 |
| *IH040T30* | 6.9 | 2.7 | -2.5 | 9.4 |

**Fig.A3-1. Test IH040T20**: *time recording of gauges 1-4.*
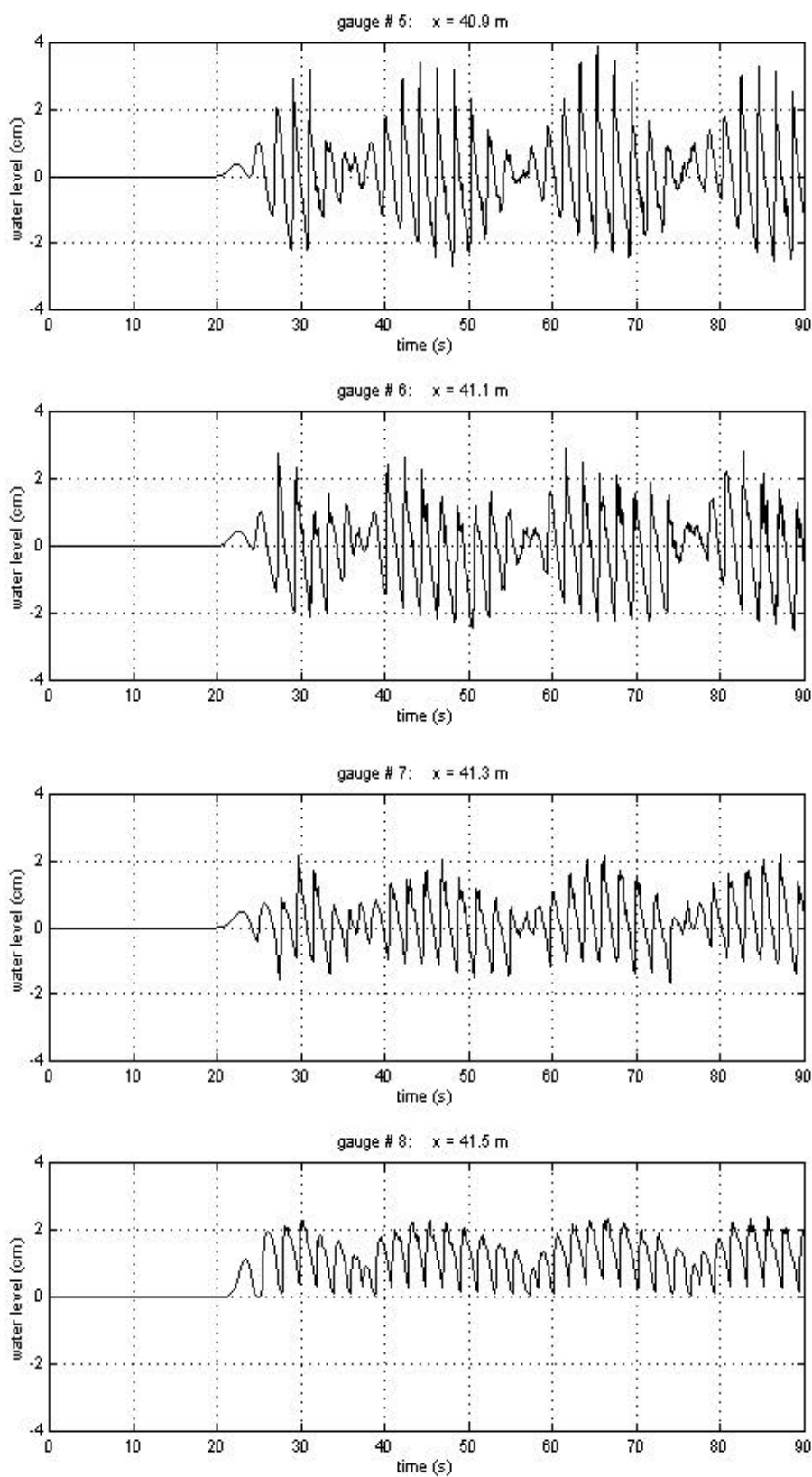
**Fig.A3-2. Test IH040T20**: *time recording of gauges 5-8.*
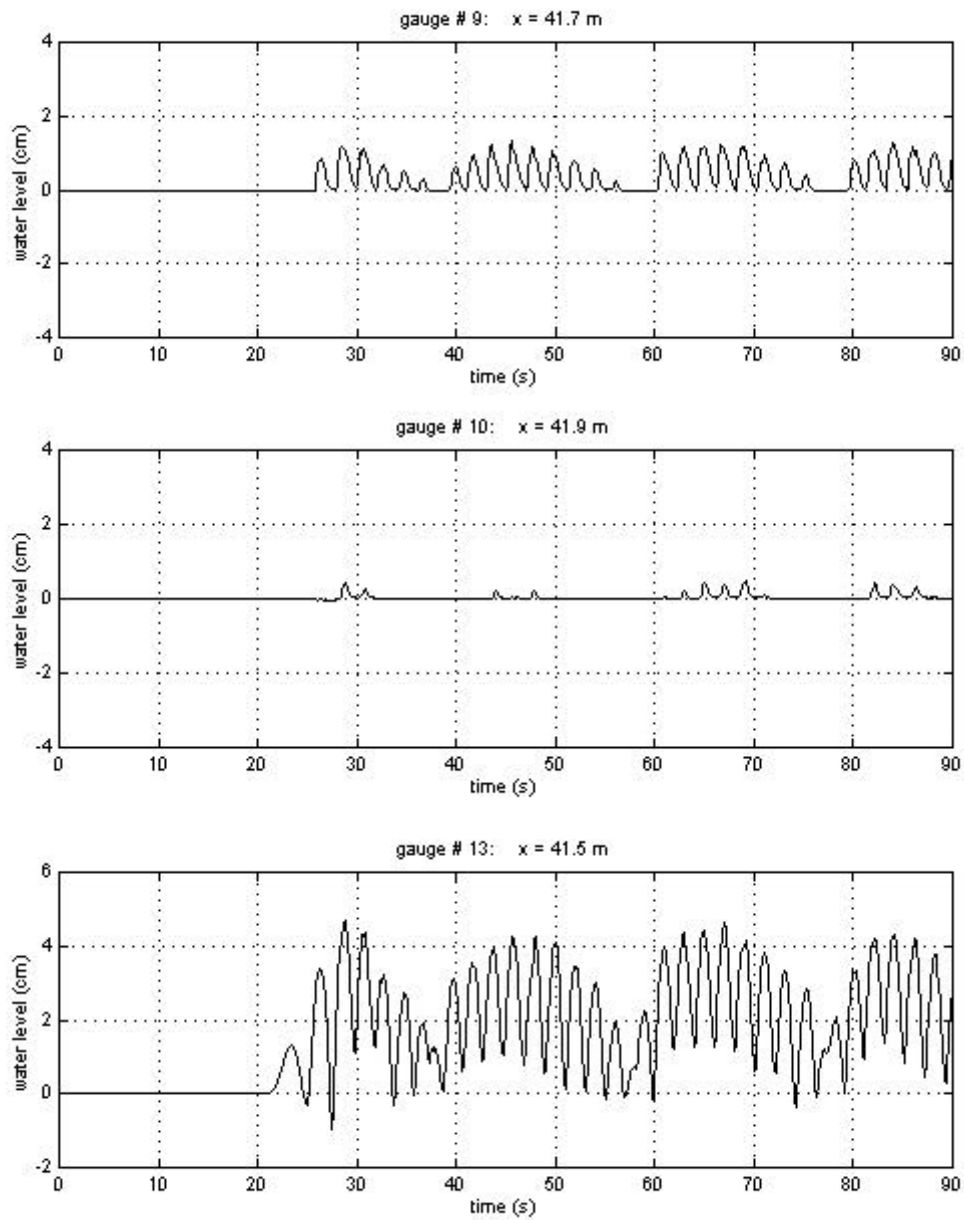
**Fig.A3-3. Test IH040T20**: *time recording of gauges 9,10 and 13.*
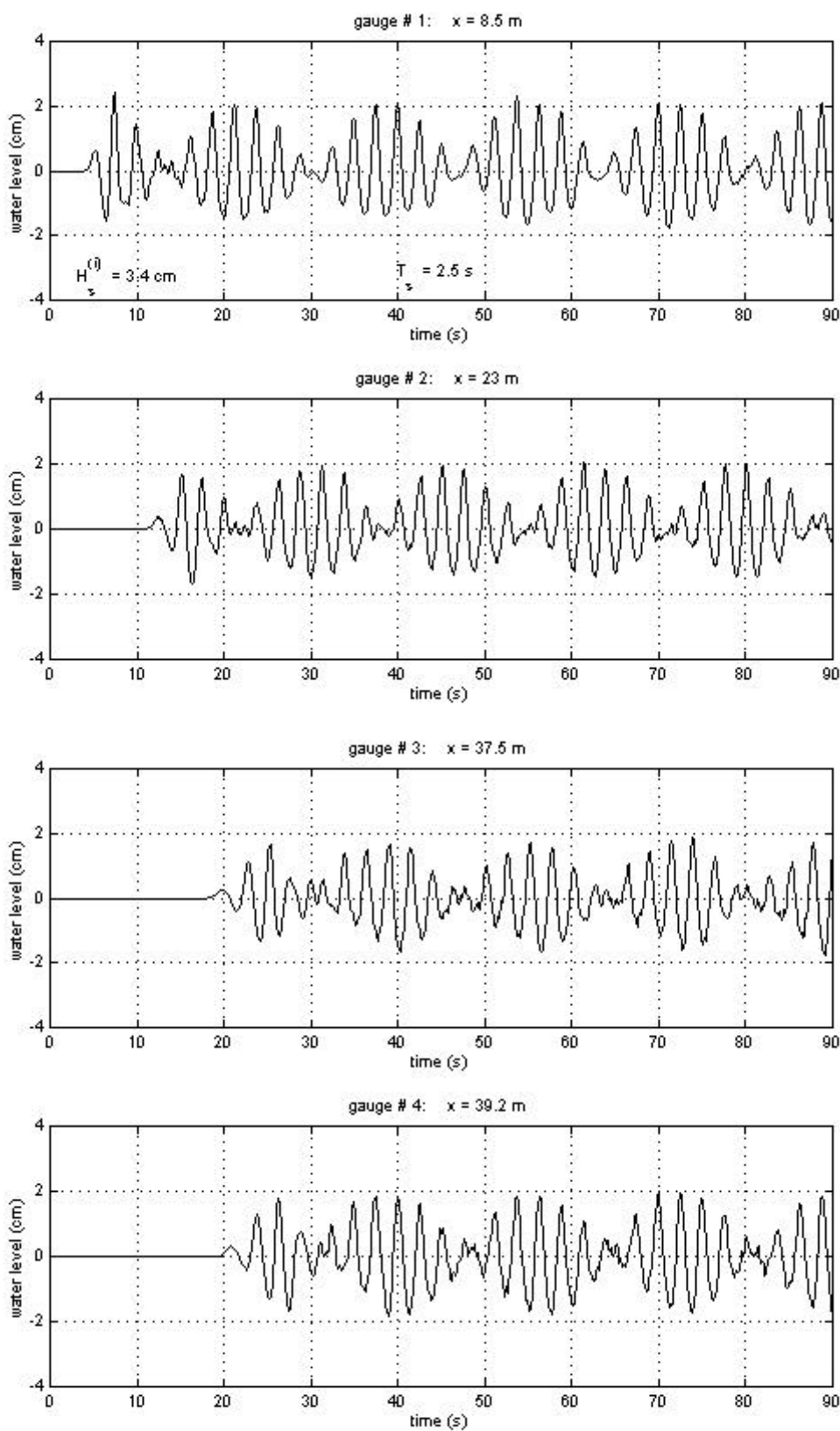
**Fig.A3-4. Test IH040T25***: time recording of gauges 1-4*.
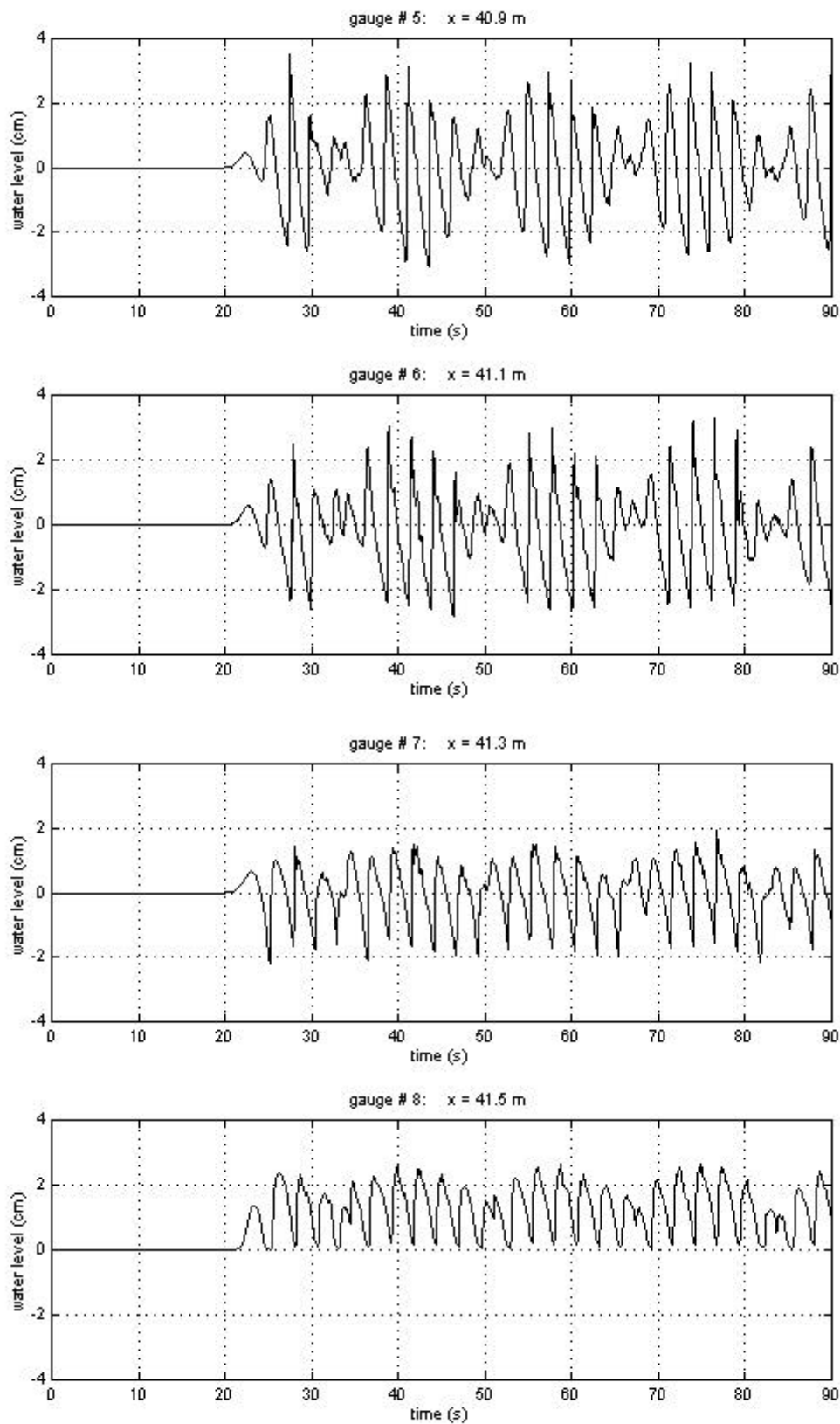
**Fig.A3-5. Test IH040T25**: *time recording of gauges 5-8.*
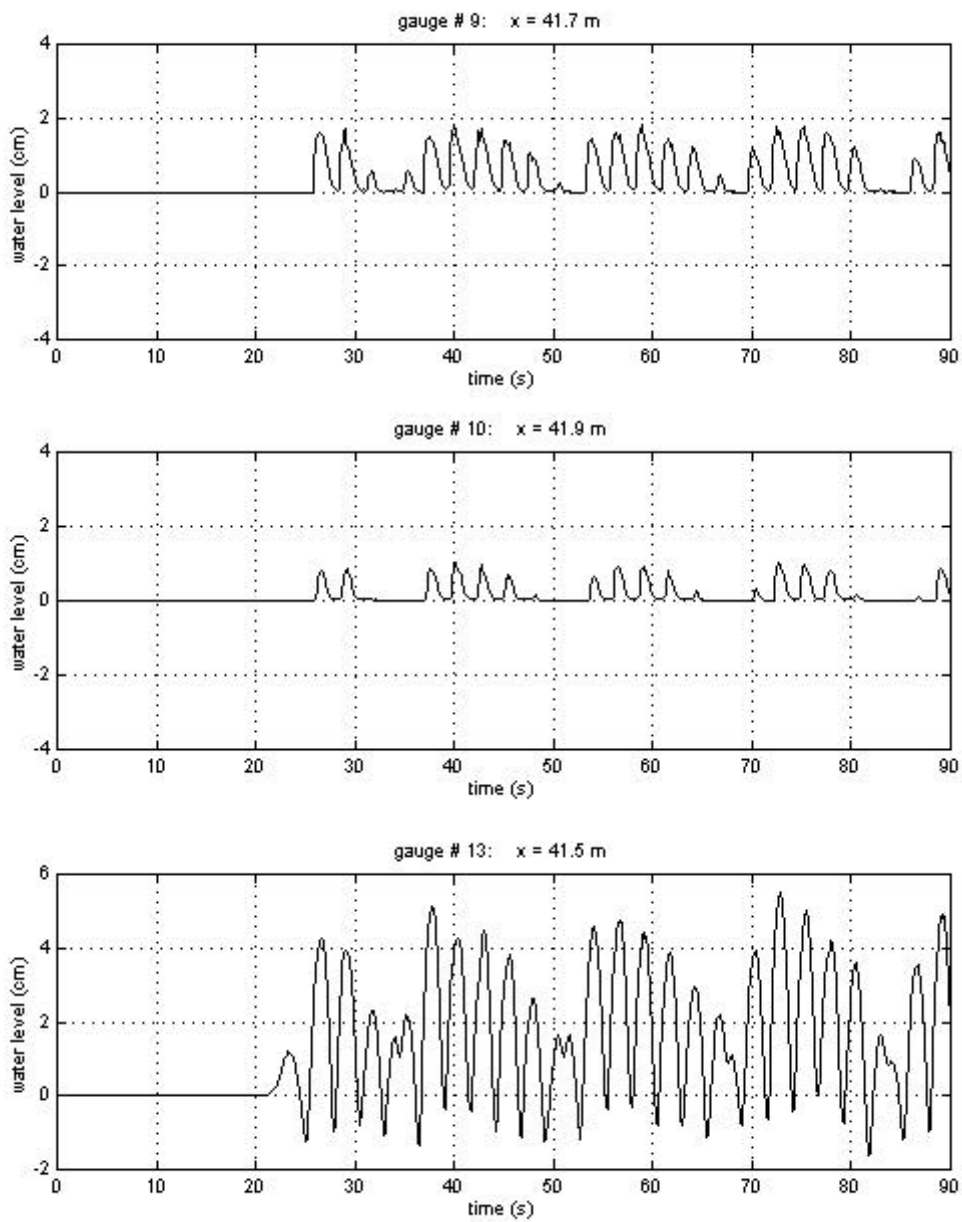
**Fig.A3-6. Test IH040T25**: *time recording of gauges 9,10 and 13*.
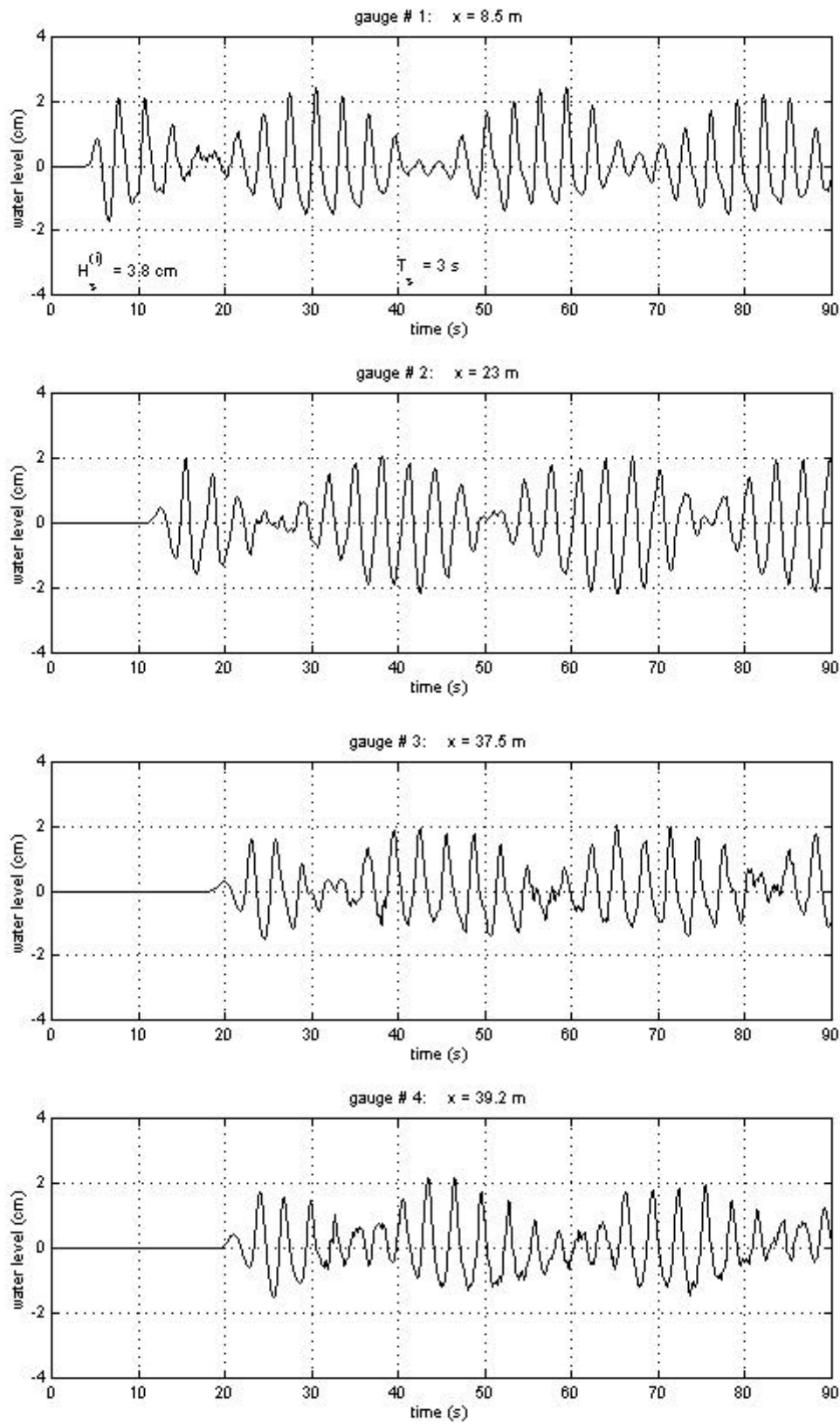
**Fig.A3-7. Test IH040T30**: *time recording of gauges 1-4.*

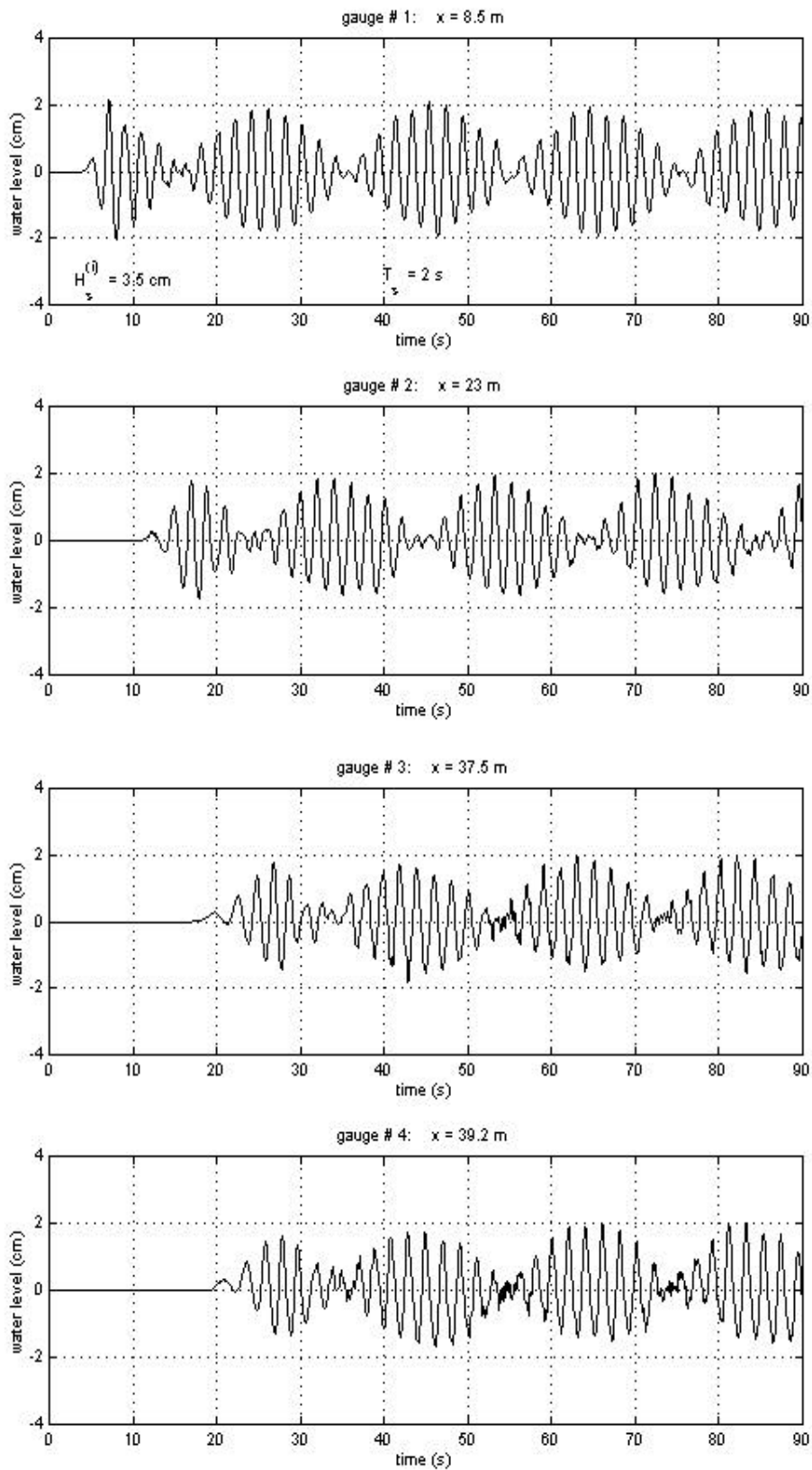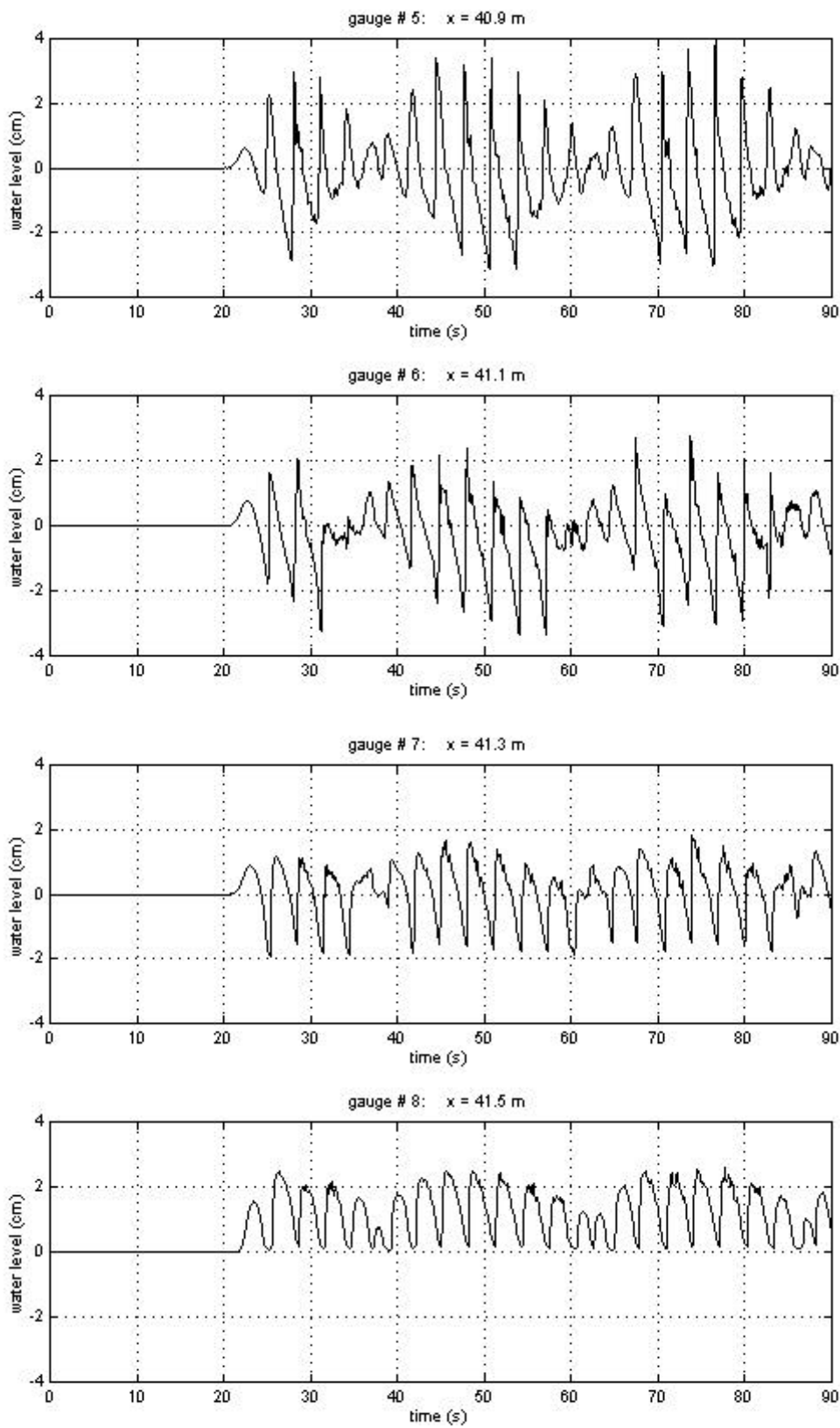**Fig.A3-8. Test IH040T30**: *time recording of gauges 5-8.*
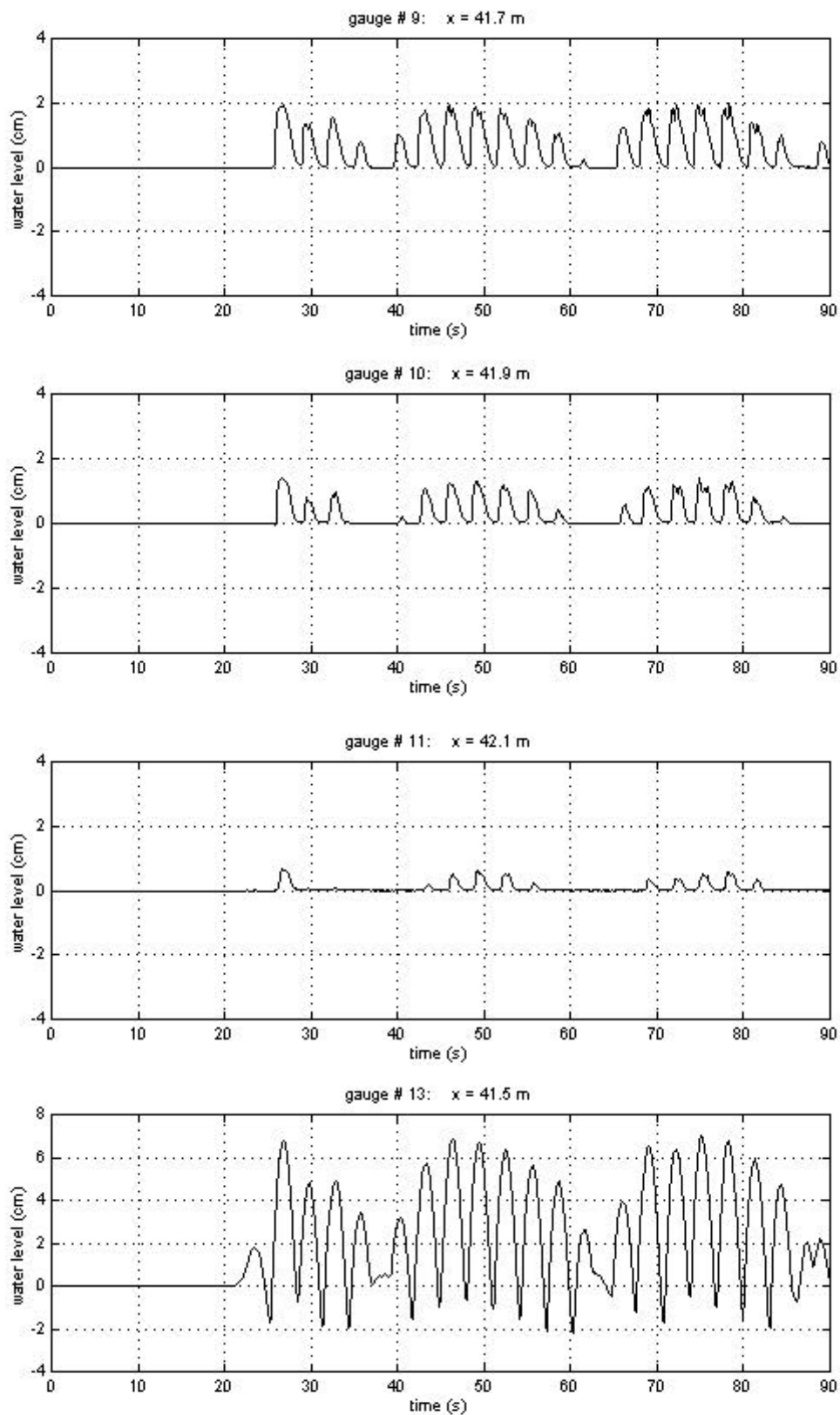
**Fig.A3-9. Test IH040T30**: *time recording of gauges 9-11, and 13.*

# Annex 4

Flux analyses of regular wave tests:

- RH040T20
- RH040T25
- RH040T30
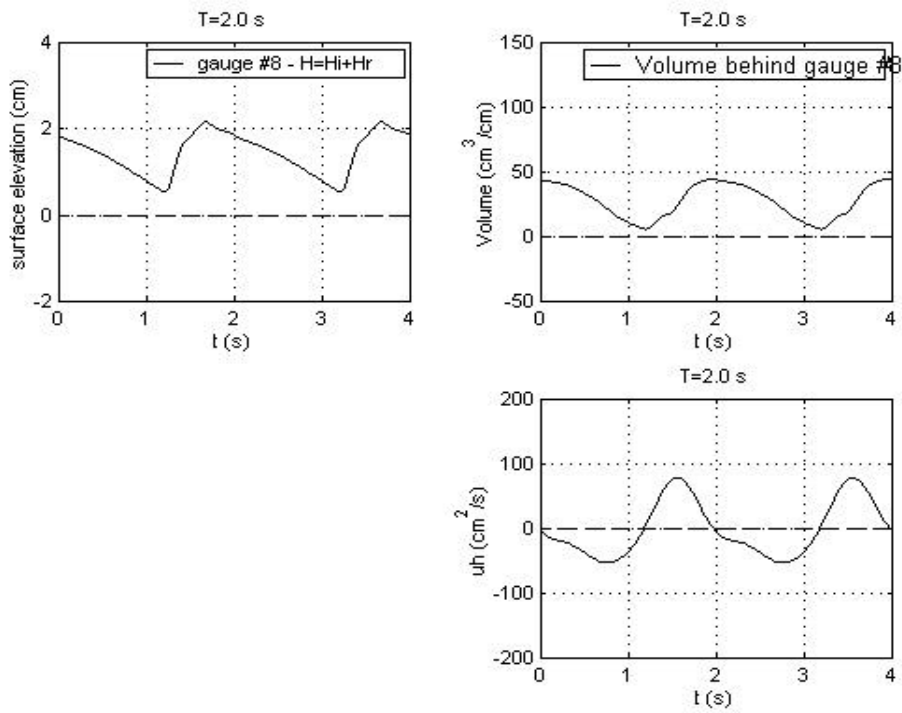
**Fig. A4-1.** *Test RH040T20: flux analysis in the zero section (gauge S8).*
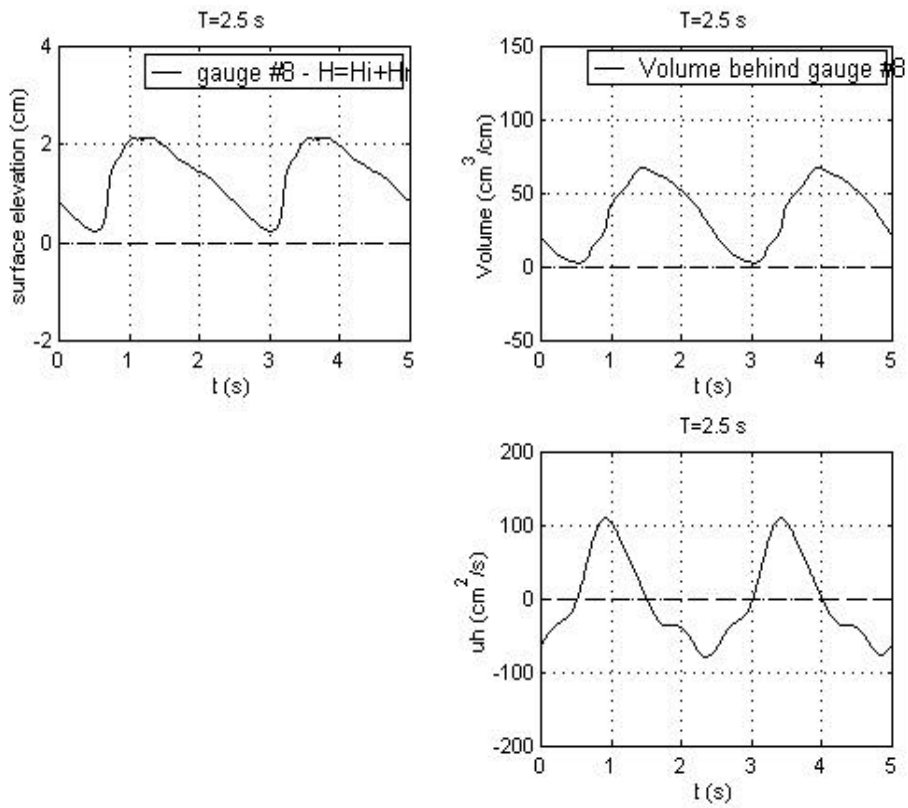


**Fig. A4-2.** *Test RH040T25: flux analysis in the zero section (gauge S8).*
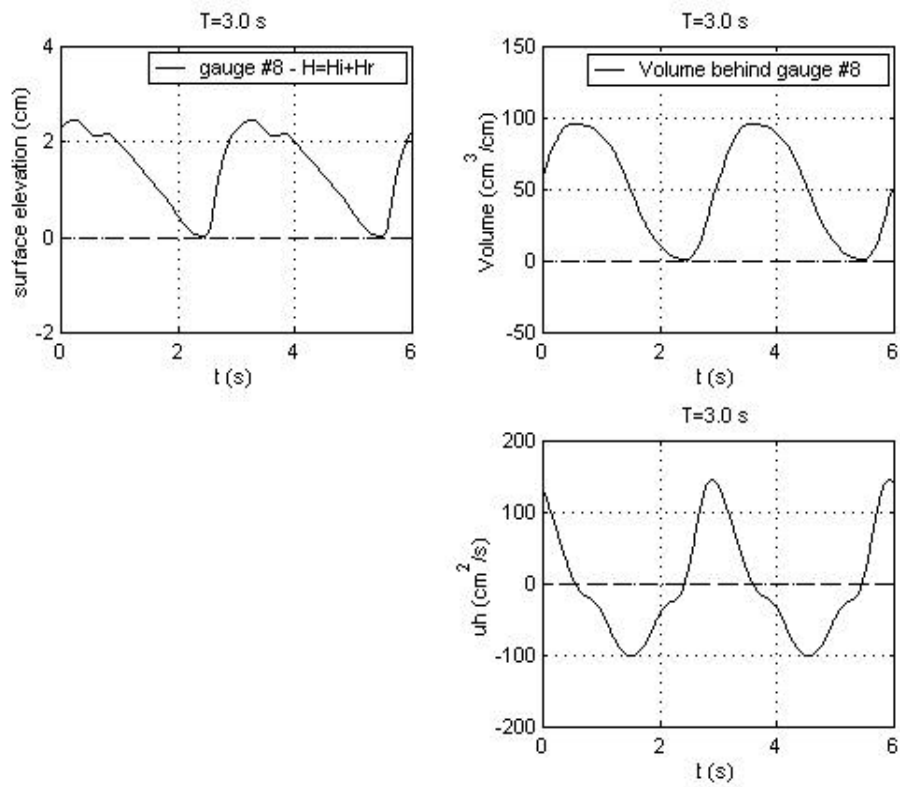
**Fig. A4-3.** *Test RH040T30*: *flux analysis in the zero section (gauge S8).*

# Annex 5

Turbulence measurements of regular wave tests:

- RH040T20
- RH040T25
- RH040T30

| Test | conditions | duration (min) | Xlaser (cm) | Zlaser (mm) | locking time (%) | Remarks : |
|---|---|---|---|---|---|---|
| RH04T20-1l | | 10 | - 20 | 0.5 | 47 | **roller section** |
| RH04T20-2l | H=3.5 cm | 10 | - 20 | 1.5 | 53 | |
| RH04T20-3l | | 10 | - 20 | 2.5 | 39 | |
| RH04T20-4l | T=2.0 s | 10 | - 20 | 3.5 | 44 | |
| RH04T20-5l | | 10 | - 20 | 4.5 | 22 | |
| RH04T20-6l | bottom slope 1 :10 | 10 | - 20 | 5.5 | 29 | |
| RH04T20-7l | | 10 | - 20 | 6.5 | 19 | disturbance of laser signal |
| RH04T20-8l | water depth = 400 mm | 10 | - 20 | 7.5 | 16 | disturbance of laser signal |
| RH04T20-9l | | 10 | - 20 | 8.5 | 14 | disturbance of laser signal |
| RH04T20-9l bis | | 10 | -20 | 8.5 | 63 | laser inclination has been changed |
| RH04T20-10l | | 10 | - 20 | 9.5 | 35 | |
| RH04T20-11l | | 10 | - 20 | 10.5 | 37 | disturbance of laser signal |

*UF1*  Swash zone hydrodynamics on a 1:10 bottom slope

**UF1**   Swash zone hydrodynamics on a 1:10 bottom slope

| | | | | | |
|---|---|---|---|---|---|
| RH04T20-12l | | 10 | - 20 | 11.5 | 38 | disturbance of laser signal |
| RH04T20-13l | | 10 | - 20 | 12.5 | 37 | disturbance of laser signal |
| RH04T20-14l | | 10 | - 20 | 13.5 | 37 | disturbance of laser signal |

**Tab. A5-I**. *Measuring programme, series RH04T20, lower section.*

| Test | conditions | duration (min) | Xlaser (cm) | Zlaser (mm) | locking time (%) | Remarks : |
|---|---|---|---|---|---|---|
| RH04T20-1m | | 10 | 0 | 0.5 | 47 | |
| RH04T20-2m | H=3.5 cm | 10 | 0 | 1.5 | 37 | |
| RH04T20-3m | | 10 | 0 | 2.5 | 37 | |
| RH04T20-4m | T=2.0 s | 10 | 0 | 3.5 | 37 | |
| RH04T20-5m | | 10 | 0 | 4.5 | 30 | |
| RH04T20-6m | bottom slope 1 :10 | 10 | 0 | 5.5 | 15 | |
| RH04T20-7m | | 10 | 0 | 6.5 | 9 | |
| RH04T20-8m | water depth = 400 mm | 10 | 0 | 7.5 | - | disturbance of laser signal |
| RH04T20-8m bis | | 10 | 0 | 7.5 | 15 | laser inclination has been changed |
| RH04T20-9m | | 10 | 0 | 8.5 | - | disregarded laser signal |

**Tab.A5-II.** *Measuring programme, series RH04T20, mid section.*

*UF1*   Swash zone hydrodynamics on a 1:10 bottom slope

*UF1*  Swash zone hydrodynamics on a 1:10 bottom slope

| Test | conditions | duration (min) | Xlaser (cm) | Zlaser (mm) | locking time (%) | Remarks : |
|---|---|---|---|---|---|---|
| RH04T20-1u | | 10 | **+5** | 0.5 | 29 | |
| RH04T20-2u | H=3.5 cm | 10 | **+5** | 1.5 | - | disregarded laser signal |
| RH04T20-2u bis | T=2.0 s | 10 | **+5** | 1.5 | 33 | laser inclination has been changed |
| RH04T20-3u | bottom slope 1 :10 | 10 | **+5** | 2.5 | 31 | |
| RH04T20-4u | | 10 | **+5** | 3.5 | 36 | laser inclination has been changed |
| RH04T20-5u | water depth = 400 mm | 10 | **+5** | 4.5 | 35 | |
| RH04T20-6u | | 10 | **+5** | 5.5 | 15 | |

**Tab.A5-III.** *Measuring programme, series RH04T20, upper section.*

| Test | conditions | duration (min) | Xlaser (cm) | Zlaser (mm) | locking time (%) | Remarks : |
|---|---|---|---|---|---|---|
| RH04T25-1l |  | 10 | - 20 | 0.5 | 52 | **roller section** |
| RH04T25-2l | H=3.5 cm | 10 | - 20 | 1.5 | 69 | |
| RH04T25-3l |  | 10 | - 20 | 2.5 | 35 | |
| RH04T25-4l | T=2.5 s | 10 | - 20 | 3.5 | 35 | |
| RH04T25-5l |  | 10 | - 20 | 4.5 | 34 | |
| RH04T25-6l | bottom slope 1 :10 | 10 | - 20 | 5.5 | 38 | |
| RH04T25-7l |  | 10 | - 20 | 6.5 | 17 | |
| RH04T25-8l | water depth = 400 mm | 10 | - 20 | 7.5 | 25 | |
| RH04T25-9l |  | 10 | - 20 | 8.5 | - | |
| RH04T25-9l bis |  | 10 | -20 | 8.5 | 60 | laser inclination has been changed |
| RH04T25-10l |  | 10 | - 20 | 9.5 | 31 | |
| RH04T25-11l |  | 10 | - 20 | 10.5 | 36 | |
| RH04T25-12l |  | 10 | - 20 | 11.5 | 37 | |
| RH04T25-13l |  | 10 | - 20 | 12.5 | 36 | |
| RH04T25-14l |  | 10 | - 20 | 13.5 | 26 | |
| RH04T25-15l |  | 10 | -20 | 14.5 | 28 | |

*UF1*    Swash zone hydrodynamics on a 1:10 bottom slope

***UF1***     Swash zone hydrodynamics on a 1:10 bottom slope

| | | | | | | |
|---|---|---|---|---|---|---|
| RH04T25-16l | | 10 | -20 | 15.5 | 34 | |
| RH04T25-17l | | 10 | -20 | 16.5 | 28 | |

**Tab.A5-IV.** *Measuring programme, series RH04T25, lower section.*

| Test | conditions | duration (min) | Xlaser (cm) | Zlaser (mm) | locking time (%) | Remarks : |
|---|---|---|---|---|---|---|
| RH04T25-1m | | 10 | 0 | 0.5 | 47 | |
| RH04T25-2m | H=3.5 cm | 10 | 0 | 1.5 | 45 | |
| RH04T25-3m | | 10 | 0 | 2.5 | 49 | |
| RH04T25-4m | T=2.5 s | 10 | 0 | 3.5 | - | disregarded laser signal |
| RH04T25-5m | | 9' 59'' | 0 | 4.5 | 38 | |
| RH04T25-6m | bottom slope 1 :10 | 10 | 0 | 5.5 | 38 | |
| RH04T25-7m | | 10 | 0 | 6.5 | 30 | |
| RH04T25-8m | water depth = 400 mm | 10 | 0 | 7.5 | - | |
| RH04T25-8m bis | | 10 | 0 | 7.5 | 41 | laser inclination has been changed |
| RH04T25-10m | | 10 | 0 | 8.5 | 31 | |
| RH04T25-11m | | 10 | 0 | 9.5 | 24 | |

*UF1*    Swash zone hydrodynamics on a 1:10 bottom slope

**UF1** Swash zone hydrodynamics on a 1:10 bottom slope

| | | | | | |
|---|---|---|---|---|---|
| RH04T25-12m | | 10 | 0 | 10.5 | 16 | |
| RH04T25-13m | | 10 | 0 | 11.5 | 4 | |

**Tab.A5-V.** *Measuring programme, series RH04T25, mid section.*

| Test | conditions | duration (min) | Xlaser (cm) | Zlaser (mm) | locking time (%) | Remarks : |
|---|---|---|---|---|---|---|
| RH04T25-1u | | 10 | +20 | 0.5 | 28 | |
| RH04T25-2u | H=3.5 cm | 10 | +20 | 1.5 | 14 | |
| RH04T25-3u | T=2.5 s | 10 | +20 | 2.5 | 0 | disturbance of laser signal |
| RH04T25-3u bis | | 10 | +20 | 2.5 | 19 | laser inclination has been changed |
| RH04T25-4u | bottom slope 1 :10 | 10 | +20 | 3.5 | 23 | |
| RH04T25-5u | water depth = 400 mm | 10 | +20 | 4.5 | 19 | |
| RH04T25-6u | | 10 | +20 | 5.5 | 15 | |

**Tab.A5-VI.** *Measuring programme, series RH04T25, upper section.*

| Test | conditions | duration (min) | Xlaser (cm) | Zlaser (mm) | locking time (%) | Remarks : |
|---|---|---|---|---|---|---|
| RH04T30-1l | | 10 | - 20 | 0.5 | 45 | |
| RH04T30-2l | H=3.5 cm | 10 | - 20 | 1.5 | 50 | |
| RH04T30-3l | | 10 | - 20 | 2.5 | 34 | |
| RH04T30-4l | T=3.0 s | 10 | - 20 | 3.5 | 61 | |
| RH04T30-5l | | 10 | - 20 | 4.5 | 37 | |
| RH04T30-6l | bottom slope 1 :10 | 10 | - 20 | 5.5 | 30 | |
| RH04T30-7l | | 10 | - 20 | 6.5 | 20 | |
| RH04T30-8l | water depth = 400 mm | 10 | - 20 | 7.5 | 27 | |
| RH04T30-9l | | 10 | - 20 | 8.5 | 20 | |
| RH04T30-9l bis | | 10 | -20 | 8.5 | 57 | laser inclination has been changed |
| RH04T30-10l | | 10 | - 20 | 9.5 | 34 | |
| RH04T30-11l | | 10 | - 20 | 10.5 | 31 | |
| RH04T30-12l | | 10 | - 20 | 11.5 | 35 | |
| RH04T30-13l | | 10 | - 20 | 12.5 | 41 | |

*UF1*   Swash zone hydrodynamics on a 1:10 bottom slope

| | | | | | | |
|---|---|---|---|---|---|---|
| RH04T30-14l | | 10 | - 20 | 13.5 | 29 | |
| RH04T30-15l | | 10 | -20 | 14.5 | 32 | |
| RH04T30-16l | | 10 | -20 | 15.5 | 34 | |
| RH04T30-17l | | 10 | -20 | 16.5 | 30 | |
| RH04T30-18l | | 10 | - 20 | 17.5 | 36 | |
| RH04T30-19l | | 10 | - 20 | 18.5 | 30 | |
| RH04T30-20l | | 10 | - 20 | 19.5 | 33 | |
| RH04T30-21l | | 10 | -20 | 20.5 | 26 | |
| RH04T30-22l | | 10 | -20 | 21.5 | 27 | |
| RH04T30-23l | | 10 | -20 | 22.5 | 24 | |

**Tab.A5-VII.** *Measuring programme, series RH04T30, lower section.*

| Test | conditions | duration (min) | Xlaser (cm) | Zlaser (mm) | locking time (%) | Remarks : |
|---|---|---|---|---|---|---|
| RH04T30-1m | | 10 | 0 | 0.5 | 67 | |
| RH04T30-2m | H=3.5 cm | 10 | 0 | 1.5 | 65 | |
| RH04T30-3m | | 10 | 0 | 2.5 | 38 | |
| RH04T30-4m | T=3.0 s | 10 | 0 | 3.5 | 38 | disregarded laser signal |
| RH04T30-5m | | 10 | 0 | 4.5 | 51 | |
| RH04T30-6m | bottom slope 1 :10 | 10 | 0 | 5.5 | 47 | |
| RH04T30-7m | | 10 | 0 | 6.5 | 43 | |
| RH04T30-8m | water depth = 400 mm | 10 | 0 | 7.5 | 38 | |
| RH04T30-9m | | 10 | 0 | 8.5 | 32 | |
| RH04T30-10m | | 10 | 0 | 9.5 | 41 | |
| RH04T30-11m | | 10 | 0 | 10.5 | 32 | |
| RH04T30-12m | | 10 | 0 | 11.5 | 17 | |
| RH04T30-12m bis | | 10 | 0 | 11.5 | 46 | laser inclination has been changed |
| RH04T30-13m | | 10 | 0 | 12.5 | 38 | |

*UF1*    Swash zone hydrodynamics on a 1:10 bottom slope

**UF1**    Swash zone hydrodynamics on a 1:10 bottom slope

| | | | | | | |
|---|---|---|---|---|---|---|
| RH04T30-14m | | 10 | 0 | 13.5 | 35 | |
| RH04T30-15m | | 10 | 0 | 14.5 | 35 | |
| RH04T30-16m | | 10 | 0 | 15.5 | 24 | |
| RH04T30-17m | | 10 | 0 | 16.5 | 7 | |
| RH04T30-18m | | 10 | 0 | 17.5 | 19 | |
| RH04T30-19m | | 10 | 0 | 18.5 | 2 | disturbance of laser signal |

**Tab.A5-VIII.** *Measuring programme, series RH04T30, mid section.*

| Test | conditions | duration (min) | Xlaser (cm) | Zlaser (mm) | locking time (%) | Remarks : |
|---|---|---|---|---|---|---|
| RH04T30-1u | | 10 | +20 | 0.5 | 42 | |
| RH04T30-2u | H=3.5 cm | 10 | +20 | 1.5 | 42 | |
| RH04T30-3u | | 10 | +20 | 2.5 | 31 | |
| RH04T30-4u | | 10 | +20 | 3.5 | 20 | |
| RH04T30-5u | T=3.0 s | 10 | +20 | 4.5 | 23 | |
| RH04T30-6u | | 10 | +20 | 5.5 | 20 | |
| RH04T30-7u | bottom slope 1 :10 | 10 | +20 | 6.5 | 47 | laser inclination has been changed |
| RH04T30-8u | | 10 | +20 | 7.5 | 36 | |
| RH04T30-9u | water depth = 400 mm | 10 | +20 | 8.5 | 31 | |
| RH04T30-10u | | 10 | +20 | 9.5 | 28 | |

**Tab.A5-IX.** *Measuring programme, series RH04T30, upper section.*

**UF1**    Swash zone hydrodynamics on a 1:10 bottom slope

*UF1*   Swash zone hydrodynamics on a 1:10 bottom slope

| Test | conditions | X (cm) | maximum free surface thickness (mm) | LDV measured points (.) | Remarks : |
|---|---|---|---|---|---|
| RH04T20-*l | H=3.5 cm | -20 | 37 | 14 | **roller** |
| RH04T20-*m | T=2.0 s | 0 | 22 | 9 | |
| RH04T20-*u | | **+5** | 19 | 6 | |
| RH04T25-*l | H=3.5 cm | -20 | 36 | 17 | **roller** |
| RH04T25-*m | T=2.5 s | 0 | 21 | 12 | |
| RH04T25-*u | | +20 | 16 | 6 | |
| RH04T30-*l | H=3.5 cm | -20 | 35 | 23 | |
| RH04T30-*m | T=3.0 s | 0 | 25 | 19 | |
| RH04T30-*u | | +20 | 21 | 10 | |

**Tab.A5-X.** *Recorded characteristics in the measuring sections.*

# Annex 6

Turbulence analysis of regular wave tests:
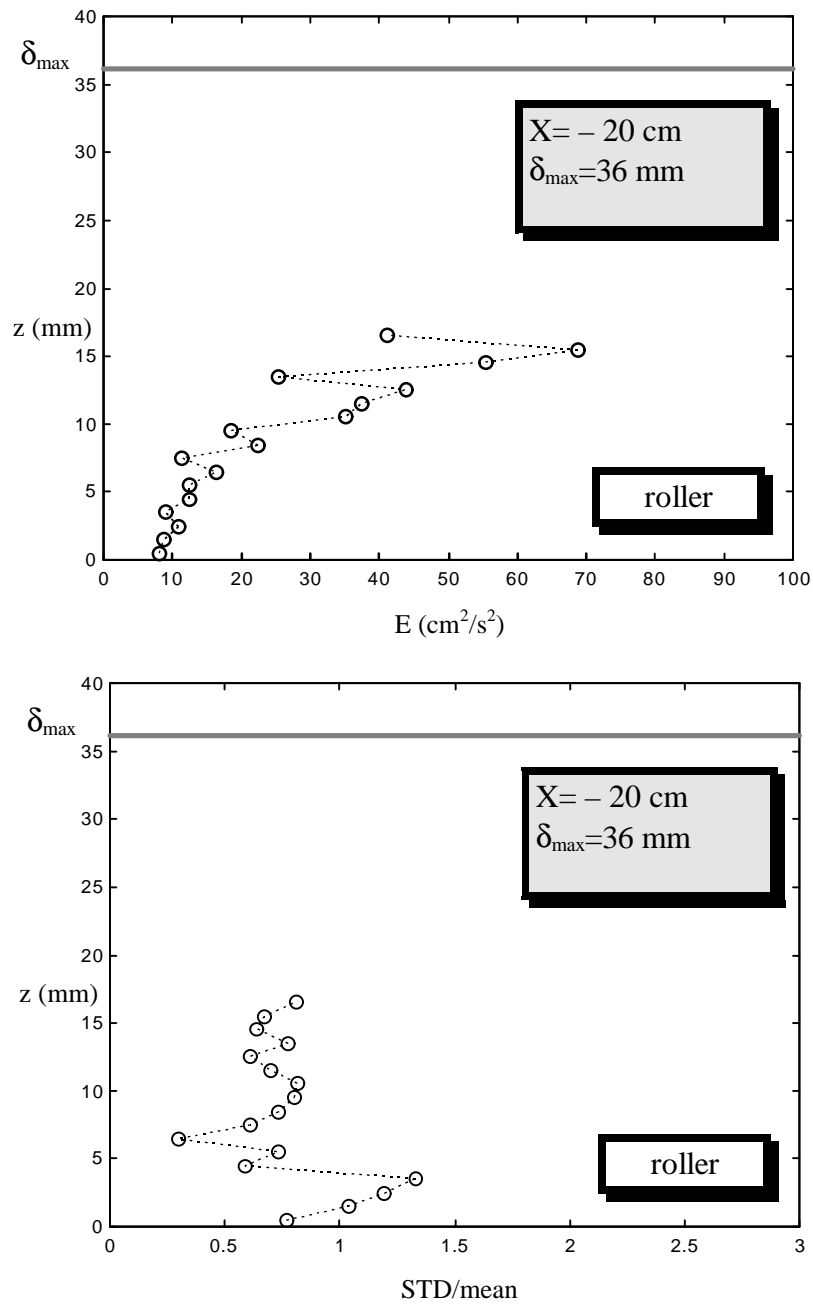
- RH040T20
- RH040T25
- RH040T30
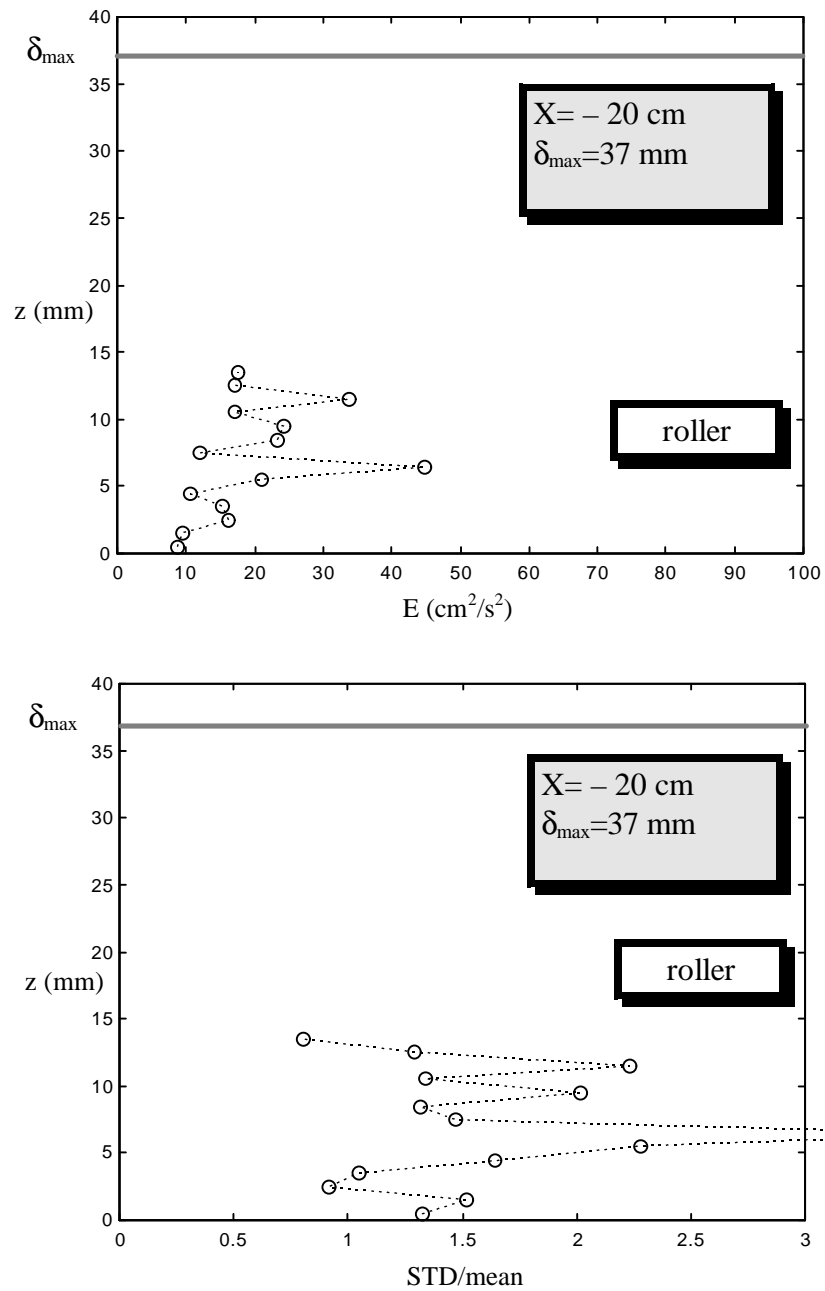
**Fig.A6- 1. Test RH040T20***: Mean turbulence energy and turbulence variation over a cycle. Lower section.*
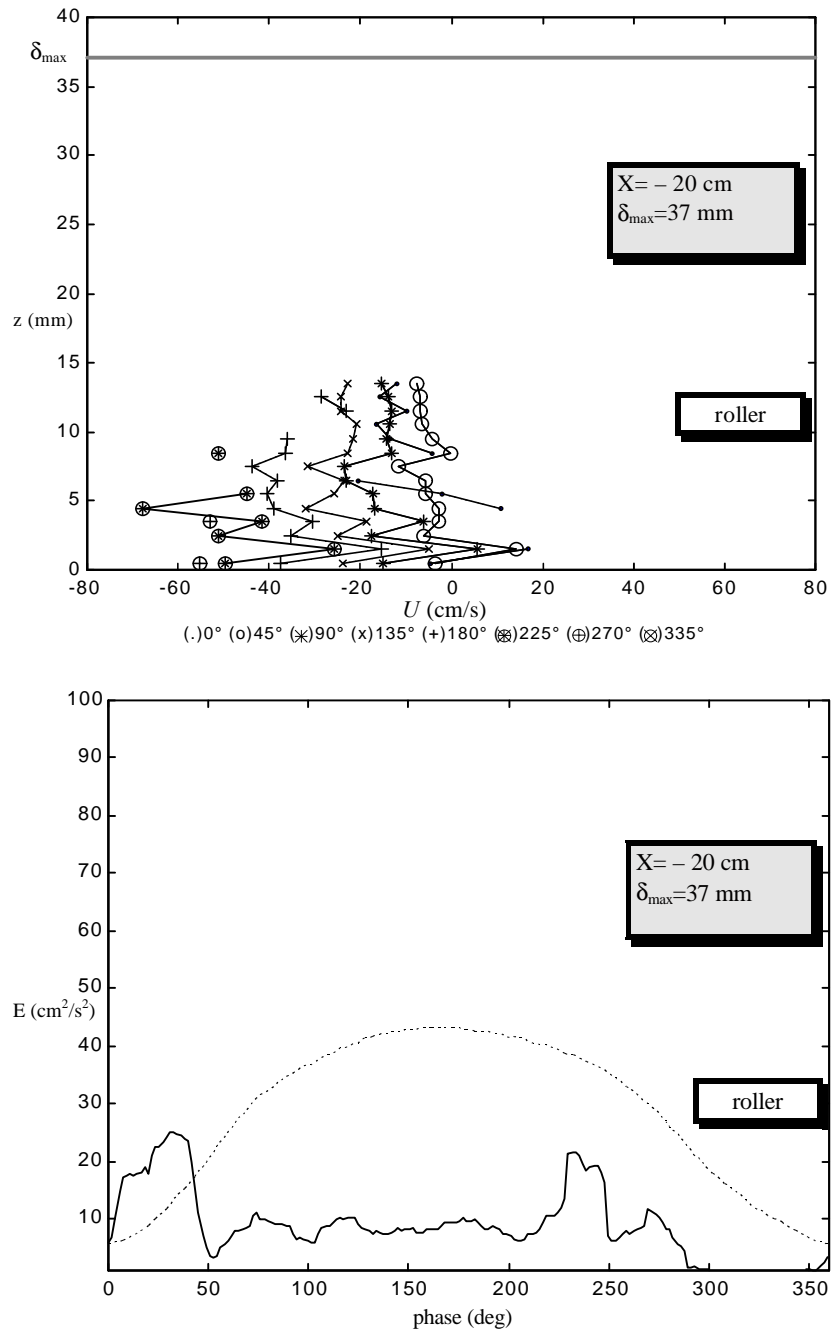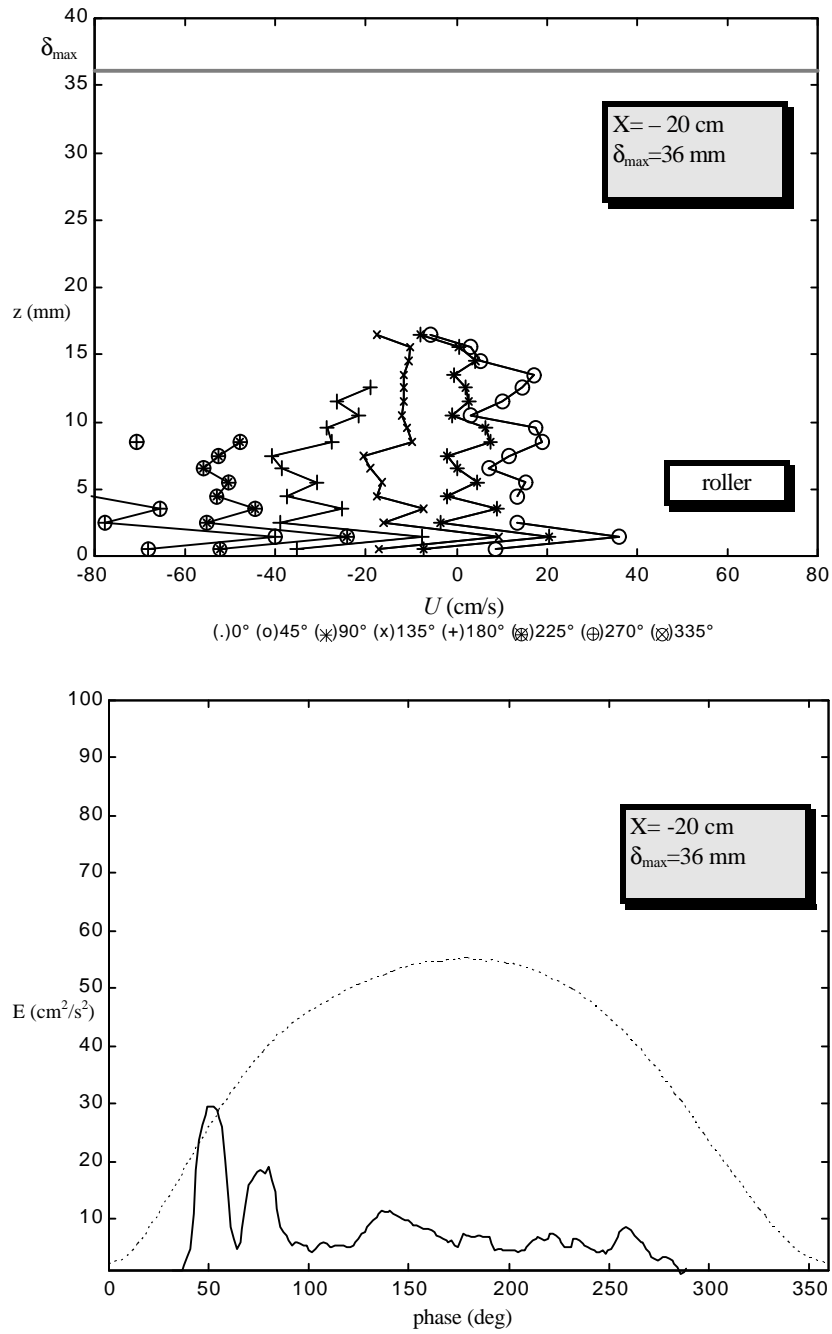
**Fig.A6- 2. Test RH040T20***: Velocity profiles and turbulence near the bottom. Lower section.*
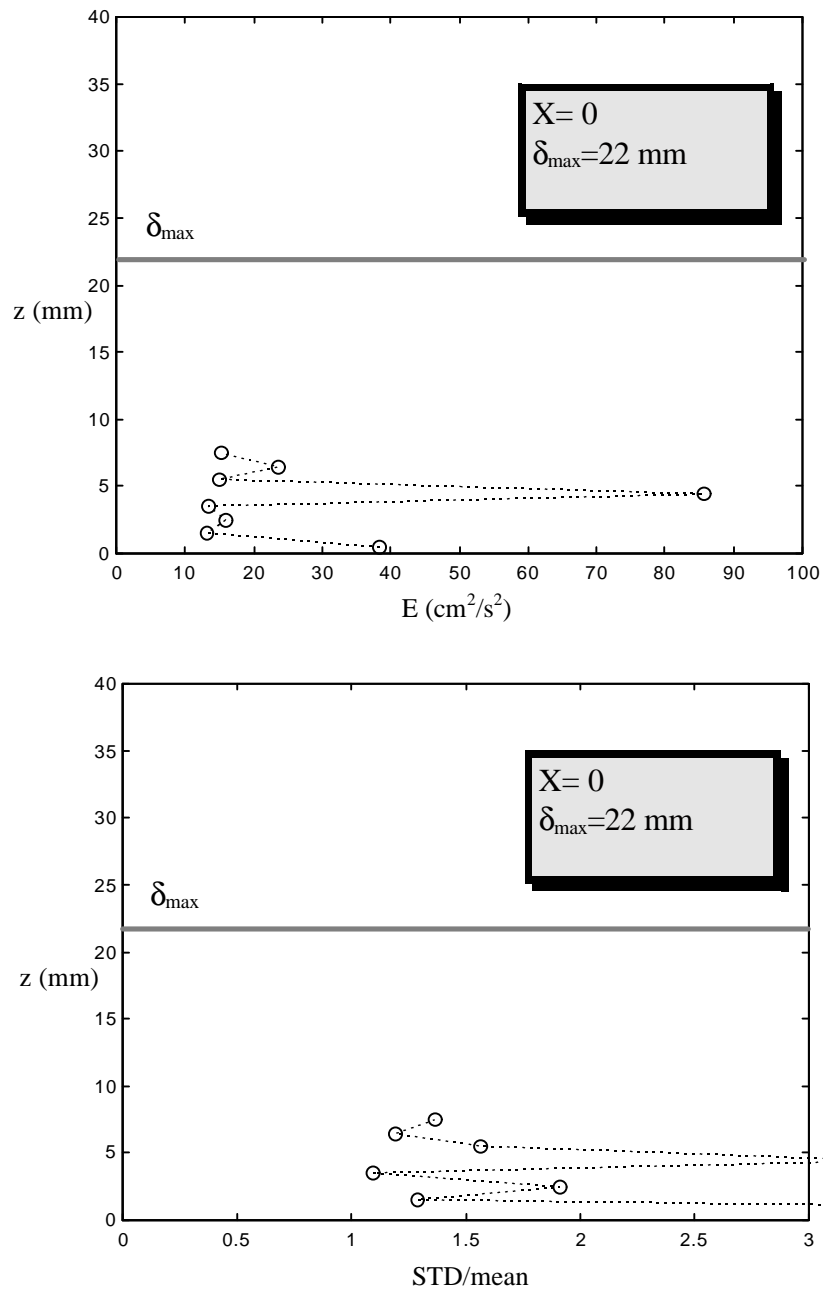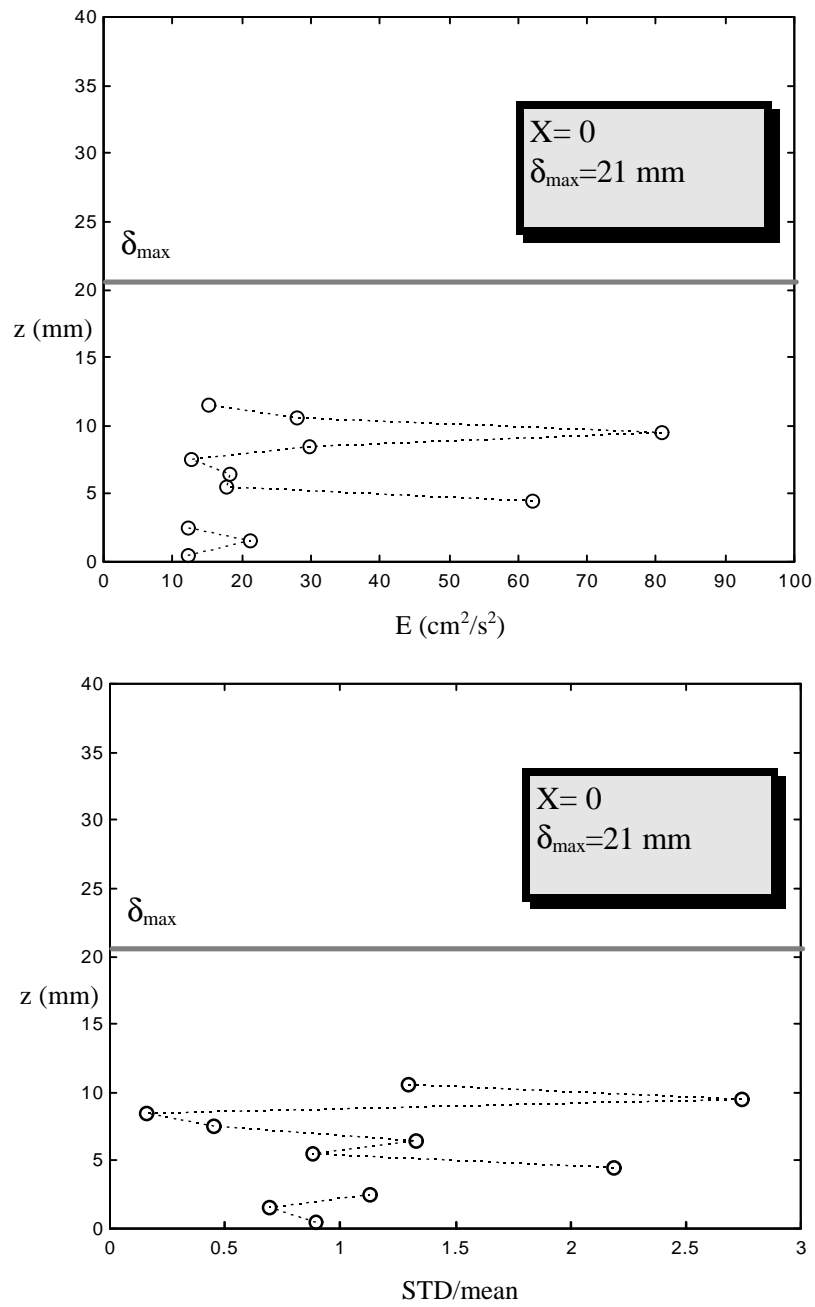
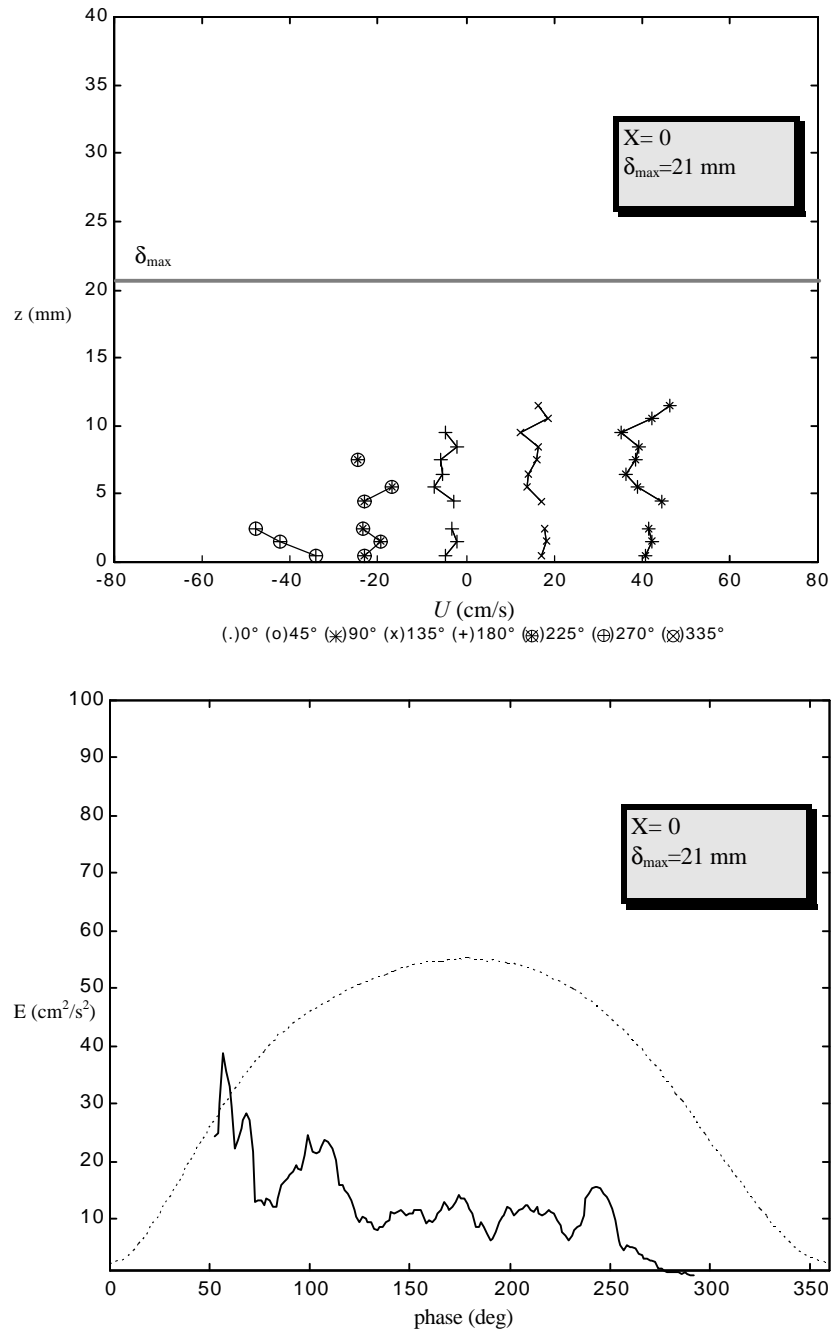**Fig.A6- 3. Test RH040T20***: Mean turbulence energy and turbulence variation over a cycle. Mid section.*

$\delta_{max}$

X= 0
$\delta_{max}$=22 mm

z (mm)

$U$ (cm/s)

(.)0° (o)45° (✳)90° (x)135° (+)180° (⊛)225° (⊕)270° (⊗)335°

E (cm$^2$/s$^2$)

X= 0
$\delta_{max}$=22 mm

phase (deg)
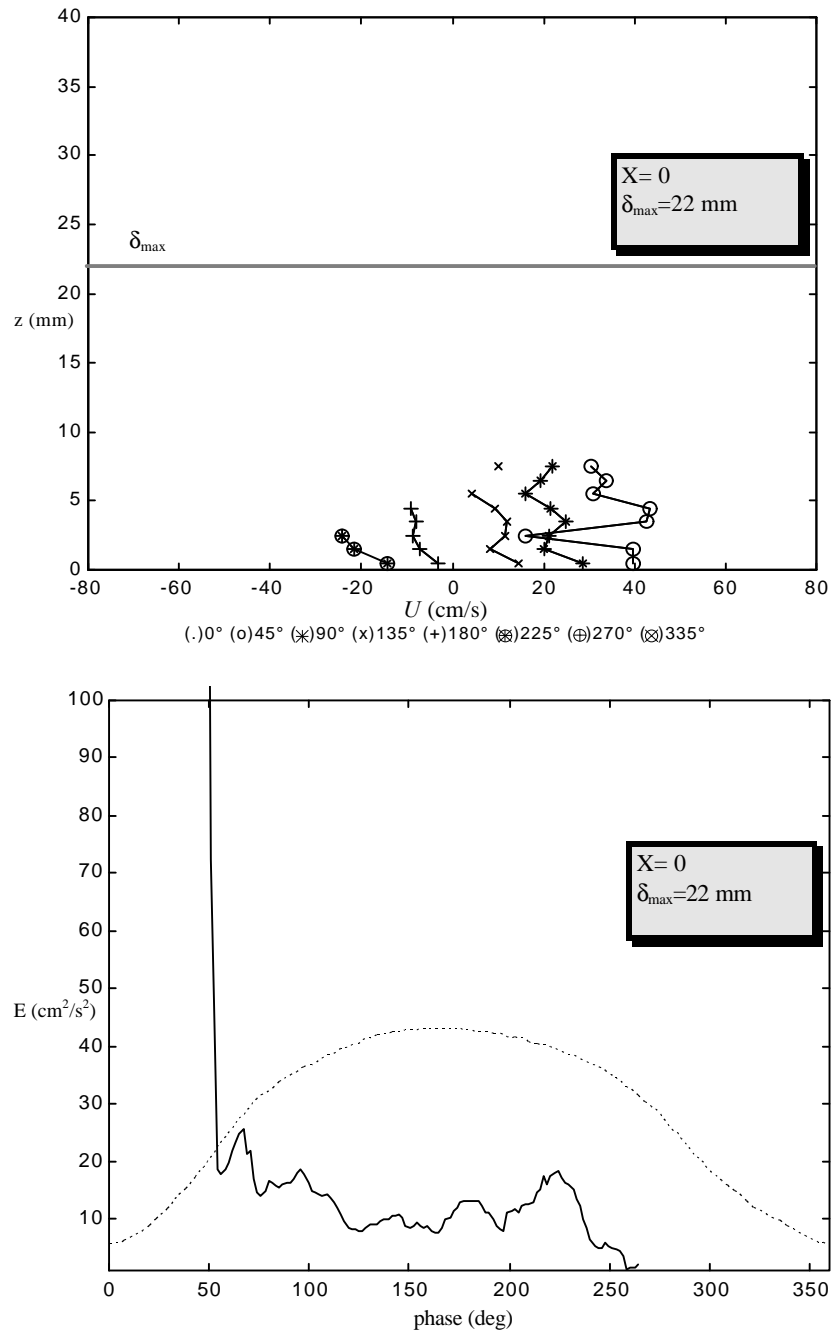
**Fig.A6- 4. Test RH040T20**: *Velocity profiles and turbulence near the bottom. Mid section.*
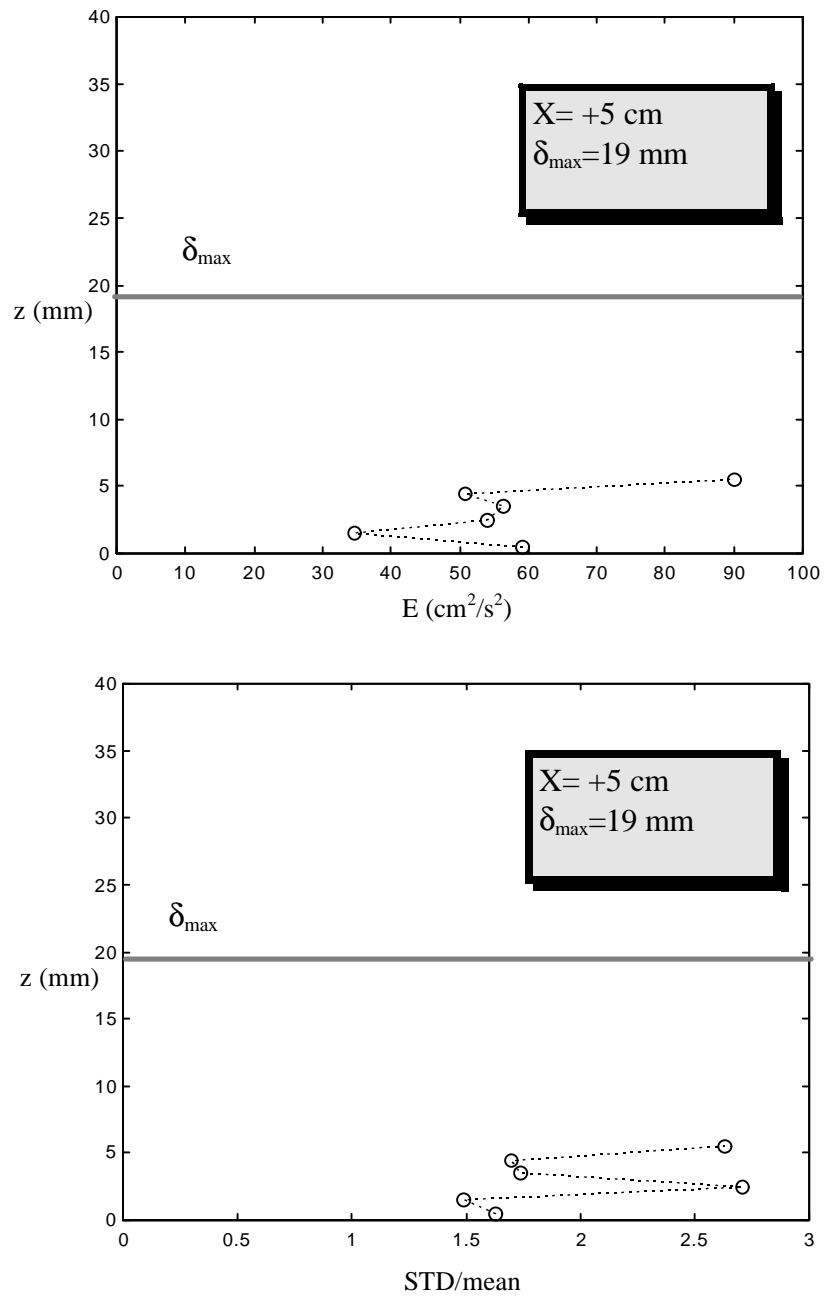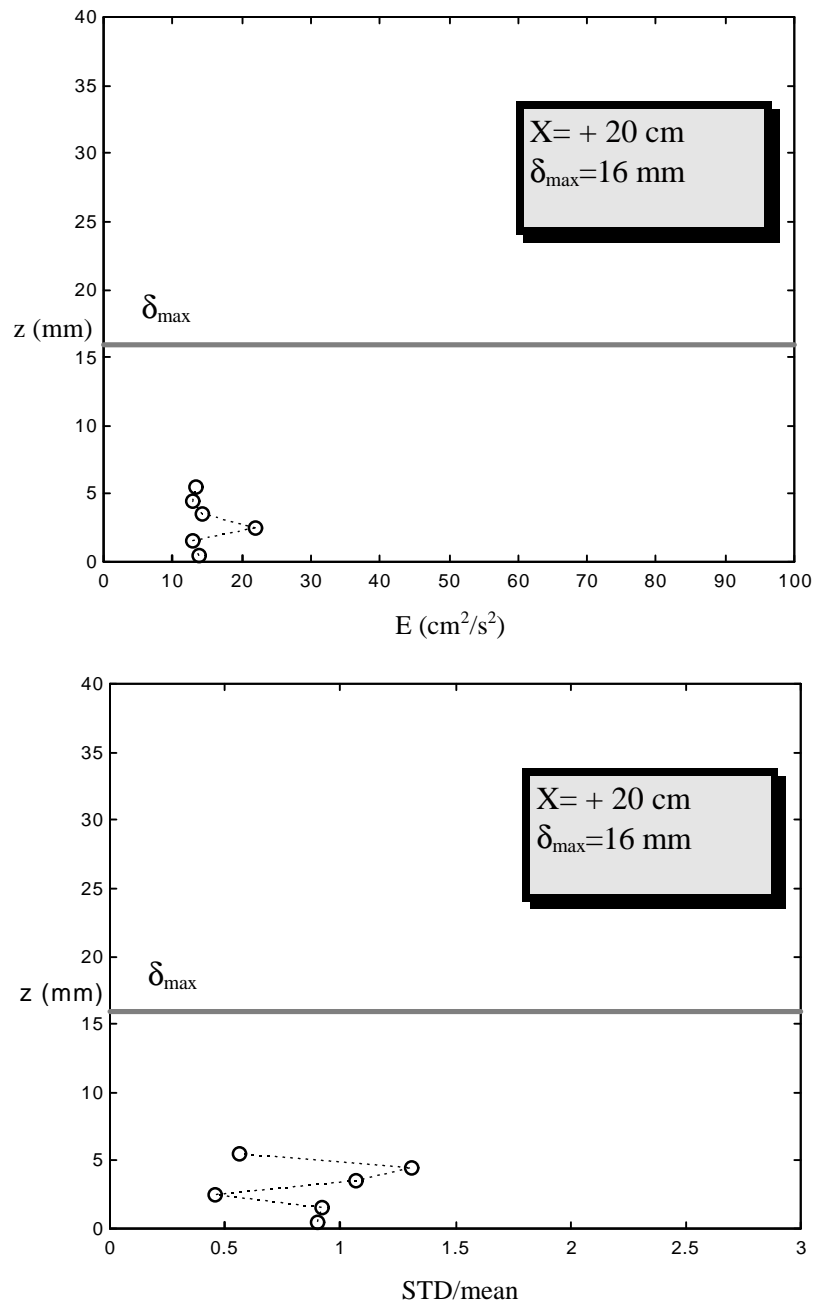
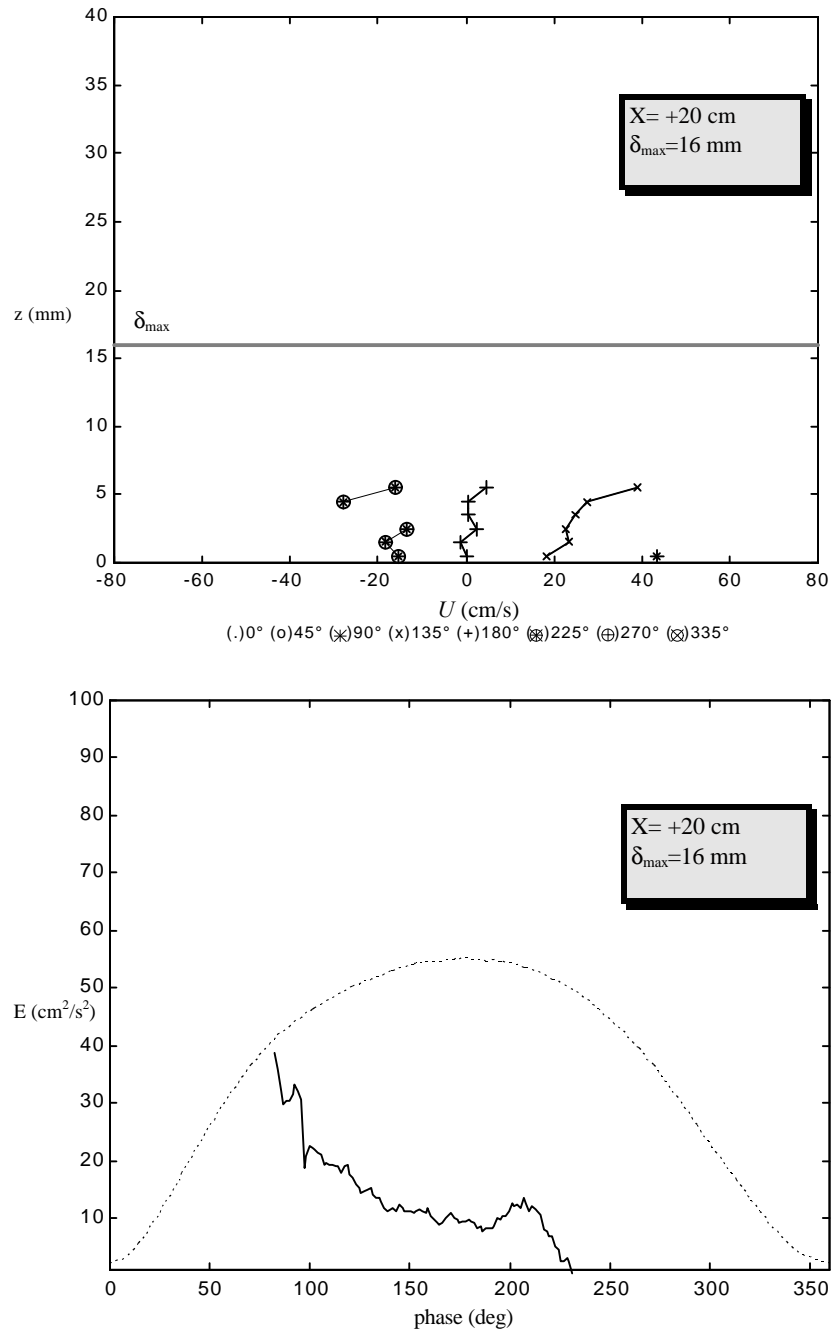**Fig.A6- 5. Test RH040T20***: Mean turbulence energy and turbulence variation over a cycle. Upper section.*
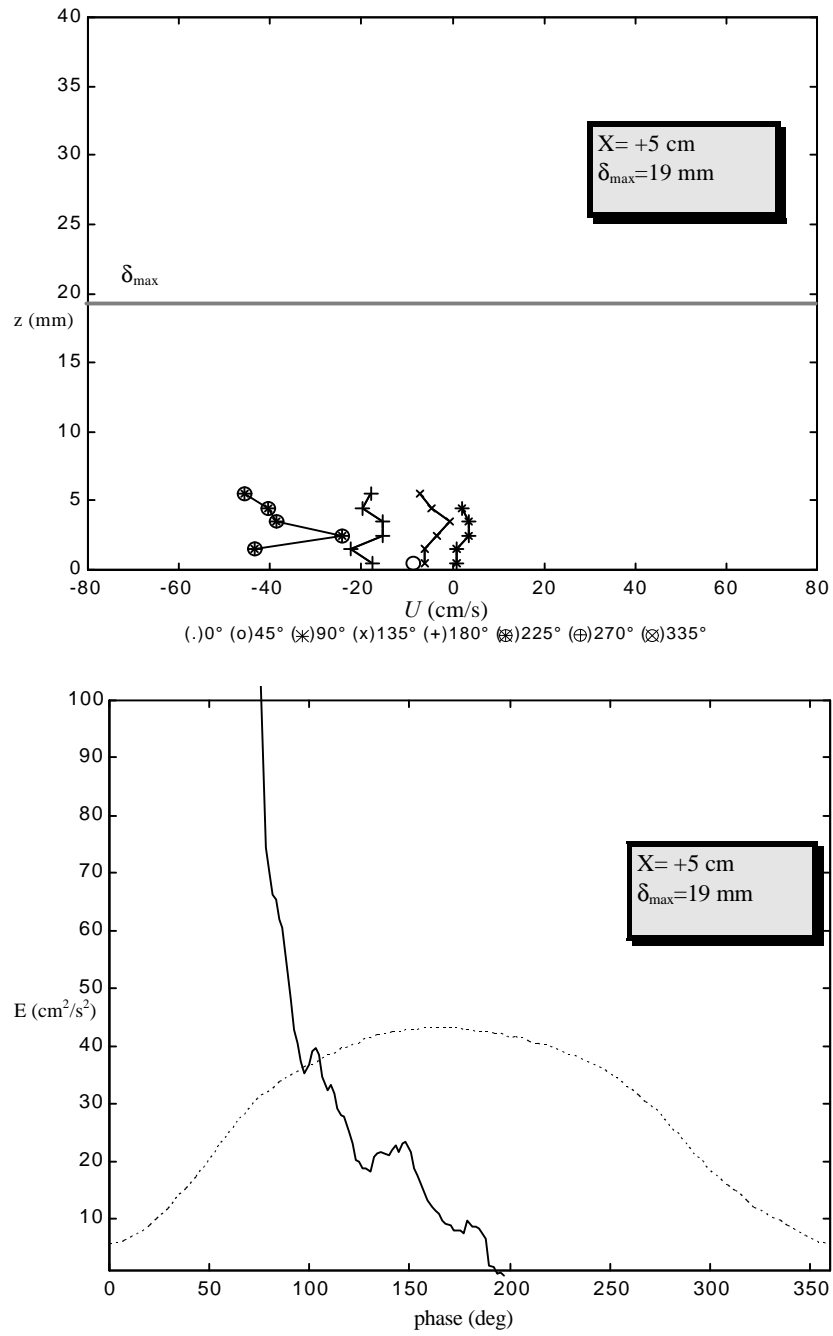
**Fig.A6- 6. Test RH040T20**: *Velocity profiles and turbulence near the bottom. Upper section.*
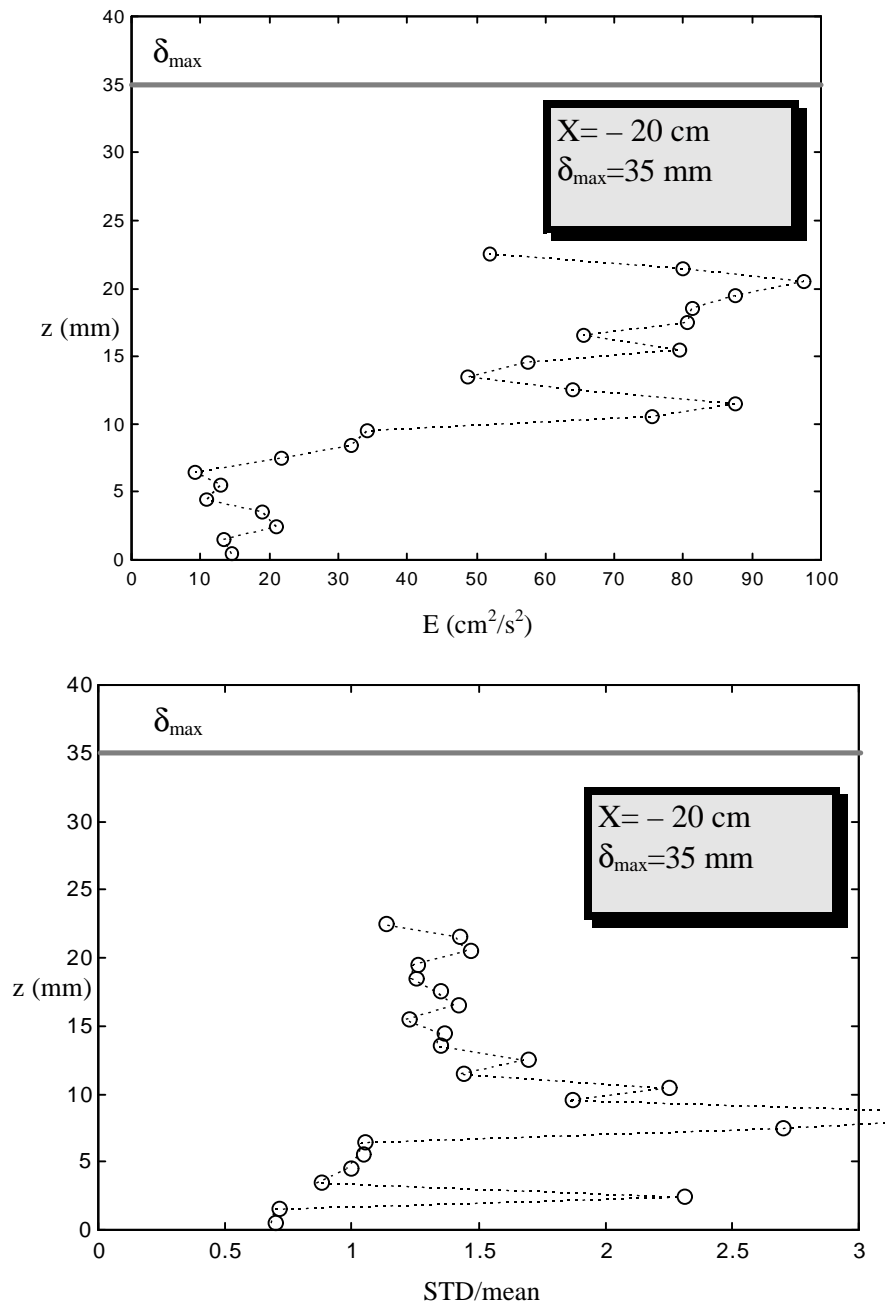
**Fig.A6- 7. Test RH040T25:** *Mean turbulence energy and turbulence variation over a cycle. Lower section.*

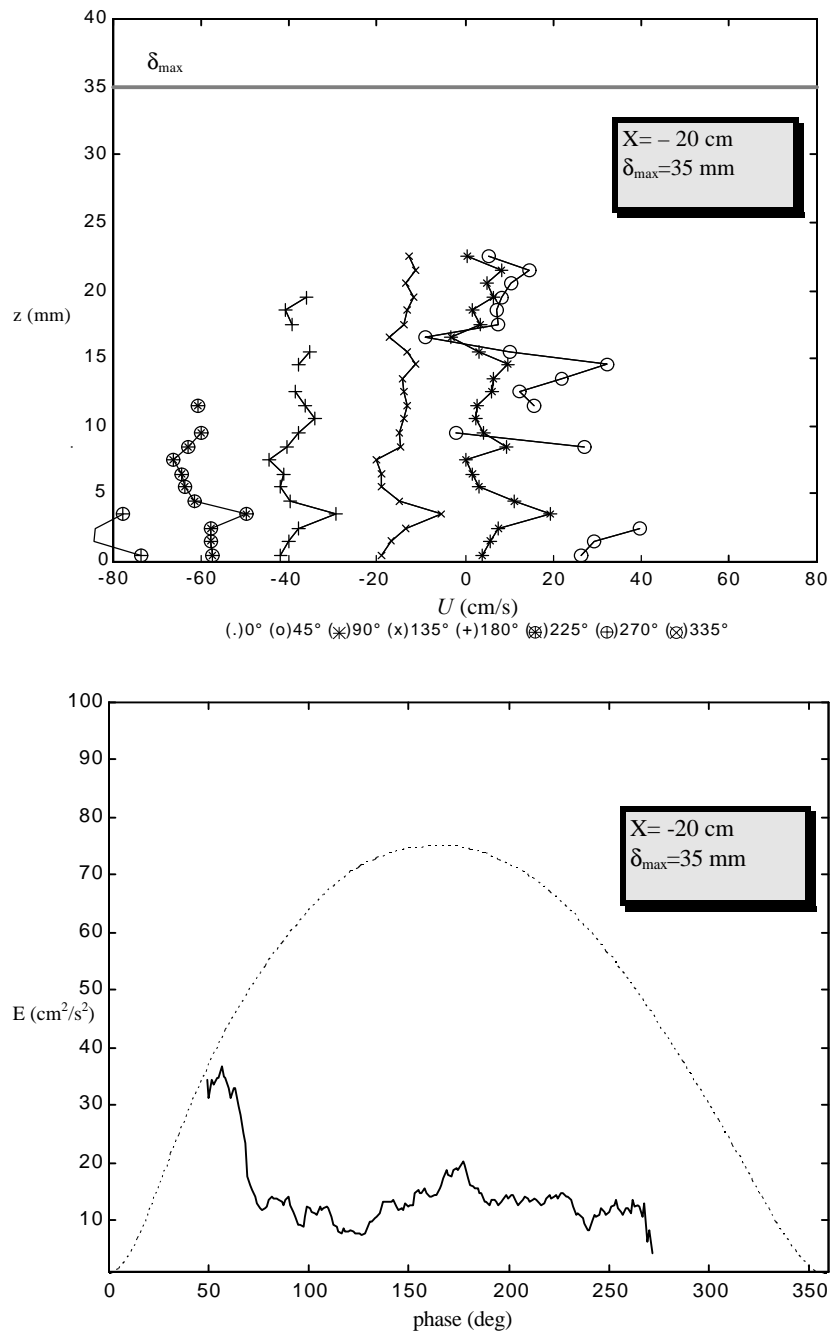(.)0° (o)45° (✳)90° (x)135° (+)180° (⊕)225° (⊕)270° (⊗)335°



**Fig.A6- 8. Test RH040T25**: *Velocity profiles and turbulence near the bottom. Lower section.*

**Fig.A6- 9. Test RH040T25***: Mean turbulence energy and turbulence variation over a cycle. Mid section.*

Fig.A6- 10. Test RH040T25: *Velocity profiles and turbulence near the bottom. Mid section.*

**Fig.A6- 11. Test RH040T25***: Mean turbulence energy and turbulence variation over a cycle. Upper section.*

**Fig.A6- 12. Test RH040T25:** *Velocity profiles and turbulence near the bottom. Upper section.*

**Fig.A6- 13. Test RH040T30***: Mean turbulence energy and turbulence variation over a cycle. Lower section.*

**Fig.A6- 14. Test RH040T30**: *Velocity profiles and turbulence near the bottom. Lower section.*
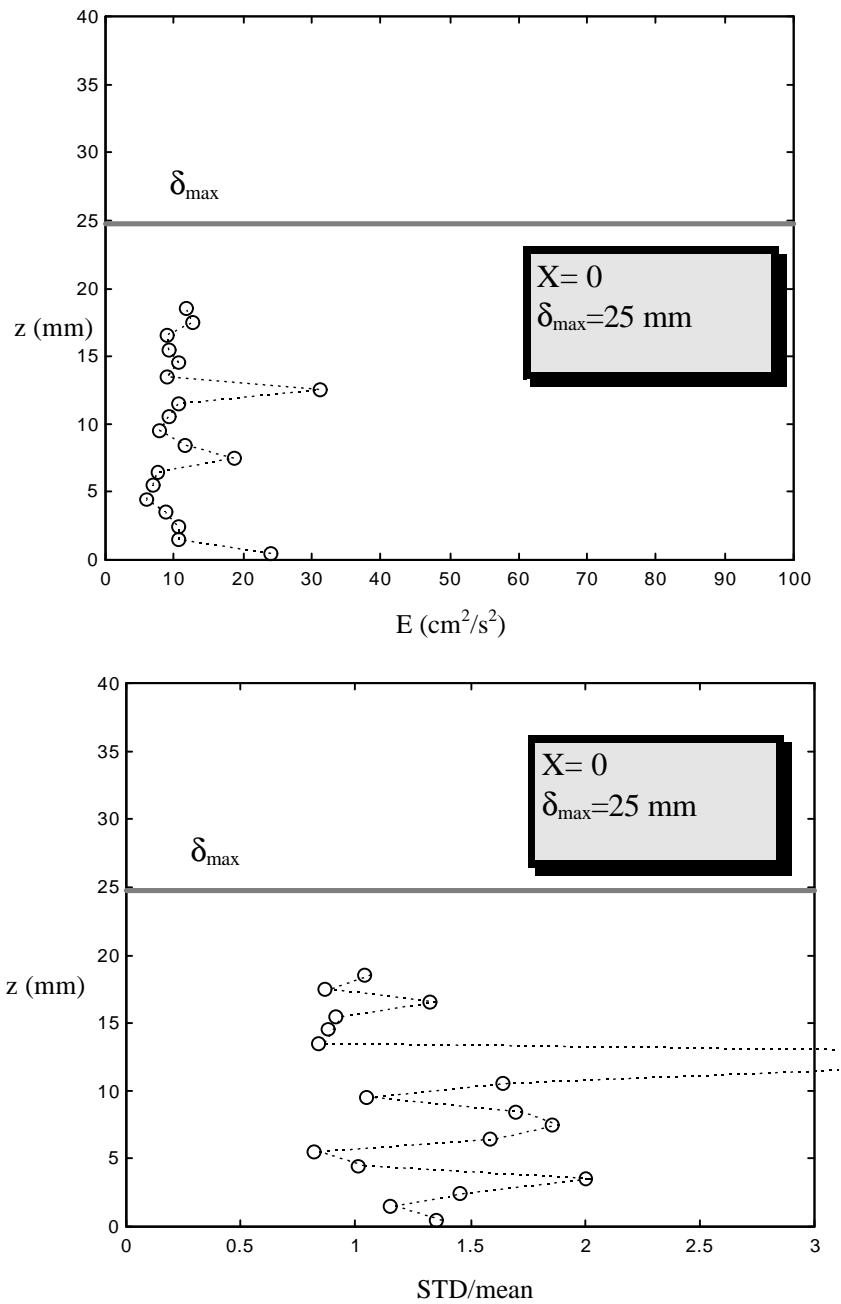
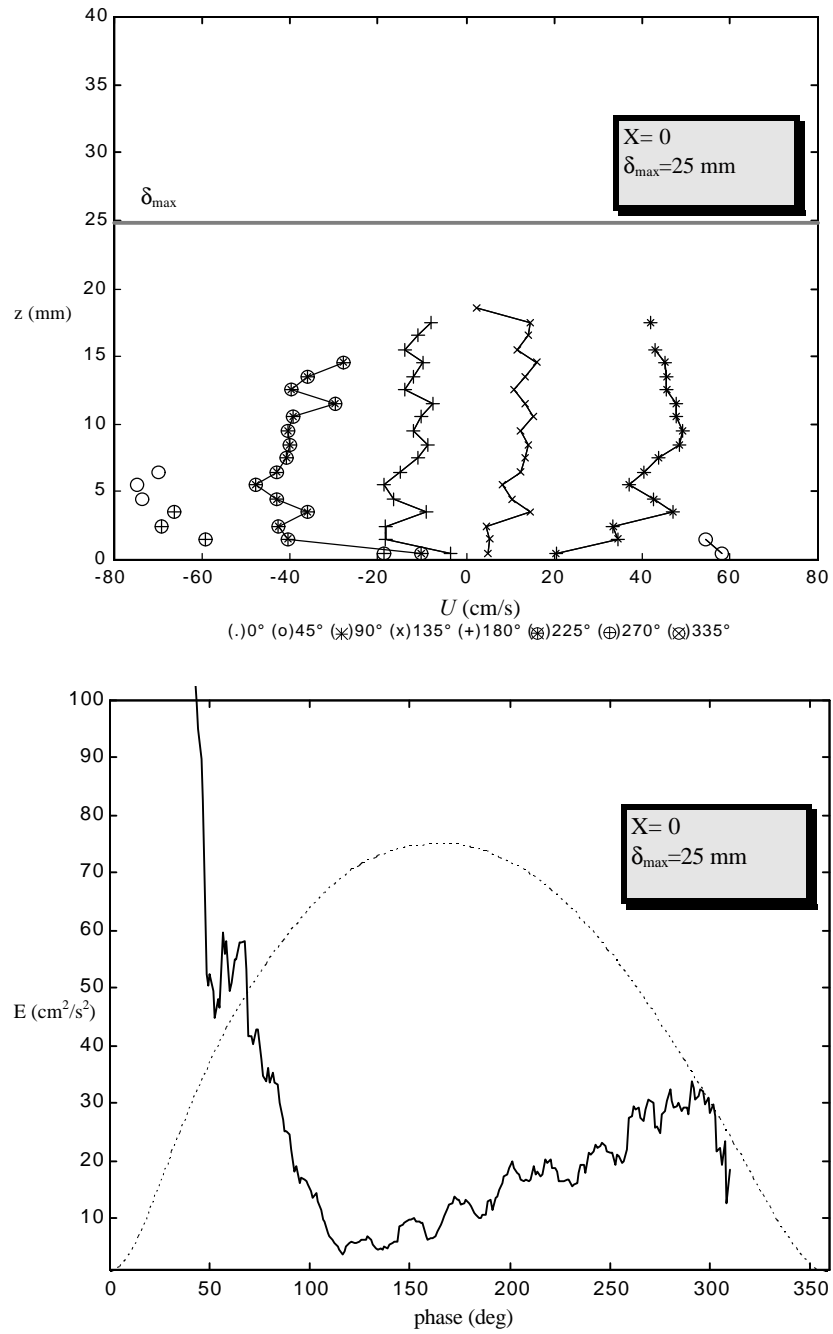**Fig.A6- 15. Test RH040T30***: Mean turbulence energy and turbulence variation over a cycle. Mid section.*

**Fig.A6- 16. Test RH040T30***: Velocity profiles and turbulence near the bottom. Mid section.*
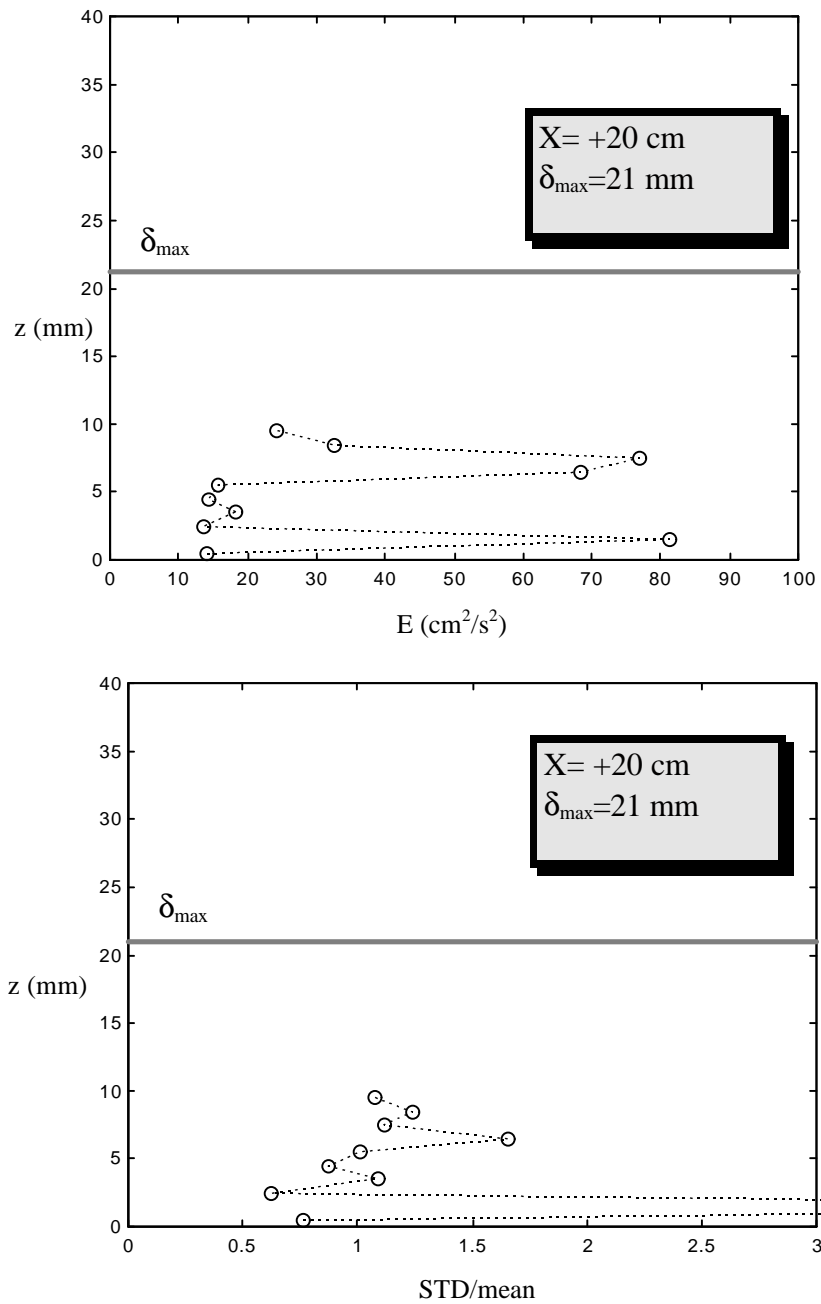
**Fig.A6- 17. Test RH040T30***: Mean turbulence energy and turbulence variation over a cycle. Upper section.*
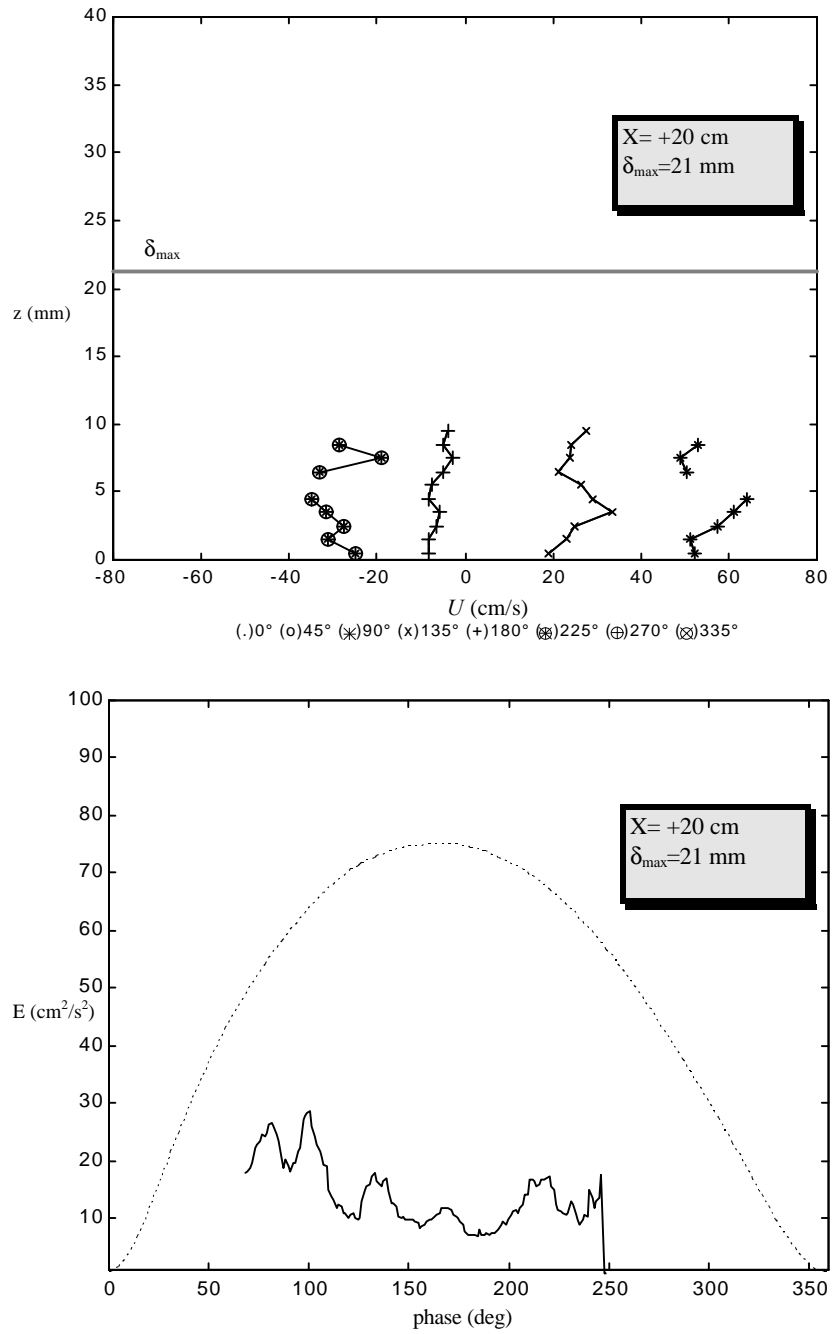
**Fig.A6- 18. Test RH040T30***: Velocity profiles and turbulence near the bottom. Upper section.*